New Optical Biosensors for Uric Acid and Glucose

DISSERTATION ZUR ERLANGUNG DES DOKTORGRADES DER NATURWISSENSCHAFTEN

(Dr. rer. nat.)

DER NATURWISSENSCHAFTLICHEN FAKULÄT IV- CHEMIE UND PHARMAZIE

DER UNIVERSITÄT REGENSBURG

vorgelegt von

Petra Schrenkhammer

aus Aidenbach, Landkreis Passau

Juli 2008

New Optical Biosensors for Uric Acid and Glucose

Doctoral Thesis

by

Petra Schrenkhammer

Für meine Familie

Diese Doktorarbeit entstand in der Zeit von April 2005 bis Juli 2008 am Institut für Analytische Chemie, Chemo- und Biosensorik an der Universität Regensburg.

Die Arbeit wurde angeleitet von Prof. Dr. Otto S. Wolfbeis.

Promotionsgesuch eingereicht am: 17.06.2008

Kolloquiumstermin:	22.07.2008	
Prüfungsausschuss:	Vorsitzender:	Prof. Dr. H. H. Kohler
	Erstgutachter:	Prof. Dr. O. S. Wolfbeis
	Zweitgutachter:	Prof. Dr. A. Göpferich
	Drittprüfer:	Prof. Dr. W. Kunz

Danksagung

Mein erster Dank gilt **Herrn Prof. Dr. Otto S. Wolfbeis** für die Vergabe des interessanten Themas, das stets mit Anregung und Diskussionen verbundene Interesse an meiner Arbeit und die sehr hervorragenden Arbeitsbedingungen am Lehrstuhl.

Für die gute Laborgemeinschaft, die anregenden Diskussionen und netten Small Talks danke ich meiner Laborkollegin **Doris Burger** und meinem Laborkollegen **Robert Meier**, der auch immer für gute Musik im Labor sorgte.

Matthias Stich danke ich für die gute Zusammenarbeit, die Bereitstellung des Tripelsensors und die Durchführung aller damit verbundenen Messungen.

Herrn **Dr. Michael Schäferling** danke ich für die gute Zusammenarbeit und die Hilfestellungen.

Weiterhin bedanke ich mich bei **Barbara Goricnik, Gisela Hierlmeier, Gisela Emmert, Edeltraud Schmid, Nadja Hinterreiter, Martin Link, Corinna Spangler, Christian Spangler, Simone Moises, Mark-Steven Steiner, Dr. Xiaohua Li, Katrin Uhlmann, Daniela Achatz, Heike Mader, Dr. Axel Dürkop** und allen weiteren Mitarbeitern für die wissenschaftlichen und nicht wissenschaftlichen Diskussionen, die netten Kaffeerunden und die sehr gute Stimmung am Lehrstuhl.

Ferner möchte ich mich bei **Rasto Serbin** und **Dilbar Mirzarakhmetova** für die Mitarbeit im Rahmen eines Forschungsaufenthaltes bedanken.

Ich bedanke mich beim Universitätsklinikum Regensburg für die Bereitstellung der Blutserumproben.

Für die finanzielle Unterstützung während dieser Arbeit danke ich dem Graduiertenkolleg „***Sensorische Photorezeptoren in natürlichen und künstlichen Systemen“***.

Abschließend möchte ich mich bei meiner Familie bedanken:

Großer Dank geht an meinen Bruder **Fritz**, der mich immer motiviert und unterstützt hat (vor allem hat er noch die nötigen Anstöße zum Chemiestudium gegeben).

Großen Dank auch an meine **Oma**, die mich immer unterstützt hat.

Mein größter Dank gebührt doch meinen Eltern **Friedrich** und **Rita Suchomel**, die mir das Studium ermöglicht und mich immer finanziell unterstützt haben, sowie mir immer bei allen Problemen und Nöten hilfestellend beistehen.

Und ganz herzlich möchte ich mich bei meinem Mann **Stephan** bedanken, der immer für mich da ist und mir immer Rückhalt auch in stressigen Zeiten gibt.

Table of Contents

Chapter 1

Introduction

1.1 Motivation

(a) Uric acid ($C_5H_4N_4O_3$) , a poorly water soluble nitrogenous end product of the purine nucleotide catabolism in humans is found in biological fluids, mainly blood, urine or serum and is excreted by kidneys.[1,2,3] Monitoring of uric acid is essential because abnormal levels of uric acid lead to several diseases like gout, Lesh-Nyhan syndrome, renal failure, hyperuricaemia, and physiological disorders. In case of leukaemia or pneumonia the uric acid level is enhanced. [1,2,4] Further on, uric acid is an antioxidant in human adult plasma and is involved in many pathological changes.[1] Therefore, uric acid determination is very important. Numerous methods have been developed for the determination of uric acid such as electrochemical and optical methods. Electrochemical methods are based on amperometry or voltammetry and the optical one on fluorometry, colorimetry, HPLC or spectrometry.[4,5,6,7,8,9,10,11] Electrochemical methods are less time-consuming, inexpensive and more sensitive compared to other methods. Interferences like ascorbic acid present in biological fluids affect electrochemical measurements due to the oxidation at the potential applied for uric acid determination. For early diagnosis e.g. for gout it is important to develop fast and easy assays or biosensors.

(b) Diabetes mellitus is a complex endocrine metabolic disorder which results from a total or partial lack of insulin.[12] Insulin is a hormone which is responsible for converting sugar, starches and other food into the daily energy requirements.[13] Diabetes mellitus is a worldwide problem because many people are diseased. Its main characteristic the glucose level, is chronically raised. Rigorous controlling of glucose level can decelerate long-term complications such as microangiopathy, kidney or nerve damages which are attributed to diabetes.[14] Hence, it is very important to maintain the glucose level near normal level for treatment of diabetes. The development of test strips allows the patient’s self controlling.

Glucose in the level of 6.1 mM ± 1.4 mM can be considered as acceptable level.[12] Therefore, numerous sensors were developed for fast monitoring of glucose levels in physiological fluids which can be done *in vivo* or *in vitro*. The currently available sensors are based on electrochemical principles where the enzyme glucose oxidase serves as molecular recognition element.[15] Several sensors for the determination of glucose are developed based on the principle of optical detection of oxygen. Glucose can be converted in hydrogen peroxide and gluconic acid under oxygen consumption catalyzed by glucose oxidase. The oxygen consumption can be detected by using an oxygen sensitive probe. In the last years several planar sensors or fiber optics were designed.[16,17,18,19]

(c) The aim of this work is the development of new assays for uric acid and glucose. One part of the work involves a microtiter plate assay for fluorimetric determination of uric acid using the effect of luminescence enhancement of the lanthanide complex europium(III) tetracycline 3:1 (Eu_3TC). Recently, Eu_3TC was introduced in literature as promising hydrogen peroxide sensitive probe.[20,21,22] It features three main characteristics such as a large Stokes´ shift, line-like emission spectrum and long luminescence lifetime. The detection of uric acid is based on the principle of luminescence enhancement of Eu_3TC in presence of hydrogen peroxide, which is released during the oxidation of uric acid catalyzed by the enzyme uricase under oxygen consumption.

Furthermore, planar optical sensors were generated for simple and sensitive continuous monitoring of uric acid and glucose. Glucose and uric acid were alternatively detected using an oxygen sensitive probe. For both sensors the enzymes uricase (for uric acid monitoring) or glucose oxidase (for glucose monitoring) is immobilized in a hydrogel matrix next to an oxygen sensitive probe incorporated in sol-gel (ormosil) beads whose luminescence is dynamically quenched in presence of oxygen. The sensing schemes are based on the measurement of the consumption of oxygen during the oxidation which is catalyzed by the corresponding enzymes.

A triple biosensor, which contains oxygen, temperature, pH sensitive beads, and the enzyme glucose oxidase, is applied for monitoring glucose via the oxygen or the pH transducer under simultaneously monitoring of the environment temperature. The experiment was performed in a microtiter plate format applying fluorescence lifetime imaging.

1.2. Lanthanide complexes

1.2.1. Luminescence Emission Mechanism of Lanthanide Complexes

Luminescence is the emission of light from fluorophores from the electronically excited state.[23] Some lanthanide ions (Eu^{3+}, Sm^{3+}, Tb^{3+}, Dy^{3+}) exhibit very low absorption and luminescence, but coordination or chelating with organic ligands result in high stability and strong luminescence. [24,25] In contrast to common fluorophores energy is absorbed by the ligand ($S_0 \rightarrow S_1$) and transferred to a triplet state (T_1) of the ligand by intersystem crossing. Then, energy is intramoleculary led across to a resonance level of the lanthanide ion which emits luminescence. For europium(III) complexes in aqueous solution all emissions emanates from the nondegenerate $^5D_0$ level. Hence, multiple emissions can be detected. The strongest emission is observed for the transitions form $^5D_0 \rightarrow {}^7F_1$ or $^5D_0 \rightarrow {}^7F_2$ whose emissions are located around 585-600 nm and 610-630 nm. Their emissions are sensitive to the ligand environment which reflects the hypersensitive character of the $^5D_0 \rightarrow {}^7F_2$ transition. The remaining emission intensities are very weak or unobservable.[26] The energy transfer for the Eu^{3+}-ion is shown in *Fig. 1*.

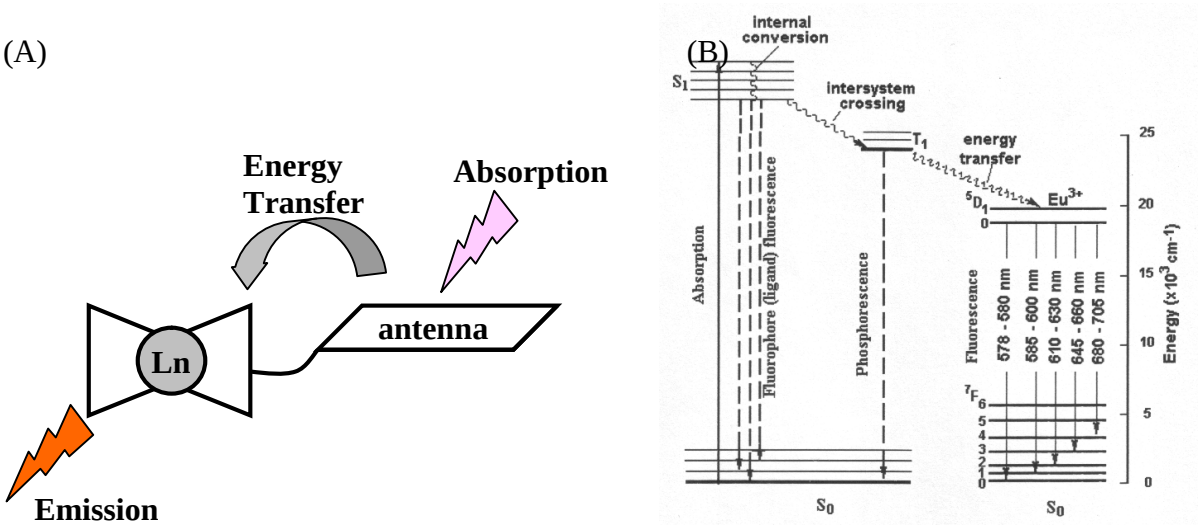

Fig. 1. *(A) The ligand (fluorophore) acts as antenna which absorbs light. The energy is transferred to the excited state of the lanthanide ion which emits luminescence. (B) Luminescence emission mechanism of a* Eu^{3+}*-complex.*

The three main characteristics for lanthanide complexes in fluorometry are (1) the large Stokes´ shift, (2) the narrow emission bands and (3) the long lifetime which make them useful as an alternative to organic dyes.

The Stokes´ shift of lanthanide complexes is between 150 and 300 nm which results in the energy consumption due to internal conversion, intersystem crossing, and in the intramolecular energy transfer. Due to this property the overlap between excitation and emission is avoided. The narrow emission bands (line-like bands) results from the shielding of the f-orbitals by the higher s and p orbitals of the lanthanide.[27] In case of the Eu^{3+}-complexes the $^5D_0 \rightarrow {}^7F_1$ emission can split into three components and the $^5D_0 \rightarrow {}^7F_2$ emission into five components. Due to spectral resolution limitations it is possible that no line splitting is observable rather than inherent structural properties of the system. The f-f electronic transitions are forbidden which results in long luminescence lifetimes. Eu^{3+}-complexes in aqueous solutions display lifetimes in the range from 0.1 to 1 ms. The lifetime is depending on the nature of the ligand environment, and the number of water molecules which occupy inner coordination sites.[26] Long luminescence lifetimes are beneficial for time-resolved measurements where typically short-lived background signals can be eliminated.

The requirements of strong lanthanide luminescence are the capability to form stable lanthanide-ligand-complexes, the efficient intramolecular energy transfer and weak radiationless energy losses.[25]

In this work the antibiotic tetracycline (TC) was applied as antenna ligand which can coordinate by its several proton-donating groups to the Eu^{3+}-ion. The resulting probe was applied to the determination of hydrogen peroxide.

1.2.2. Time-Resolved Detection of Lanthanide Luminescence

The application of time-resolved luminescence measurements reduces the background signals. The principle for time-resolved luminescence detection for lanthanide complexes, especially Eu^{3+}-complexes, is shown in *Fig. 2*. The Eu^{3+} complex is excited via a pulsed light source such as a xenon flash lamp. Luminescence intensity is collected after a delay time of 30 to 100 µs when the scattering light (Tyndall, Raman scatter, Rayleigh scatter) and the background from microtiter plates, cuvettes or sample matrix (e.g. proteins, cells) are completely eliminated. The lifetime of such signals is in the ns range whereas the lifetime of the Eu(III)-complex, applied in this work, is around 30 µs. [28,29] The implementation of time-

gated methods enables a highly sensitive detection of the lanthanide specific signals without background interference.[30;31]

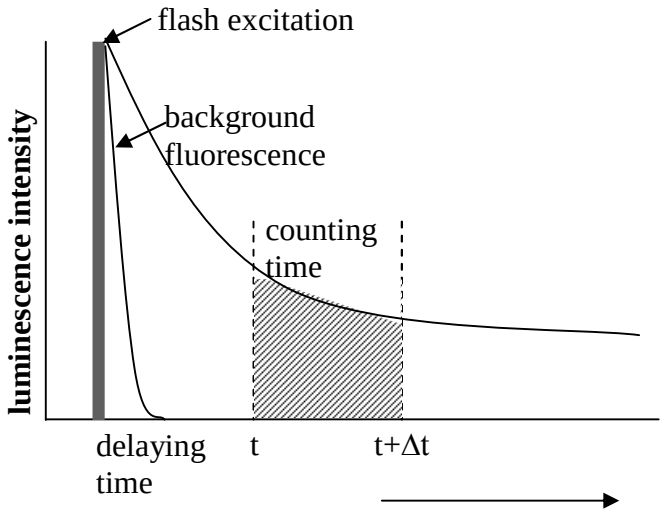

Fig.2. *Principle of time-resolved (gated) luminescence assays*

1.2.3. Methods for Determination of H_2O_2 in Fluorescent Analysis

Hydrogen peroxide (HP) is a product of reactions which are catalyzed by oxidases such as glucose oxidase or uricase. It is essential in industrial and clinical chemistry. In the industry it is used for wastewater treatment or as source of oxygen. [32,33] HP and its derivatives are oxidizing agents which can be applied in the chemical synthesis of organic compounds.[32] In some cases the determination of low HP levels is required. For example, the determination of nanomolar concentrations is very crucial in marine water, air, drinking water, or in many immunoassays.[34] There are many methods for detection of HP such as titrimetry, spectrophotometry, fluorimetry and chemiluminescence. Electrochemical methods are very popular as well.[32,34] For analytical application direct reduction or oxidation of HP at a bare electrode is not suitable because the electrode kinetics are too slow and high overpotentials are required for the redox oxidation of HP. Mediators like cobalt phthalocyanine or Prussian blue are applied for decreasing the overpotential and increasing the electron transfer kinetics.[32]

Spectrophotometry is one of the most applied methods for HP determination. HP is detected by reaction with a chromogenic hydrogen donor in the presence of peroxidase. Several hydrogen donors were suggested e. g. a mixture of 4-aminoantipyrine and phenol, 4-chlorophenol or 2,4-dichlorophenol-6-sulphonic acid. These donors are oxidized in presence of peroxidase and form chromophores that exhibit absorption maxima between 500 and 520

nm. When HP is detected in blood serum these chromophores are not suitable because the absorption maximum of the hemoglobine decomposition product bilirubin is in the range from 380 nm to 530 nm.[35] Titanium(IV) complexes are applied as well for spectrophotometric determination of HP. In this case the enzyme peroxidase is not required. In acid solutions the presence of HP decreases the absorbance of the titanium(IV) complex at 432 nm.[36] Nowadays fluorometric methods for HP determination are very popular. One common used fluorogenic probe is Amplex Red. In presence of hydrogen peroxide Amplex Red is converted to resorufin catalyzed by peroxidase. Resorufin can be detected at a 580 nm when excited at 570 nm.[37] A new probe for HP determination is based on a europium coordination complex called Eu_3TC (europium(III)-tetracycline). In numerous publications the application of this complex is described where the luminescence of Eu_3TC is enhanced in presence of HP. This method can be used for rapid determination of HP at neutral pH without requiring an enzyme such as peroxidase. Compared to common fluorophores this complex features the advantages of (1) long lifetime in the excited state (~30 µs), (2) large Stokes´ shift (~210 nm) and (3) line like emission bands. Hence, time-resolved measurements are possible.[29,38,39] Further on, Eu_3TC can be applied in sensor technology, where Eu_3TC was incorporated in a hydrogel matrix for hydrogen peroxide sensing and reversibility of the sensor is given compared to methods based on formation of a chromophoric product.[22]

1.3. Sensor Technology

1.3.1. State of the Art of O_2 Sensing

The determination of dissolved oxygen is of great importance in environmental, biomedical and industrial analysis.[40,41] In food industry low oxygen levels are important to keep good quality of many food products especially for those which are stored over long time. Hence, foods are packed under vacuum and the residual oxygen is the key determinant of food quality.[42] In the medical field, the measurement of the oxygen partial pressure of blood and tissue is a standard diagnostic tool.[43] In the environmental analysis monitoring of oxygen is important in the atmosphere and in water.[40,44] In industrial process control the monitoring oxygen supply is essential in case of anaerobic processes or processes which utilize metabolizing organisms. In biotechnology oxygen monitoring is required to control the

cultivation conditions of aerobic organisms or for monitoring of oxygen which is consumed by enzymes during the fermentation process.[45,46,47]

For determination of oxygen in aqueous solutions several methods are proposed like Winkler titration, oxygen sensitive electrodes, extraction of the dissolved gas from the liquid phase followed by mass spectroscopy or optical measurements of fluorescence quenching in oxygen sensitive membranes.[48] Winkler titration was the first method for determination of dissolved oxygen in water samples which was developed by Lajos Winkler in 1888. The development of the Clark electrode for determination of oxygen was revolutionary and is applied nowadays. This oxygen sensor is based on polarography. For oxygen measurements a platinum and a silver reference electrode are merged which are immersed in a KCl solution. The electrodes are separated by an oxygen permeable membrane from the test sample. The electric current flow between the electrodes when polarised with a potential between -0.6 and -0.8 V (vs Ag/AgCl) is proportional to the oxygen partial pressure in the sample. The disadvantage of this sensor is the oxygen consumption by the system which causes wrong data at determination of low pO_2 levels and the application of the electrodes is limited because the anode reaction can slowly passivate the reference electrode.[49]

In consequence of these disadvantages optical sensors for oxygen monitoring have been developed. They have the significant advantage that no reference element is required and the miniaturization can be easily performed. Most of the optical oxygen sensors are based on the principle of collisional quenching of the excited state of a luminescent indicator dye by oxygen. In 1968 Bergman developed the first pO_2 optode which consists of fluoranthene absorbed on a porous glass support.[50] The properties of the sensing film are mostly depending on the polymer properties. In most of the optical oxygen sensors the dye is immobilized in oxygen permeable and non-polar polymers. Further on, the polymer has to be impermeable for potential quencher such as heavy metals. The most applied polymers are silicone rubbers, polystyrene (PS), poly(vinyl chloride) (PVC), poly(methyl methacrylate) (PMMA) and cellulose derivatives.[17,51,52,53,54,55] Silicon rubbers show the best oxygen permeability. This yields in high quenching effect of the oxygen sensitive dye. The oxygen permeability of PS, PMMA and PVC is lower than silicon rubbers, but their mechanically stability is much better. Furthermore, sol gels matrices are applied for detection of dissolved oxygen. They exhibit the advantages of good optical transparency in the spectral region of the dopant dye, chemical stability, high porosity, rigidity, chemical inertness, and their swelling in liquids is negligible. Sol-gels are widely applicable as sensor films, micro-or nanospheres, and powder. When

molecules are entrapped in a sol-gel matrix, their chemical and physical characteristics are maintained.[56,57]

Optical sensing of oxygen is based on dynamic quenching of the luminescence intensity or lifetime of numerous dyes by oxygen. A variety of luminescent species can be used as indicators and are useful when the quenching efficiency and rate is large enough. Photostability, high quantum yields, long lifetimes, high molar absorbance, solubility in the sensor polymer and excitation with low-price sources such LED or diode laser are the main characteristics for the choice of an indicator.[49] The fluorescent polycyclic aromatic hydrocarbons (PAH) were one of the first oxygen indicators. PAH are pyrene, pyrene derivates, decacyclene, fluoranthene or anthracene derivatives. [58,59] These indicators are photostable, exhibit lifetimes between 40-300 ns and are highly soluble in the extremely oxygen permeable silicon matrices.[60] Ruthenium(II) complexes such as tris(4,7-diphenyl-1,10-phenanthroline) ruthenium(II) ($Ru(dpp)_3^{2+}$) or tris(2,2´-bipyridine) ruthenium(II) ($Ru(bpy)_3^{2+}$) gain considerable interest as oxygen sensitive material due to their high quantum yields (up to 0.4), the large Stokes´ shift (> 150 nm), the long lifetimes (0.1-7 µs), strong visible absorption (~ 450 nm) and intense luminescence (550-800 nm). [59,61] Other promising indicators are Pd(II) or Pt(II) porphyrin complexes e. g. platinum(II) tetrakis(pentafluorophenyl)-porphyrin due to its long lifetimes (> 10 µs).[60] Disadvantageous is that these complexes show the effect of oxidation when they illuminated in presence of oxygen.[60] Hence, for oxygen sensing it is important to combine appropriate indicators and polymers to obtain sensors with the desired stability and sensitivity.

1.3.2. State of the Art of pH Sensing

One of the most applied instruments for pH detection is the glass electrode which was first described by Cremer in 1906 and later by MacInnes and Dole.[62] The potentiometric electrode is made up of an Ag^+/AgCl reference electrode and an Ag^+/AgCl working electrode which is immersed in a KCl buffer solution with defined pH. The working electrode is connected with the external test sample via a glass membrane. At this membrane the potential is generated which is used for the pH measurement. Ion-sensitive field effect transistors (ISFETs) are another alternative for chemical sensing of pH, which were first introduced in 1970 by Bergveld.[63,64] Recently iridium oxide (IrO_x) electrodes have been investigated for pH sensing. The advantages are the good stability over a wide pH range at high temperatures, at high pressure, in aggressive environments (e. g. HF solution) and the fast response even in

non-aqueous solutions. These are the advantages compared to conventional glass electrodes and other metal oxide electrodes.[65] pH electrodes exhibit a Nernstian response to the pH and are applicable over a wider pH range (2 to 12).[49]

An optical pH sensor consists of indicator dye which is immobilized in a proton permeable polymer matrix by covalently linking, entrapment or adsorption.[49] pH sensitive dyes are weak acids or bases which revise their optical properties by protonation or deprotonation. The polymer matrix can be used as planar sensor spot or as fiber optic.[66,67,68] In recent years, optical fibers are introduced for pH sensing. They have many advantages such as small size, immunity to electromagnetic and radio frequency, and multiplexing capability.[69] They are reversible and the pH induced changes can be monitored by changing the absorbance, reflectance, fluorescence, energy transfer or refractive index.[69] The first fiber optic sensor was investigated by Peterson et al. in the early eighties. It was developed for monitoring blood pH based on absorbance changes of the pH sensitive indicator phenol red.[70] Bromthymol blue, methyl orange, bromocresol green and alizarin are further typically absorption based pH indicators.[71] One of the first fluorescent fiber optical pH sensors were reported by Saari and Seitz where fluorescein amine was immobilized on controlled pore glass or on cellulose. [72] The most frequently applied fluorescent pH indicators are 8-hydroxypyrene-1,3,6-trisulfonic acid sodium salt, fluorescein derivatives, hydroxycoumarins, seminaphtho-rhodafluors (SNARF) and seminaphtho-fluoresceins (SNAFL). The choice of the right pH indicator is depending on photostability, high quantum yield, large Stokes´ shift, pK_a value, excitation and emission wavelengths.[49] The pH indicator of optical pH sensors can be immobilized onto ion exchangers, in sol-gel glasses or in poly(vinyl chloride).[67,73,74] The widely used polymer hydrogels are based on polyurethane, cellulose or pHEMA, which exhibit excellent proton permeability.[68,75,76]

1.3.3. Optical Biosensors and Methods for Enzyme Immobilization

Biosensors are a fast and growing field which combine biochemistry, biology, chemistry, and physics. The first biosensors were presented by Clark in 1956, and Clark and Lyons in 1962. Here, the enzyme glucose oxidase was coupled to an amperometric oxygen electrode for determination of glucose. [77] In the following years there was a great progress in the development of biosensors. IUPAC defines a biosensor as a chemical sensor which transforms chemical information into an analytical signal. In biosensors there has to be a biomolecule as recognition and a physico-chemical transducer.[77,78,79] The function of the

recognition element is the translation of the information e.g. of the analyte concentration in a chemical and physical signal.

Optical biosensors can be divided in two types of biosensors: catalytic and affinity biosensors. Affinity biosensors rely on the principle that the analyte binds to the recognition element. Immunosensors, nucleic acid biosensors, and biosensor based on the interaction of a ligand (analyte) with a biological receptor are affinity biosensors. Catalytic biosensors are mostly enzyme biosensors where the recognition element is the enzyme. They are based on catalytic reactions between the analyte and the enzyme which results in a measureable change of a solution property e g. of oxygen depletion or formation of a product. Further on, a transducer is necessary for converting the changes into an optical signal like emission, absorption, or reflectance.[77,80] The changes are detected by a photodetector which transforms it to an electrical signal. By virtue of the high enzyme substrate interaction and the high turnover rates of enzymes, enzyme-based biosensors are highly sensitive and specific. The usual format of an enzyme biosensor is that the enzyme is immobilized on the surface of a transducer. Immobilization of enzymes is required for avoiding the washing out by liquid solutions. There are three methods which have to be accentuated for the immobilization of enzymes: (1) binding to a support, (2) encapsulation, and (3) crosslinking.[77]

Support binding can be occurred physically such as hydrophobic interactions or Van der Waals forces, ionically or covalently. Physically immobilization is not the best method because the enzyme molecules are loosely bound to the surface and desorption is given. Application of this method causes no loss in enzyme activity and is very easy. Covalent and ionic binding are promising methods in contrast to physical binding. No leaching of the enzyme is given, but during the binding process the enzyme could be completely deactivated.[77,81,82]

Entrapment of enzymes in a polymer network or sol-gel prevents the leaching out from the membrane. The pore size of the membrane is smaller than the larger enzyme molecules but the analyte molecules can pass through the membrane. The encapsulation of the enzyme can be carried out during the crosslinking process of the polymer. [81,83,84]

Crosslinking is further chemical method for preparation of carrierless enzyme macroparticles where enzyme aggregates or crystals are crosslinked with a bifunctional reagent. The developed crosslinked enzyme crystals (CLECs) and crosslinked enzyme aggregates (CLEAs) exhibit high stability, high activity and low production costs.[81,85,86,87]

In this work enzyme biosensors were prepared for determination of uric acid or glucose. The technique of protein crosslinking via the reaction of glutaraldehyde with primary

amino groups on the enzyme surface was applied and combined with the entrapment in a polymer matrix.

1.3.4. Optical Sensor versus Electrochemical Sensor

The two main groups of biosensors are electrochemical and optical biosensors. The combination of the Clark amperometric oxygen electrode as transducer and the enzyme glucose oxidase as sensing element for glucose monitoring was the first electrochemical biosensor.[77] Electrochemical and optical biosensors are prepared in a similar way but display different features. Due to their disadvantages and advantages the situation and problem has to balance which kind of biosensor is the best choice. Optical sensors have the following advantages over electrochemical sensors:[88]

(1) No reference element is required as a reference electrode applying electrochemical biosensors.[88]

(2) Optical biosensors can be easy miniaturized such as fiber optics. This is advantageous for in vivo measurements like for continuous glucose monitoring in subcutaneous tissue.[89]

(3) No electrical interferences such as magnetic, ionic, or electrical fields influence the signal.[88]

(4) Optical sensors offer the possibility to measure one or more analytes simultaneously. Several dual sensors for monitoring oxygen and pH or oxygen and carbon dioxide were developed in recent years.[90,91]

(5) Optical sensors do not consume the analyte in contrast to electrochemical sensors e.g. the Clark electrode consumes oxygen.[92]

(6) Optical sensors or biosensors are non-invasive.

Optical biosensors or sensor display disadvantageous as well.[88]

(1) Ambient light can interfere. Based on this, the measurements have to be performed in dark environment, or optical isolations and pulse technique have to minimize interferences by ambient light.

(2) Optical sensors exhibit the effect of photobleaching or leaching out of the indicator from a polymer matrix. Therefore, the long-term stability is reduced.

(3) The dynamic range of optical sensors is smaller than for electrochemical ones. In case of pH optodes the dynamic is extended over 2 units compared to the glass electrode which includes the pH range from 1 to 13.[68]

(4) Optical sensors or biosensors have to be calibrated at two points because of depending on the light source and the slope. The intensity of the light source can be varying form instrument to instrument or with increasing time the intensity of the light source (xenon lamp) is decreasing.

1.4. References

[1] Goyal R. N., Gupta V. K., Sangal A., Bachheti N., **Voltammetric determination of uric acid at a fullerene-C_{60}-modified glassy carbone electrode** 2005. Electroanalysis 17, 2217-2223

[2] Ramesh P., Sampath S., **Selective determination of uric acid in presence of ascorbic acid and dopamine at neutral pH using exfoliated graphite electrodes** 2004. Electroanalysis 16, 866-869

[3] Becker B. F., **Towards the physiological function of uric acid** 1992. Free Rad. Biol. Med. 14, 615-631

[4] Galbán J., Andreu Y., Almenara M. J., de Marcos S., Castillo J. R., **Direct determination of uric acid in serum by a fluorometric-enzymatic method based on uricase** 2001. Talanta 54, 847-854

[5] Kalimuthu P., Suresh D., John S. A., **Uric acid determination in the presence of ascorbic acid using self-assembled submonolayer of dimercaptothiadiazole-modified gold electrodes** 2006. Anal. Biochem. 357, 188-193

[6] da Silva R. P., Lima A. W. O., Serrano S. H. P., **Simultaneous voltammetric detection of ascorbic acid, dopamine and uric acid using a pyrolytic graphite electrode modified into dopamine solution** 2008. Anal. Chim. Acta 612, 89-98

[7] Dai X., Fang X., Zhang C., Xu R., Xu B., **Determination of serum uric acid using high-performance liquid chromatography (HPLC)/isotope dilution mass spectrometry (ID-MS) as a candidate reference method** 2007. J. Chromatography B 857, 287-295

[8] Jauge P., Del-Razo L. M., **Urinary uric acid determination by reversed-phase high pressure liquid chromatography** 1983. J. Liquid Chromatography 6, 845-860

[9] Martinez-Perez D., Ferrer M. L., Mateo C. R., **A reagent less fluorescent sol-gel biosensor for uric acid detection in biological fluids** 2003. Anal. Biochem. 322, 238-242

[10] Odo J., Shinmoto E., Shiozaki A., Hatae Y., Katayama S., Jiao G. S., **Spectrofluorometric determination of uric acid and glucose by use of Fe(III)-thiacalix[4]arenetetrasulfonate as a peroxidase mimic** 2004. J. Health Sci. 50, 594-599

[11] Duncan P. H., Gochman N., Cooper T., Smith E., Bayse D., **A candidate reference method for uric acid in serum. I. Optimization and evaluation** 1982. Clin. Chem. 28, 284-290

[12] Wilkins E., Atanasov P., **Glucose monitoring: state of the art and future possibilities** 1996. Med. Eng. Phy. 18, 273-288

[13] Wang X. D., Zhou T. Y., Chen X., Wong K. Y., Wang X. R., **An optical biosensor for the rapid determination of glucose in human serum** 2008. Sens. Actuators B 129, 866-873

[14] Russell R. J., Pishko M. V., Gefrides C. C., McShane M. J., Coté G. L., **A fluorescence-based glucose biosensor using concanavalin A and dextran encapsulated in a poly(ethylene glycol) hydrogel** 1999. Anal. Chem. 71, 3126-3132

[15] Pasic A., Koehler H., Schaupp L., Pieber T. R., Klimant I., **Fiber-optic flow-through sensor for online monitoring of glucose** 2006. Anal. Bioanal. Chem. 386, 1293-1302

[16] Schaffar B. P. H., Wolfbeis O. S., **A fast responding fiber optic glucose biosensor based on an oxygen optrode** 1990. Biosens. Bioelectron. 5, 137-148

[17] Moreno-Bondi M. C., Wolfbeis O. S., Leiner M. J. P., Schaffar B. P. H., **Oxygen optrode for use in a fiber-optic glucose biosensor** 1990. Anal. Chem. 62, 2377-2380

[18] Zhou Z., Qiao L., Zhang P., Xiao D., Choi M. M. F., **An optical glucose biosensor based on glucose oxidase immobilized on a swim bladder membrane** 2005. Anal. Bioanal. Chem. 383, 673-679

[19] Trettnak W., Leiner M. J. P., Wolfbeis O. S., **Fibre optic glucose biosensor with an oxygen optode as the transducer** 1988. Analyst 113, 1519-1523

[20] Wu M., Lin Z., Wolfbeis O. S., **Determination of the activity of catalase using a europium(III)-tetracycline-derived fluorescent substrate** 2003. Anal. Biochem. 320, 129-135

[21] Wu M., Lin Z., Schaeferling M., Duerkop A., Wolfbeis O. S., **Fluorescence imaging of the activity of glucose oxidase using a hydrogen peroxide sensitive-europium probe** 2005. Anal. Biochem. 340, 66-73

[22] Schaeferling M., Wu M., Enderlein J., Bauer H., Wolfbeis O. S., **Time-resolved luminescence imaging of hydrogen peroxide using sensor membranes in a microwell format** 2003. Appl. Spectrosc. 57, 1386-1392

[23] Lakowicz J. R., **Principles of fluorescence spectroscopy** 1999. 2th edition, Kluwer Academic / Plenum Publishers, 4-6

[24] Yuan J., Wang G., **Lanthanide complex-based fluorescence label for time-resolved fluorescence bioassay** 2005. J. Fluoresc. 15, 559-568

[25] Arnaud N., Georges J., **Comprehensive study of the luminescent properties and lifetimes of Eu^{3+} and Tb^{3+} chelated with various ligands in aqueous solutions: influence of the synergic agent, the surfactant and the energy level of the ligand triplet** 2003. Spectrochim. Acta Part A 59, 1829-1840

[26] Richardson F. S., **Terbium(III) and europium(III) ions as luminescent probes and stains for biomolecular systems** 1982. Chem. Rev. 82, 541-552

[27] Lin Z., **Time-resolved fluorescence-based europium-derived probes for peroxidase bioassays, citrate cycle imaging and chirality sensing** 2004. Dissertation, 1-5

[28] Dickson E. F., Pollak A., Diamandis E. P., **Ultrasensitive bioanalytical assays using time-resolved fluorescence detection** 1995. Pharmacology and therapeutics 66, 207-235

[29] Wolfbeis O. S, Duerkop A., Wu M., Lin Z., **A europium-ion-based luminescent sensing probe for hydrogen peroxide** 2002. Angew. Chem. Int. Ed. 41, 4495-4498

[30] Handl H. L., Gillies R. J., **Lanthanide-based luminescent assays for ligand-receptor interactions** 2005. Life Sci. 77, 361-371

[31] Lakowicz J. R., **Principles of fluorescence spectroscopy** 1999. 2th edition, Kluwer Academic / Plenum Publishers, 86-88

[32] Salimi A., Hallaj R., Soltanian S., Mamkhezri H., **Nanomolar detection of hydrogen peroxide on glassy carbon electrode modified with electrodeposited cobalt oxide nanoparticles** 2007. Anal. Chim. Acta 594, 24-31

[33] Cosgrove M., Moody G. J., Thomas J. D. R., **Chemically immobilized enzyme electrodes for hydrogen peroxide determination** 1988. Analyst 113, 1811-1815

[34] Razola S. S., Aktas E., Viré J. C., Kauffman J. M., **Reagentless enzyme electrode based on phenothiazine mediation of horseradish peroxidase for subnanomolar hydrogen peroxide determination** 2000. Analyst 125, 79-85

[35] Tamaoku K., Murao Y., Akiura K., Ohkura Y., **New water-soluble hydrogen donors for the enzymatic spectrophotometric determination of hydrogen peroxide** 1982. Anal. Chim. Acta 136, 121-127

[36] Matsubara C., Kawamoto N., Takamura K., **Oxo[5,10,15,20-tetra(4-pyridyl)porphyrinato]titanium(IV): an ultrahigh sensitive spectrophotometric reagent for hydrogen peroxide** 1992. Analyst 117, 1781-1784

[37] Haugland R. **Handbook of fluorescent probes and research products** 2002. 9th edition, 440-442

[38] Lei W., Duerkop A., Lin Z., Wu M., Wolfbeis O. S., **Detection of hydrogen peroxide in river water via a luminescence assay with time-resolved ("gated") detection** 2003. Microchim. Acta 143, 269-274

[39] Duerkop A., Wolfbeis O. S., **Nonenzymatic direct assay of hydrogen peroxide at neutral pH using theEu_3TC fluorescent probe** 2005. J. Fluoresc. 15, 757-761

[40] Guo L., Ni Q., Li J., Zhang L., Lin X., Xie Z., Chen G., **A novel sensor based on the porous plastic probe for determination of dissolved oxygen in seawater** 2008. Talanta 74, 1032-1037

[41] Xiao D., Mo Y., Choi M. M. F., **A hand – held optical sensor for dissolved oxygen measurement** 2003. Meas. Sci. Technol. 14, 862-867

[42] Fitzgerald M., Papkovsky D. B., Smiddy M., Kerry J. P., O´Sullivan C. K., Buckley D. J., Guilbault G. G., **Nondestructive monitoring of oxygen profiles in packaged food using phase-fluorimetric oxygen sensor** 2001. J. Food Sci. 66, 105-110

[43] Peterson J. I., Fitzgerald R. V., Buckhold D. K., **Fiber-optic probe for in vivo measurement of oxygen partial pressure** 1984. Anal. Chem. 56, 62-67

[44] Li H., Wen J., Cai Q., Wang X., Xu J., Jin L., **A novel nano-Au-assembled gas sensor for atmospheric oxygen determination** 2001. Analyst 126, 1747-1750

[45] Wittmann C., Kim H. M., John G., Heinzle E., **Characterization and application of an optical sensor for quantification of dissolved O_2 in shake-flasks** 2003. Biotechnol. Letters 25, 377-380

[46] Gupta A., Rao G., **A study of oxygen transfer in shake flasks using a non-invasive oxygen sensor** 2003. Biotechnol. Bioeng. 84, 351-358

[47] Jamnik P., Raspor P., **Methods for monitoring oxidative stress response in yeast** 2005. J. Biochem. Molecular Toxicology 19, 195-2003

[48] Nestle N., Baumann T., Niessner R., **Oxygen determination in oxygen-supersaturated drinking waters by NMR relaxometry** 2003. Water Resarch 37, 3361-3366

[49] Schröder C. R., **Luminescent planar single and dual optodes for time-resolved imaging of pH, pCO_2 and pO_2 in marine systems** 2006. Dissertation

[50] Bergman I., **Rapid-response atmospheric oxygen monitor based on fluorescence quenching** 1968. Nature 218, 396

[51] Schaffar B. P., Wolfbeis O. S., **A fast responding fibre optic glucose biosensor based on oxygen optrode** 1990. Biosens. Bioelec. 5, 137-148

[52] Borisov S. M., Klimant I., **Ultrabright oxygen optodes based on cyclometalated iridium(III) coumarin complexes** 2007. Anal. Chem. 79, 7501-7509

[53] Mills A., Lepre A. **Controlling the response characteristics of luminescent porphyrin plastic film sensors for oxygen** 1997. Anal. Chem. 69, 4653-4659

[54] Mills A., **Controlling the sensitivity of optical oxygen sensors** 1998. Sens. Actuators B 51, 60-68

[55] Douglas P., Eaton K., **Response characteristics of thin film oxygen sensors, Pt and Pd octaethylporphyrins in polymer films** 2002. Sens. Actuators B 82, 200-208

[56] García E. A., Fernádez R. G., Díaz-García M. E., **Tris(bipyridine)ruthenium(II) doped sol-gel materials for oxygen recognition in organic solvents** 2005. Micropor. Mesopor. Mat. 77, 235-239

[57] Pang H. L., Kwok N. Y., Chow L. M. C., Yeung C. H., Wong K. Y., Chen X., Wang X., **Ormosil oxygen sensors on polystyrene microtiter plate for dissolved oxygen measurement** 2007. Sens. Actuators B 123, 120-126

[58] Wolbeis O. S., Posch H. E., Kroneis H. W., **Fiber optical fluorosensor for determination of halothane and/or oxygen** 1985. Anal. Chem. 57, 2556-2561

[59] Xu W., Schmidt R., Whaley M., Demas J. N., DeGraff B. A., Karikari E. K., Farmer B. L., **Oxygen sensors based on luminescence quenching: interactions of pyrene with the polymer supports** 1995. Anal. Chem. 67, 3172-3180

[60] García-Fresnadillo D., Marazuela M. D., Moreno-Bondi M. C., Orellana G., **Luminescent nafion membranes dyed with ruthenium(II) complexes as sensing materials for dissolved oxygen** 1999. Langmuir 15, 6451-6459

[61] McGee K. A., Veltkamp D. J., Marquardt B. J., Mann K. R., **Porous crystalline ruthenium complexes are oxygen sensors** 2007. J. Am. Chem. Soc. 129, 15092-15093

[62] Dole M., **The early history of the development of the glass electrode for pH measurements** 1980. J. Chem. Edu. 57, 134

[63] Pan T. M., Liao K. M., **Influence of oxygen content on the structural and sensing characteristics of Y_2O_3 sensing membrane for pH-ISEFT** 2007. Sens. Actuators B 128, 245-251

[64] Van Den Berg A., Bergveld P., Reinhoudt D. N., Sudhoelter E. J. R., **Sensitivity control of ISFETs by chemical surface modification** 1985. Sens. Actuators 8, 129-148

[65] Wang M., Yao S., Madou M., **A long-term stable iridium oxide pH electrode** 2002. Sens. Actuators B 81, 313-315

[66] Wencel D., Higgins C., Klukowska A., MacCraith B. D., McDonagh C., **Novel sol-gel derived films for luminescence-based oxygen and pH sensing** 2007. Mat. Science 25, 767-779

[67] Turel M., Čajlaković M., Austin E., Dakin J. P., Uray G., Lobnik A., **Direct UV-LED lifetime pH sensor based on a semi-permeable sol-gel membrane immobilized luminescent Eu^{3+} chelate complex** 2008. Sen. Actuators B 131, 247-253

[68] Weidgans B. M., Krause C., Klimant I., Wolfbeis O. S., **Fluorescent pH sensors with negligible sensitivity to ionic strength** 2004. Analyst 129, 645-650

[69] Dong S., Luo M., Peng G., Cheng W., **Broad range pH sensor based on sol-gel entrapped indicators on fiber optic** 2008. Sens. Actuators B 129, 94-98

[70] Motellier S., Noiré M H., Pitsch H., Duréault B., **pH determination of clay interstitial water using a fiber-optic sensor** 1995. Sens. Actuator B 29, 345-352

[71] Arain S. **Microrespirometry with sensor-equipped microtiterplates** 2006. Dissertation, 20

[72] Saari L. A., Seitz W. R., **pH sensor based on immobilized fluoresceinamine** 1982. Anal. Chem. 54, 821-823

[73] Vishnoi G., Goel T. C., Pillai P. K. C., **A pH-optrode for the complete working range** 1999**.** Proc. SPIE 3538, 319-325

[74] Daffy L. M., de Silva A. P., Gunaratne H. Q. N., Huber C., Lynch P. L. M., Werner T., Wolfbeis O. S., **Arenedicarboximide building blocks for fluorescent photoinduced**

electron transfer pH sensors applicable with different media and communication wavelengths 1998. Chem. Eur. J. 4, 1810-1815

[75] Yang X. H., Wang L. L., **Fluorescence pH probe based on microstructured polymer optical fiber** 2007. Optics Express 15, 16478-16483

[76] Hakonen A., Hulth S., **A high-precision ratiometric fluorosensor for pH: Implementing time-dependent non-linear calibration protocols for drift compensation** 2008. Anal. Chim. Acta 606, 63-71

[77] Choi M. M. F., **Progress in enzyme-based biosensors using optical transducers** 2004. Microchim. Acta 148, 107-132

[78] Thevenot D. R., Toth K., Durst R. A. Wilson G. S., **Electrochemical biosensors: recommended definitions and classifications** 1999. Pure Appl. Chem. 71, 2333-2348

[79] Turner A. P. F., **Techview: Biochemistry: Biosensors-sense and sensitivity** 2000. Science 290, 1315-1317

[80] Borisov S. M., Wolfbeis O. S., **Optical biosensors** 2008. Chem. Rev. 108, 423-461

[81] Sheldon R. A., **Enzyme immobilization: the quest for optimum performance** 2007. Adv. Synth. Catal. 349, 1289-1307

[82] Mateo C., Grazú V., Pessela B. C. C., Montes T., Palomo J. M., Torres R., López-Gallego F., Fernández-Lafuente R., Guisan J. M., **Advances in the design of new epoxy supports for enzyme immobilization-stabilization** 2007. Biochem. Soc. Transactions 35, 1593-1601

[83] Vidinha P., Augusto V., Almeida M., Fonseca I., Fidalgo A., Ilharco L., Cabral J. M. S., Barreiros S., **Sol-gel encapsulation: an efficient and versatile immobilization technique for cutinase in non-aqueous media** 2006. J. Biotechnol. 121, 23-33

[84] Choi D., Lee W., Lee Y., Kim D. N., Park J., Koh W. G., **Fabrication of macroporous hydrogel membranes using photolithography for enzyme immobilization** 2008. J. Chem. Technol. Biotechnol. 83, 252-259

[85] Sheldon R. A., **Cross-linked enzyme aggregate (CLEAs). Stable and recyclable biocatalysts** 2007. Biochem. Soc. Transactions 35, 1583-1587

[86] Roy J. J., Abraham T. E., Abhijith K. S., Kumar P. V. S., Thakur M. S., **Biosensor for the determination of phenols based on cross-linked enzyme crystals (CLEC) of lactase** 2005. Biosens. Bioelectron. 21, 206-211

[87] van Pelt S., Quignard S., Kubac D., Sorokin D. Y., van Rantwijk F., Sheldon R. A., **Nitrile hydratase CLEAs: the immobilization and stabilization of an industrially important enzyme** 2008. Green Chem. 10, 395-400

[88] Blum L. J., Coulet P. R., **Biosensor principles and applications** 1991. Marcel Dekker, Inc., 163-165

[89] Pasic A., Koehler H., Klimant I., Schaupp L., **Miniaturized fiber-optic hybrid sensor for continuous glucose monitoring in subcutaneous tissue** 2007. Sens. Actuators 122, 60-68

[90] Schroeder C. R., Neurauter G., Klimant I., **Luminescent dual sensor for time-resolved imaging of pCO2 and pO2 in aquatic system**s 2007. Microchim. Acta 158, 205-218

[91] Borisov S. M., Vasylevska A. S., Krause C., Wolfbeis O. S., **Composite luminescent material for dual sensing of oxygen and temperature** 2006**.** Adv. Funct. Mater. 16, 1536-1542

[92] Weidgans B. M., **New fluorescent optical pH sensors with minimal effects of ionic strength** 2004. Dissertation, 15-16

Chapter 2

Microtiter Plate Assay for Uric Acid Using the Europium Tetracycline Complex as a Luminescent Probe

A kinetic enzymatic assay is presented for the fluorometric determination of uric acid (UA) using the effect of luminescence enhancement of the europium(III)-tetracycline 3:1 complex (Eu_3TC). Its luminescence at a wavelength of 617 nm, when excited at 405 nm, is enhanced strongly in presence of hydrogen peroxide. Uric acid is enzymatically oxidized to allantoin and hydrogen peroxide (HP) which coordinates to Eu_3TC and enhances its luminescence intensity as a result of displacement of water from the inner coordination sphere of the central metal Eu^{3+}. The time-resolved measurement is applied to get larger signal changes than in the steady state measurements of the luminescence. The limit of detection for uric acid is 9.9 µM.

2.1. Introduction

Uricase is an enzyme which catalyzes the degradation of uric acid to allantoin and hydrogen peroxide in the purine metabolism.[1] This enzyme is found in mammals, fungi, plants, yeast and bacteria.[2,3,4,5,6,7] Uric acid, the primary end-product of the purine metabolism, is contained in blood serum and urine.[8] Different disease patterns are responsible for the increase of the uric acid level in biological fluids. These conditions cause gout, Lesch Nyhan syndrome or chronic renal diseases.[1] Numerous optical, electrochemical, amperometric, potentiometric or voltammetric methods are developed for the determination of uric acid. Many methods are based on enzymatic oxidation of uric acid. Uric acid is oxidized to allantoin and hydrogen peroxide under oxygen consumption catalyzed by the enzyme uricase. Hence, uric acid can be determined by measuring (a) the production of

hydrogen peroxide or (b) the consumption of oxygen according to following equation.

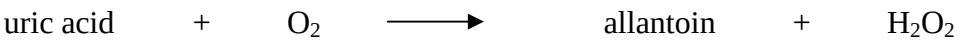

In 1947, Kalckar presented a method where uric acid is directly determined by measurement the absorbance decrease of uric acid at a wavelength of 293 nm at presence of uricase.[9] Fossati and Tamaoku developed colorimetric methods by coupling the uricase reaction with an oxidation of a chromophore catalyzed by peroxidase under hydrogen peroxide consumptions.[10,11] The concentration of uric acid is proportional to the oxidized chromophore which can be detected fluorimetrically or photometrically.

Methods based on the direct determination of hydrogen peroxide are of great importance.[12] Optical hydrogen peroxide indicators are not reversible. Several methods for detection of hydrogen peroxide are given. Onoda et al. developed a simple and rapid method using phosphine-based fluorescent reagents with sodium tungstate dehydrate.[13] The workgroup of Chen designed a spectrometric method using rhodamine B hydrazide as fluorogenetic substrate catalyzed by iron(III)-tetrasulfonatophthalocyanine. The colorless non fluorescent rhodamine B hydrazide is oxidized by hydrogen peroxide to the highly fluorescent rhodamine B.[14] Tahirović et al. prepared a chemiluminescent one-shot sensor for hydrogen peroxide determination. A hydroxyethyl cellulose matrix containing cobalt chloride and sodium lauryl sulphate is fixed on a microscope cover glass where a mixture of luminol, sodium phosphate and the probe is added and therefore chemiluminescence of luminol can be detected.[15] In 1992 Matsubara generated a spectrophotometric method for detection of hydrogen peroxide. A water soluble titanium(IV)-porphyrin complex is used, whose absorbance shows a decrease at 432 nm after addition of hydrogen peroxide.[16] Hydrogen peroxide can be determined with a commercial available detection kit from Molecular Probes. In the presence of horseradish peroxidase hydrogen peroxide and Amplex Red react to resorufin which can be detected spectrophotometrically or fluorometrically.[17] Further on, fluorogenetic reagents like homovanillic acid or p-hydroxyphenylacetic acid undergo dimerization reactions in presence of hydrogen peroxide catalyzed by peroxidase and form strongly fluorescent products. These results can be applied for detection of hydrogen peroxide or the activity of oxidases.[18,19]

Recently the europium(III)-tetracycline 3:1 complex was introduced for the determination of hydrogen peroxide.[20] A stoichiometry of 3:1 is necessary for a sensitive detection. This reversible response in luminescence emission is used for microtiter plate

assays or sensor membranes.[21] This complex is used for detection of hydrogen peroxide, glucose and phosphate or for the determination of enzyme activities based on the production or the consumption of hydrogen peroxide. Fluorescence measurements of the Eu_3TC complex are done by time-resolved fluorescence techniques or by imaging.[12,22,23,24,25]

In this work a microtiter plate assay is developed for determination of uric acid. The principle is based on the enzymatically oxidation of uric acid to allantoin and hydrogen peroxide. Hydrogen peroxide coordinates to the weakly luminescent Eu_3TC complex. The result is a significant increase of its luminescence intensity and lifetime. In *Fig. 1* the mechanism is shown.

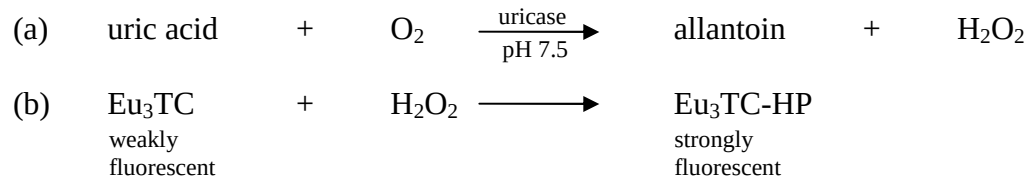

Fig. 1. *(a) Oxidation of uric acid by uricase. (b) Reaction of weakly fluorescent europium(III)-tetracycline (Eu_3TC) with hydrogen peroxide to the strongly fluorescent Eu_3TC-HP.*

2.2. Material and Methods

2.2.1. Instrumentation

Luminescence spectra were acquired on an Aminco Bowman AB2 luminescence spectrometer, as shown in *Fig. 2* (from SLM Spectronic Unicam; www.thermo.com) equipped with a continuous wave 150 W xenon lamp as light source. Luminescence was excited at 398 nm, and emission was detected at 617 nm. Bandpasses were set to 4 nm for excitation and emission.

Fig. 2. *Aminco Bowman AB2 luminescence spectrometer*

Luminescence measurements with microtiter plates were performed on a microwell plate reader GENios+ (from Tecan, www.tecan.com) (see *Fig. 3*). The excitation filter was set to 405 nm and the emission filter to 612 nm, which was the best filter for the emission maximum of Eu_3TC (617 nm). A 30 W quartz halogen lamp was used as light source. Temperature was kept constant at 37 °C by an internal incubator. All experiments were performed in transparent, flat bottom microwell plates (product no. 655101) from Greiner Bio-One (www. greiner.bioone.com).

Fig. 3. *microwell plate reader GENios+ from Tecan*

pH measurements were done with a pH meter CG 842 (from Schott, www.schottinstruments.com), which was calibrated with standard buffers of pH 7.0 and 4.0 (from Roth, Karlsruhe, www.carlroth.de).

2.2.1. Chemicals and Buffers

Europium(III) chloride hexahydrate (99,99%), uricase (EC 1.7.3.3., from Bacillus fastidious lyophylized, 14.6 unit/mg), and uric acid sodium salt were purchased from Sigma (www. sigmaaldrich.com); tetracycline hydrochloride from Serva (www.serva.de); 3-(N-morpholino) propanesulfonate sodium salt (MOPS sodium salt, 98%) from ABCR (www.abcr.de). Hydrogen peroxide was obtained from Merck (www.merck.de). Water was doubly distilled. All used chemicals were of analytical grade and used without further purification.

2.2.2. Preparation of Stock Solutions

MOPS buffer (*solution A*): 3.00 g MOPS sodium salt was dissolved in 990 mL of doubly distilled water, adjusted to pH 7.5 with 72% perchloric acid, and filled up to 1000 mL.

Eu_3TC stock solution (*solution B*): 9.66 mg of Eu_3Cl hexahydrate and 4.22 mg tetracycline hydrochloride were dissolved in 100 mL of *solution A*.

Uric acid (*solution C*): 0.08 mg of uric acid sodium salt was dissolved in 100 mL of *solution A* at a temperature of 90 °C.

Uric acid stock solution (*solution D*): 1.60 mL of solution C was filled up to 25 mL with *solution A*.

Uricase (*solution E*): 0.274 mg was dissolved in 2 mL of *solution A*.

2.2.3. Standard Operational Protocol (SOP) for Uric Acid Assay

For the determination of uric acid in the micromolar range (as found in blood serum) the assay was optimized for the determination in a time range of 20 minutes. A 96-well microtiter plate was filled in rows of four replicates with varying volumes (0-90 µL) of uric acid *solution C*, varying volumes of MOPS buffer *solution A* (30-112.5 µL) and 50 µL of Eu_3TC *solution B*. The mixture was equilibrated for 10 min at 37 °C and then filled up with 30 µL of uricase *solution E*. The overall volume in each well was 200 µL. The mixture was incubated for 10 min at 37 °C and then luminescence intensity was measured. The optical filters of the microtiter plate reader were set to 405 nm for excitation and 612 nm for emission. Luminescence measurements were done in the time-resolved mode with a lag time of 60 µs and an integration time of 100 µs.

2.3. Results

2.3.1. Choice of Indicator and Spectral Characterization of Eu_3TC and Eu_3TC-HP

Previous studies show the detection of tetracycline or ciprofloxacin with europium(III) or terbium (III) ions.[26,27] Tetracycline is an antibiotic with the chemical structure as shown in *Fig. 4*. In this work a complex consisting of the europium (III) ion and the antibiotic tetracycline in the molar ratio 3:1 is used as a probe for detection of hydrogen peroxide.

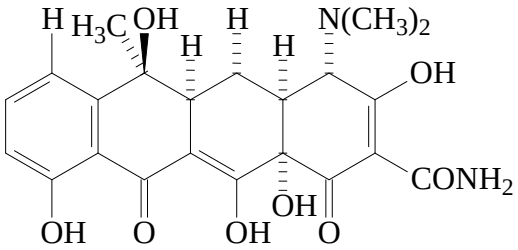

Fig. 4. *Chemical structure of tetracycline*

The probe Eu_3Tc shows a broad excitation spectrum with its maximum around 400 nm (see *Fig. 5*). It can be excited at a wavelength range 390 to 405 nm by using a 405 nm diode laser or a purple LED. The Eu_3Tc complex exhibits several side bands and two main emission bands, located at 585 nm and 617 nm with an intensity ratio 1:7. The luminescence of Eu_3TC is the result of an energy transfer from the antenna ligand tetracycline to the central Eu^{3+} ion like in other lanthanide complexes.[28] The emission of europium (III) complexes in aqueous solutions emanates from the nondegenerate $^5D_0$ level. The strongest emissions are observed in the $^5D_0 \rightarrow {}^7F_1$ and $^7F_2$ transition regions.[29] The excitation and emission spectrum of Eu_3TC is shown in *Figure 5*. Hydrogen peroxide (*spectrum B, C, D*) cause the intensity of the emission at 617 nm increased by a factor of more than 5 compared with Eu_3TC *(spectrum A)*. Most probably HP displaces strong quenching water molecules which are coordinated to the 8^{th} or 9^{th} coordination site of Eu^{3+}. This effect can be applied for determination of HP and consequently for the determination of uric acid. In literature it is reported that HP can be detected in the linear concentration range from 2 to 400 µM of HP.[25]

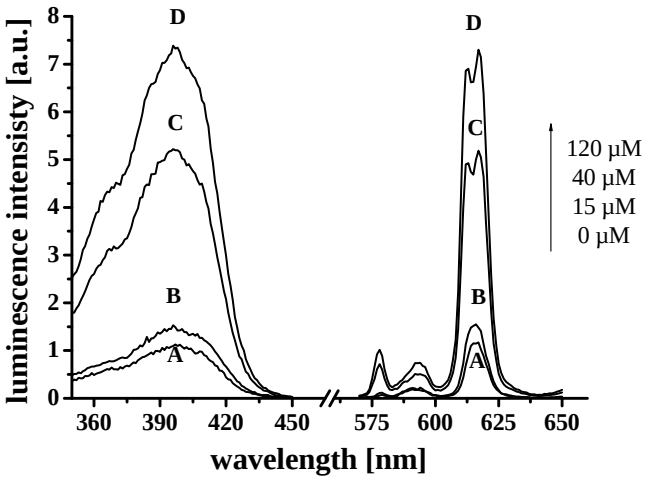

Fig. 5. *Excitation (left) and emission (right) spectra of Eu_3TC and Eu_3TC-HP (A) 66 µM Eu^{3+} and 22 µM tetracycline. (B-D) Eu_3TC in the presence of hydrogen peroxide in the concentration range 15 to 120 µM after 15 minutes.*

2.3.2. Assay Principle

The fluorescent probe Eu_3TC is used for determination of uric acid. The principle of the assay is based on the oxidation of uric acid by the enzyme uricase to allantoin and hydrogen peroxide. Subsequently the released hydrogen peroxide coordinates to the weakly fluorescent Eu_3TC complex under formation of the strongly fluorescent Eu_3TC-HP complex according to *Fig. 1*. The excitation and emission spectra of Eu_3TC and Eu_3TC-HP are shown in *Fig. 5*. In *Fig. 6* the excitation and emission spectra of Eu_3TC, Eu_3TC-uricase and Eu_3TC-HP (HP released by enzymatically catalyzed oxidation of uric acid) are given where the enzyme uricase enhances the luminescence intensity of Eu_3TC only slightly. HP released by enzymatically catalyzed oxidation of UA enhances the luminescence intensity of Eu_3TC by a factor of 4. These results are again clarified in *Fig. 7*.

For the performance of the assay, various concentrations of uric acid to Eu_3TC have to be mixed and equilibrated. After addition of uricase to the mixture the complexation of released HP to Eu_3TC takes place. The kinetic response of the system uricase/Eu_3TC in correlation with increasing concentrations of uric acid is shown in *Fig. 7*. Higher concentrations of uric acid increase the production of HP and cause an increase of the luminescence intensity due to formation of the Eu_3TC-HP complex. UA can be detected after 20 minutes or by the endpoint method (approximately 60 minutes). Uric acid in the concentration range from 0 to 120 µM has no effect on the fluorescence intensity of Eu_3TC. Higher concentrations show a strong quenching effect of Eu_3TC.

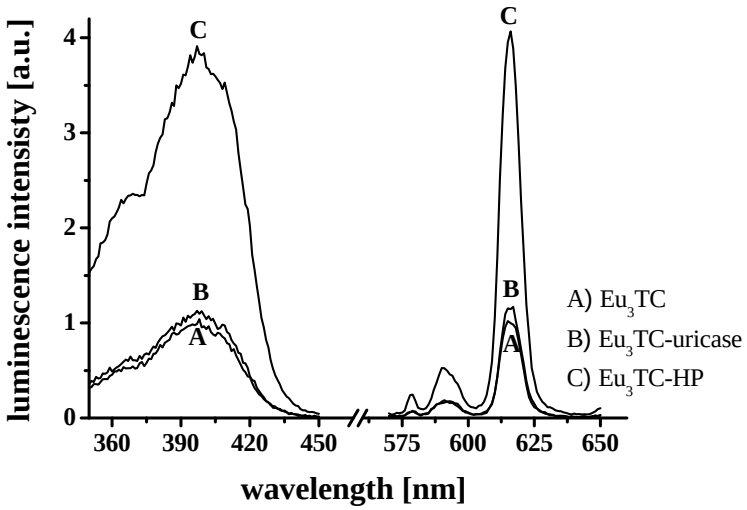

Fig. 6. *Excitation (left) and emission (right) spectra of Eu_3TC, Eu_3TC-uricase, and Eu_3TC-HP (HP released from UA by uricase) (A) Eu_3TC; (B) Eu_3TC-uricase; and (C) Eu_3TC-HP (HP released from UA by uricase); All measurements are done at 37 °C, pH 7.5, and luminescence was measured after 20 min; c_{Eu}^{3+}: 66 µM; c_{TC}: 22 µM; uricase: 0.3 unit/mL; UA: 120 µM.*

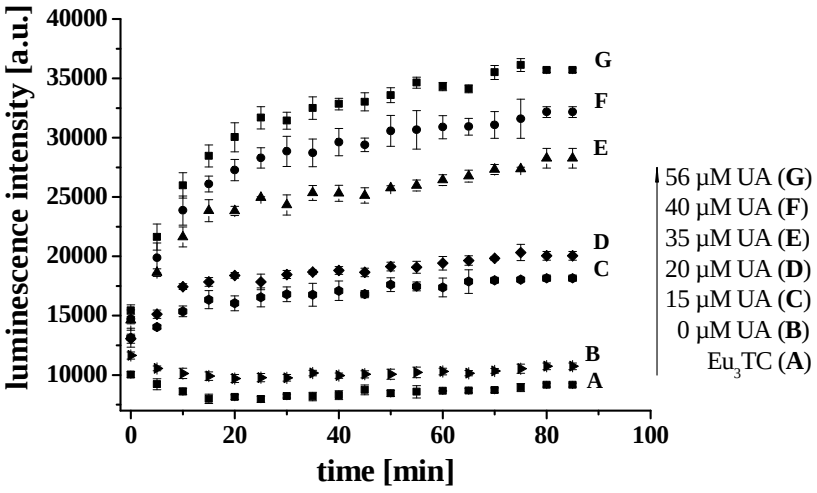

Fig. 7. *Time trace of luminescence intensity. (A) Eu_3TC, (B) Eu_3TC-uricase, (C-D) Eu_3TC-HP (HP released from UA in the concentration range from 0 to 56 µM by uricase); c_{Eu}^{3+}: 66 µM; c_{TC}: 22 µM; uricase: 0.3 unit/mL; Measurements were performed at 37 °C and pH 7.5.*

2.3.3. Effect of pH, and Temperature

Uricase exhibits its maximum activity at a pH of 9.1.[30] That is why measurements at pH lower than 7.5 are not useful. For pH higher than 9 the measurement cannot be performed due to the instability of the Eu_3TC complex. Therefore, the effect of pH was studied for the complex Eu_3TC-HP (HP was released from uric acid by uricase) in the pH range from 7.5 to 8.8 at 37 °C. The luminescence maximum was found at pH 8.5 whereas in literature is reported the luminescence maximum for Eu_3TC-HP is found at pH 6.9.[31] The reason for the optimum pH at 8.5 is the interaction of the uricase activity with pH. At pH 6.9 the uricase activity is very low which results in slight HP release. For all measurements a pH of 7.5 was chosen. This represents approximately the real pH of urine or blood serum and in addition the intense of the luminescence of Eu_3TC is strong enough at this pH. A temperature of 37 °C was applied for all measurements because best results were achieved at that temperature compared to 25 °C and 30 °C. The best assay conditions were at 37 °C and pH 7.5. For activation of the enzyme no other substances like Mg^{2+} ions are required.

2.3.4. Luminescence Decay Times and Time-Resolved Detection

Lanthanide derived complexes show very long luminescence decay times, and the Eu_3TC complex has a triple exponential decay profile. The respective decay times of Eu_3TC are 8.7 µs (relative amplitude 58%), 30.4 µs (40%), and 174 µs (2%).[20] Eu_3TC-HP shows two main components with 13.2 µs (34%) and 59.4 µs (64%). The third component shows a decay time of 158 µs with the relative amplitude of 2%. Based on these facts the best time-resolved measurements were performed at lag times of 30 µs in order to detect the main component (59.4 µs) of the Eu_3TC-HP complex.

The application of time-resolved measurements have the advantage that background luminescence such as intrinsic fluorescence of proteins, cuvettes or microtiter plates, which is in the nanosecond range, can be eliminated.[12] For the gated microtiter plate assay the lag and the integration time were optimized. The lag time was varied from 40 to 80 µs. Best results were achieved with a lag time of 60 µs which gives good signal to noise ratio. The variation of the integration time from 40 to 100 µs has no effect. An integration time of 100 µs was chosen for all further measurements.

2.3.5. Effect of Uricase Activity

For performance of the uric acid assay an optimum uricase concentration is required. In this work the assay was performed applying different uricase activities in the range from 0 to 10 unit/mL. The application of uricase with an activity of 5 to 10 unit/mL shows no satisfying results. High uricase concentrations strongly enhance the luminescence intensity of Eu_3TC and the separation of the single signals towards different uric acid concentrations cannot be done. High uricase amounts are favourably because of faster reaction rates. Best results are achieved with uricase activities in the range from 0.1 to 1 unit/mL. *Fig. 8* shows the kinetic response of the system Eu_3TC-uricase-uric acid. Eu_3TC was incubated at 37 °C in presence of varying UA concentrations and subsequently uricase (0.3 units/mL) was added. The oxidation of uric acid catalyzed by uricase was started and the formation of the Eu_3TC-HP complex was detected fluorimetrically by an increase of the luminescence of Eu_3TC. After 20 minutes the resulting fluorimetrically intensities of the formed Eu_3TC-HP complexes can be clearly assigned to varying uric acid concentrations, and UA can be determined after this time. By applying the endpoint method lower uric acid concentrations can be detected. The endpoint of the formation of the Eu_3TC-HP complexes is obtained after 60 minutes since the luminescence signal is stable.

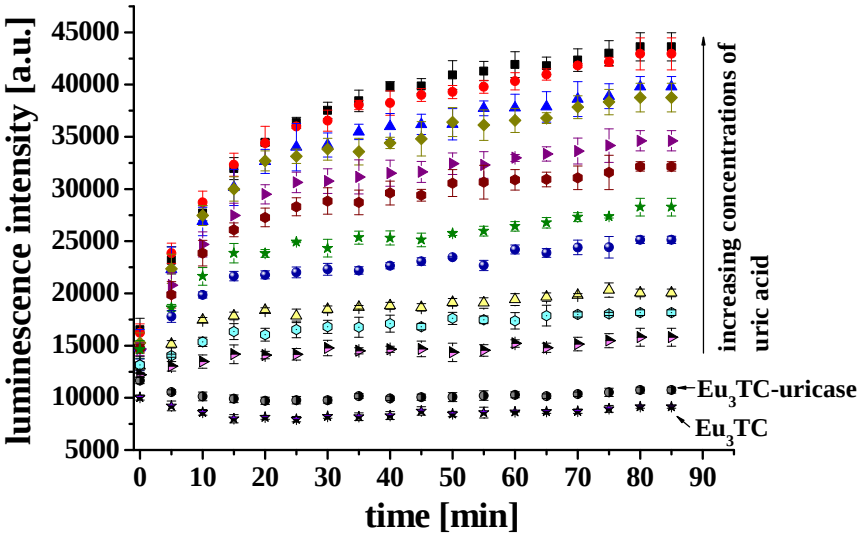

Fig. 8. *Kinetic response of the Eu_3TC-uricase system to increasing concentrations of uric acid in the micromolar range (0 to 120 µM). Experimental conditions: uricase 0.3 unit/mL, c_{Eu}^{3+}: 66 µM, c_{TC}: 22 µM.*

2.3.6. Calibration Plot

The calibration plots for the time-resolved uric acid assays are shown in *Fig. 9 (A, B)*. The assays were carried out under optimized experimental conditions as described in the experimental part *2.2.4*. *Fig. 9A* shows the calibration plot for the determination of UA after 20 minutes and *Fig. 9B* the endpoint method for UA detection after 60 minutes. The linear range for both methods is from 0 to 35 µM and can be fitted by the equation y = 1.014 + 0.041 x (R = 0.996, n = 3 for each point; after 20 minutes) and y = 1.004 + 0.046 x (R = 0.993, n = 3 for each point; after 60 minutes). For both methods y is defined as I/I_0, where I is the luminescence intensity after 20 or 60 minutes, I_0 is the blank (Eu_3TC-uricase) and x is the concentration of UA. The limit of detection at a signal to noise ratio of 3 is 9.9 µM for the determination after 20 minutes and 7.0 µM for the endpoint method.

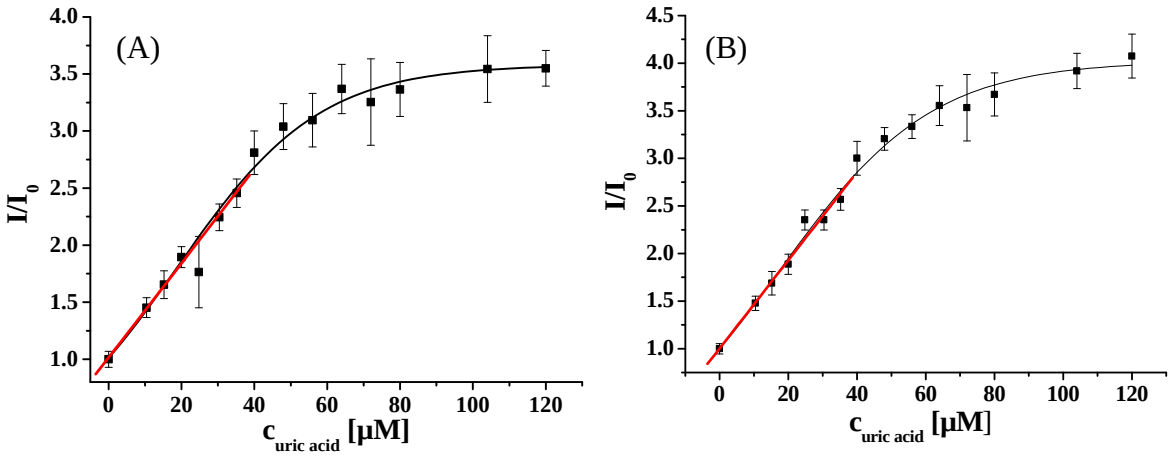

Fig. 9. *Calibration plots for UA determination by the gated mode. (A) determination after 20 minutes; (B) endpoint method; uricase: 0.3 unit/mL, c_{Eu}^{3+}: 66 µM, c_{TC}: 22 µM.*

2.3.7. Interferences and Application to Urine Samples

Interferences can affect the luminescence of the probe Eu_3TC seriously. The components of urine as urea, creatinine, human serum albumine (HSA), alkali- and earth alkali ions, and anions were applied for testing the effect on the luminescence of Eu_3TC. In urine the concentration of the present ions is in the millimolare range. Eu_3TC was separately exposed towards all named interferences where the luminescence of Eu_3TC was observed in presence and in absence of the interferences. Creatinine in the concentration range from 0 to 35 mg/mL enhances the luminescence of Eu_3TC whereas in the range from 1.2 to 3.0 mg/mL the luminescence is quenched. Urea has an enhancing effect on the luminescence of Eu_3TC.

The alkali ions Na^+ and K^+ show no effect in the concentration range up to 100 mM, but show an increasing effect for higher concentrations. The earth alkali ion Ca^{2+} enhances slightly the luminescence of Eu_3TC in the concentration range up to 10 mM and Mg^{2+} in the range up to 15 mM. The anions chloride and sulphate have no effect but phosphate enhances the luminescence of Eu_3TC already strongly in the micromolar range. The presence of low amounts of HSA shows always an enhancing effect. Same results were achieved for the system Eu_3TC-HP but phosphate decreases the luminescence of Eu_3TC-HP strongly.

The developed assay was applied for the determination of UA in urine. For minimizing the effect of proteins the urine samples were heated up to 100 °C. After cooling down to room temperature they were filtered by a syringe filter for removing denaturated proteins. The filtrate was diluted in order to minimize the effect of the sample matrix and applied to the microtiter plate assay. The obtained results were not satisfactory because the luminescence of Eu_3TC was continuously decreasing instead of increasing (see *Fig. 10A*). In *Fig. 10A* the time trace of Eu_3TC, Eu_3TC-urine as well as Eu_3TC-urine-uricase is shown. The luminescence of Eu_3TC is stable. In presence of urine the luminescence of Eu_3TC is enhanced and in presence of urine and uricase a continuously decrease is given where generally the luminescence has to be increased due to the release of HP during the oxidation of UA catalyzed by uricase. The system urine-uricase was verified for working. Here the absorption of UA was detected at a wavelength of 293 nm after addition of uricase. *Fig. 10B* shows the decrease of absorbance of uric acid which confirms the system urine-uricase works. Phosphate is the only interference which affects the luminescence of Eu_3TC-HP strongly. Hence, we assume the presence of phosphate in the sample matrix affects the assay strongly.

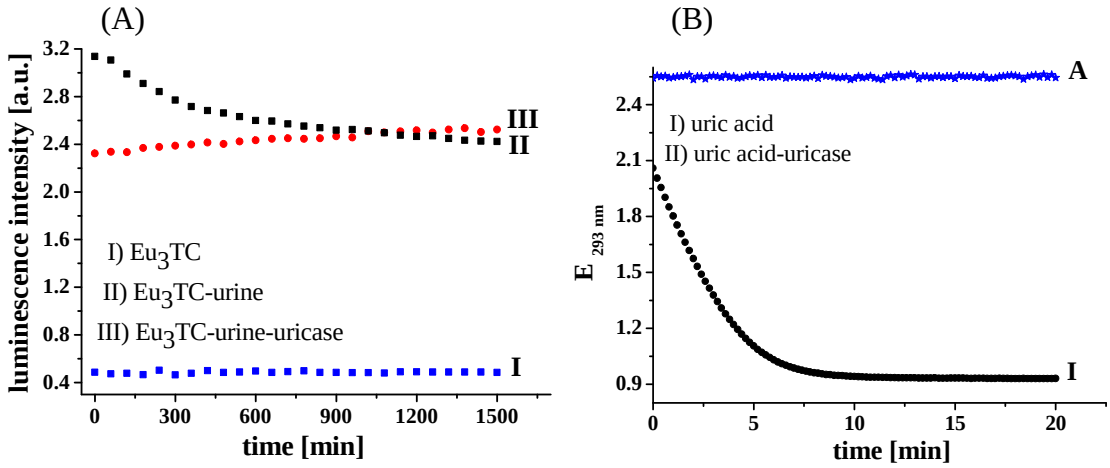

***Fig. 10A** and **B**. (A) Time trace of luminescence intensity of Eu_3TC (I), Eu_3TC-urine (II) and Eu_3TC-urine-uricase (III). (B) Time trace of absorbance at 293 nm for UA (I) and UA-uricase (II).*

2.4. Discussion

Various methods for the determination of uric acid are developed. It is necessary to distinguish between optical or electrochemical methods. Most of them are based on voltammetry, potentiometry or amperometry.[8,32,33,34] As described in *chapter 2.1* most of the methods are based on the enzymatic oxidation of uric acid which can be detected by measuring the production of hydrogen peroxide or by consumption of oxygen during the oxidation process. In this work an assay for uric acid determination is developed based on the detection of hydrogen peroxide produced, therefore the luminescent probe Eu_3TC was chosen. Nowadays lanthanide complexes are often used as fluorescent probes. In the early nineties Evangelista developed a new method called EALL (enzyme-amplified lanthanide luminescence) for enzyme detection in bioanalytical assays.[35] Another application is the synthesis of novel lanthanide sensor molecules for detecting Zn^{2+}.[36] Further on, it was reported on a norfloxacin-terbium complex for the spectrofluorimetrically detection of nicotinamide adenine dinucleotide phosphate (NADP).[37] Lanthanide complexes feature perfect spectroscopic properties for biological applications.[36] They show long luminescence lifetimes up to the millisecond range, a large Stokes´ shift of more than 200 nm, a longwave excitation maximum at ~ 400 nm and high water solubility.[36] The complex Eu_3TC used in this work exhibits all these properties. As a result of the long lifetime of this complex time-resolved measurements can be performed and therefore disturbing background signals can be eliminated.

In previous studies, EuTC in the molar ratio 1:1, was used as an indicator for phosphate and Cu (II).[38,39] In the stoichiometric ratio 3:1 of Eu/TC numerous applications for detection of hydrogen peroxide are published.[25,40,41] We propose for the luminescence enhancement of Eu_3TC in presence of hydrogen peroxide, a water ligand, which exerts a quenching effect, will be replaced by hydrogen peroxide. The binding of the HP ligand causes a structural rearrangement of the Eu_3TC complex in solution, so that the TC ligands come closer to the Eu^{3+} ion. Hence, more energy can be transferred from the ligand to the metal ion. This indicates an increase of the luminescence intensity and lifetime.[20] The luminescence of the Eu_3TC complex is strongly dependent from temperature, which has to be kept constant at 37 °C. Consequently, europium complexes can be applied as temperature probes.[42]

Table 1 gives an overview of known optical methods. All listed methods cannot detect hydrogen peroxide directly compared to electrochemical methods. [10,43,44,45,46] The presence of an additional enzyme peroxidase is required in order to convert the non fluorescent substrates in fluorescent products.[10,43,44,45] UA can be directly determined by few methods which are

based on chromatography or on enhancement of the chemiluminescence intensity of the complex luminol-hexacyanoferrate(III)-hexacyanoferrate(II) in the presence of cetyltrimethylammonium bromide and UA.[47,48,49] In the late eighties a nonenzymatic stopped-flow fluorimetric method for direct determination of uric acid was developed. This method is based on the fluorescent reaction between UA and 1,1,3-tricyano-2-amino-1-propene in the presence of hydrogen peroxide.[46] A great instrumental effort compared to the method developed in this work is required.

Compared to all methods given in *table 1* the new developed assay is the first one which is applicable to time-resolved fluorescence detection at pH 7.5. The benefit of the new method is that excitation of Eu_3TC can be carried out in the range of visible light compared to the fluorimetric methods based on the usage of thyramine, L-tyrosine, homovanillic acid and TRIAP.[44,45,46] The generated fluorescent products have their excitation maximum in the range from 315 to 360 nm. Excitation in the UV causes a strong background fluorescence of cuvettes, microtiter plates and the sample itself.

The incubation time of the system Eu_3TC-uric acid and uricase is in the same time range as most of the other methods except the spectrophotometric methods using Amplex Red, 3,5-dichloro-2-hydroxybenzensulfonic acid and 4-aminophenanzone.[10,43,44,45] All these analytical methods require a working pH between 7.0 and 7.5 except the methods using homovanillic acid or the fluorimetric stopped–flow method.[45,46] All methods have a broad analytical range except the fluorimetric-stopped method with a limit of detection of 0.2 µM. In this work uric acid can be developed in microtiter plates applying endpoints methods after a time of 20 or 60 minutes, but in view of developing a fast and simple method the determination of UA after 20 minutes is the best choice.

In this work a new method for determination of uric acid was developed. The application of Eu_3TC offers several advantages: On the one hand a very easy preparation of the Eu_3TC complex (only 2 commercial available reagents have to be mixed), on the other hand the large Stokes´ shift, the differences in the average decay time of the Eu_3TC complex (~ 30 µs) and Eu_3TC-HP complex (~ 60 µs) and the application to gated measurements at the working pH 7.5. Generally, all these advantages can make this assay as an alternative tool in biotechnology or diagnosis. The determination of UA in urine did not work well enough but possibly the quantitative elimination of phosphate in the urine sample avoid the effect of the luminescence decreasing of Eu_3TC-HP.

Table 1. *Overview of selected assays for determination of uric acid*

Reagent	Structure	LOD/ µM	Linear Range/ µM	Remarks	Ref
Amplex Red and POx		100 nM	-	Absorbance measured at 560 nm; fluorescence measured at exc/em at wavelengths of 530-560 nm/ ~ 590 nm; incubation time 30 min or longer at 37 °C; pH 7.5	43
3-methyl-benzothiazoline-2-one (MBTH) and 3-dimethylaminobenzoic acid (DMAB) and POx	**MTBH** **DMAB**	-	119-1785	Absorbance measured at 590 nm; incubation time 20 min at 37 °C; pH 7.5; peroxidase	44
Tyramine and POx		-	60-715	Fluorescence measured at exc/em at wavelengths of 315 nm/ 405 nm; incubation time 20 min at 37 °C; pH 7.2	44
L-Tyrosine		-	60-715	Fluorescence measured at exc/em at wavelengths of 315 nm/ 405 nm; incubation time 20 min at 37 °C; pH 7.2	44

3,5-dichloro-2-hydroxybenzenesulfonic acid (I) and 4-aminophenanzone (II) and POx	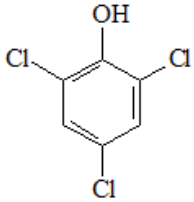 **(I)** 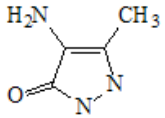 **(II)**	-	0-1500	Absorbance measured at 520 nm; incubation time 15 min at room temperature; pH 7.0.	10
Homovanillic acid and POx	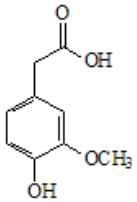	-	0-900	Fluorescence measured at exc/em at wavelengths of 315 nm/ 425nm; incubation time 20 min at 25°C; pH 9.0.	45
1,1,3-tricyano-2-amino-1-propene (TRIAP)	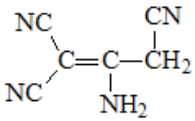	0.2	0.5-18	Fluorescence measured at exc/em at wavelengths of 360 nm/ 430nm; reaction temperature 40°C; pH 9.2; stopped flow method.	46
Eu_3TC	-	9.9	0-35	Time-resolved fluorescence method; fluorescence measured at exc/em 398 nm/ 612nm; fluorescence detection after 20 min at 37°C; pH 7.5.	this work

2.5. References

[1] Huang S. H., Shih Y. C., Wu C. Y., Yuan C. J., Yang Y. S., Li Y. K., Wu T. K., **Detection of serum uric acid using the optical polymeric enzyme biochip system** 2004. Biosens. Bioelectron. 19, 1627-1633

[2] Keilin J., **The biological significance of uric acid and guanine excretion** 1959. Biol. Revs. 34, 265-296

[3] Wallrath L. L., Friedman T. B., **Species differences in the temporal pattern of Drosophila urate oxidase gene expression are attributed to trans-acting regulatory changes** 1991. Proc. Natl. Acad. Sci. U.S.A. 88, 5489-5493

[4] Montalbini P., Aguilar M., Pineda M., **Isolation and characterization of uricase from bean leaves and its comparison with uredospore enzymes** 1999. Plant Sci. 147, 139-147

[5] Montalbini P., Redondo J., Caballero J. L., Cardenas J. Pineda M., **Uricase from leaves. Its purification and characterization from three different higher plants** 1997. Planta 202, 277-283

[6] Yuichi H., Tetsuhiko S., Hajime I., **Cloning, sequence analysis and expression in Escherichia coli of the gene encoding a uricase from the yeast-like symbiont of the brown planthopper, Nilaparvata lugens** 2000. Insect. Biochem. Mol. Biol. 30, 173-182.

[7] Yamamoto K., Kojima Y. Kikuchi T., Shigyo T., Sugihara K., Takashio M., Emi S., **Nucleotide sequence of the uricase gene from *Bacillus* sp. TB-90** 1996. J. Biochem. 119, 80-84

[8] Wang Z., Wang Y., Luo G., **A selective voltammetric method for uric acid detection at β-cyclodextrin modified electrode incorporating carbon nanotubes** 2002. Analyst 127, 1353-1358

[9] Kalckar H. M., Shafran M., **Differential spectrophotometry of purine compounds by means of specific enzymes. I. Determination of hydroxypurine compounds** 1947. J. Biol. Chem. 167, 429-443

[10] Fossati P., Prencipe L., Berti G., **Use of 3,5-dichloro-2-hydroxybenzenesulfonic acid/4-aminophenazone chromogenic system in direct enzymatic assay of uric acid in serum and urine** 1980., Clin. Chem. 26, 227-231

[11] Tamaoku K., Ueno K., Akiura K., Ohkura Y., **New water-soluble hydrogen donors for the enzymatic photometric determination of hydrogen peroxide. II. N-ethyl-**

N-(2-hydroxy-3-sulfopropyl) aniline derivatives 1982. Chem. Pharm. Bull. 30, 2492-2497

[12] Wu M., Lin Z. Duerkop A., Wolfbeis O. S., **Time-resolved enzymatic determination of glucose using a fluorescent europium probe for hydrogen peroxide** 2004. Anal. Bioanal. Chem. 380, 619-626

[13] Onoda M., Uchiyama T., Mawatari K. I., Kaneko K., Nakagomi K., **Simple and rapid determination of hydrogen peroxide using phosphine-based fluorescent reagents with sodium tungstate dihydrate** 2006. Anal. Sci. 22, 815-817

[14] Chen X., Zou J., **Application of rhodamine B hydrazide as a new fluorogenic indicator in the highly sensitive determination of hydrogen peroxide and glucose based on the catalytic effect of iron(III)-tetrasulfonatophthalocyanine** 2007. Microchim. Acta 157, 133-138

[15] Tahirović A., Čopra A., Omanović-Mikličanin E., Kalcher K., **A chemiluminescence sensor for the determination of hydrogen peroxide** 2007. Talanta 72, 1378-1385

[16] Matsubara C., Kawamoto N., Takamura K., **Oxo[5,10,15,20-tetra(4-pyridyl)porphyrinato]titanium(IV): an ultrahigh-sensitive spectrophotometric reagent for hydrogen peroxide** 1992. Analyst 117, 1781-1784

[17] Haugland R. P., 2002. **Handbook of Molecular Probes** 9th ed., 440-442

[18] Guilbault G. G., Brignac P., Zimmer M., **Homovanillic acid as a fluorometric substrate for oxidative enzymes. Analytical applications of the peroxidase, glucose oxidase, and xanthine oxidase systems** 1968. Anal Chem. 40, 190-196

[19] Guilbault G. G., Brignac P. J., Juneau M., **New substrates for the fluorometric determination of oxidative enzymes** 1968. Anal Chem. 40, 1256-1263

[20] Wolfbeis O. S., Duerkop A., Wu M., Lin Z., **A Europium-ion-based luminescent sensing probe for hydrogen peroxide** 2002. Angew. Chem. Int. Ed. 41, 4495-4498

[21] Wolfbeis O. S., Schaeferling M., Duerkop A., **Reversible optical sensor membrane for hydrogen peroxide using an immobilized fluorescent probe, and its application to a glucose biosensor** 2003. Microchim. Acta 143, 221-227

[22] Schrenkhammer P., Rosnizeck I. C., Duerkop A., Wolfbeis O. S., Schaeferling M., **Time-resolved fluorescence-based assay for the determination of alkaline phosphatase activity and application to the screening of its inhibitors** 2008. J. Biomol. Screening 13, 9-16

[23] Wu M., Lin Z., Schaeferling M., Duerkop A., Wolfbeis O. S., **Fluorescence imaging of the activity of glucose oxidase using a hydrogen-peroxide-sensitive europium probe** 2005. Anal. Biochem. 340, 66-73

[24] Lin. Z., **Time-resolved fluorescence-based europium-derived probes for peroxidase bioassays, citrate cycle imaging and chirality sensing** 2004. Dissertation

[25] Duerkop A., Wolfbeis O. S., **Nonenzymatic direct assay of hydrogen peroxide at neutral pH using the Eu_3Tc fluorescent probe** 2005. J. Fluoresc. 15, 755-761

[26] Rodríguez-Díaz R. C., Aguilar-Caballos M. P., Gómez-Hens A., **Simultaneous determination of ciprofloxacin and tetracycline in biological fluids based on dual-lanthanide sensitised luminescence using dry reagent chemical technology** 2003. Anal. Chim. Acta 494, 55-62

[27] Hirschy L. M., Dose E. V., Winefordner J. D., **Lanthanide-sensitized luminescence for the detection of tetracyclines** 1983. Anal. Chim. Acta 147, 311-316

[28] Courrol L. C., de Oliveira S. F. R., Gomes L., Vieira Júnior N. D., **Energy transfer study of europium-tetracycline complexes** 2007. J. Luminescence. 122-123, 288-290

[29] Richardson F. S., **Terbium(III) and europium(III) ions as luminescent probes and stains for biomolecular systems** 1982. Chem. Rev. 82, 541-552

[30] http://www.sigmaaldrich.com/catalog/search/ProductDetail/FLUKA/94310

[31] Wu M., **Time-resolved quantitative assays and imaging of enzymes and enzyme substrates using a new europium fluorescent probe for hydrogen peroxide** 2003. Dissertation, 29-30

[32] Matos R. C., Augelli M. A., Lago C. L., Angnes L., **Flow injection analysis-amperometric determination of ascorbic and uric acids in urine using arrays of gold microelectrodes modified by electrodeposition of palladium** 2000. Anal. Chim. Acta 404, 151-157

[33] Khoo S. B., Chen F., **Studies of sol-gel ceramic film incorporating methylene blue on glassy carbon: an electrocatalytic system for the simultaneous determination of ascorbic and uric acids** 2002. Anal. Chem. 74, 5734-5741

[34] Kamel A. H., **Conventional and planar chip sensors for potentiometric assay of uric acid in biological fluids using flow injection analysis** 2007. J. Pharm. Biomed. Anal. 45, 341-348

[35] Evangelista R. A., Pollak A., Templeton A., Gudgin E., F., **Enzyme-amplified lanthanide luminescence for enzyme detection in bioanalytical assays** 1991. Anal. Biochem. 197, 213-224

[36] Hanaoka K., Kikuchi K., Kojima H., Urano Y., Nagano T., **Development of a zinc ion-selective luminescent lanthanide chemosensor for biological applications** 2004. J. Am. Chem. Soc. 126, 12470-12476

[37] Wang Y., Liu J., Jiang C., **Spectrofluorimetric determination of trace amounts of coenzyme II using norfloxacin-terbium complex as a fluorescent probe** 2005. Anal. Sciences 21, 709-711

[38] Cano-Raya C., Ramos M. D. F., Vallvey L. F. C., Wolfbeis O. S., Schaeferling M., **Fluorescence quenching of the europium tetracycline hydrogen peroxide complex by copper (II) and other metal ions** 2005. Applied Spec. 59, 1209-1216

[39] Duerkop A., Turel M., Lobnik A., Wolfbeis O. S., **Microtiter plate assay for phosphate using a europium-tetracycline complex as a sensitive luminescent probe** 2006. Anal. Chim. Acta 555, 292-298

[40] Lin Z., Wu M., Wolfbeis O. S., Schaeferling M., **A novel method for time-resolved fluorimetric determination and imaging of the activity of peroxidase, and its application to an enzyme-linked immunosorbent assay** 2006. Chem Eur. J. 12, 2730-2738

[41] Wu M., Lin Z., Wolfbeis O. S., **Determination of the Activity of Catalase Using a Europium(III)-Tetracycline-Derived Fluorescent Substrate** 2003. Anal. Biochem. 320, 129-135

[42] Borisov S. M., Wolfbeis O. S., **Temperature-sensitive europium(III) probes and their use for simultaneous luminescent sensing of temperature and oxygen** 2006. Anal. Chem. 78, 5094-5101

[43] **http://probes.invitrogen.com/media/pis/mp22181.pdf**

[44] Kovar K. A., El Bolkiny M. N., Rink R., Abdel Hamid M., **An enzymatic asaay for the colorimetric and fluorimetric determination of uric acid in sera** 1990. Arch. Pharm. 323, 235-237

[45] Kuan J. C. W., Kuan S. S., Guilbault G. G., **An alternative method for the determination of uric acid in serum** 1975. Clin. Chim. Acta 64, 19-25

[46] Perez-Bendito D., Gómes-Hens A., Gutiérrez M. C., Antón S., **Nonenzymatic stopped-flow fluorimetric method for direct determination of uric acid in serum and urine** 1989. Clin. Chem. 35, 230-233

[47] Ingebretsen O. C., Borgen J., Farstad M., **Uric acid determinations: reversed-phase liquid chromatography with ultraviolet detection compared with kinetic and equilibrium adaptations of the uricase method** 1982. Clin. Chem. 28, 496-498

[48] Jen J. F., Hsiao S. L., Liu K. H., **Simultaneous determination of uric acid and creatinine in urine by an eco-friendly solvent-free high performance liquid chromatographic method** 2002. Talanta 58, 711-717

[49] Han S., Liu E., Li H., **Cetyltrimethylammonium bromide-enhanced chemiluminescence determination of uric acid using a luminol-hexacyanoferrate(III)-hexacyanoferrate(II) system** 2005. Anal. Sciences 21, 111-114

Chapter 3

Fully Reversible Uric Acid Biosensors Using Oxygen Transduction

An optical biosensor is presented for continuous determination of uric acid. The scheme is based on the measurement of the consumption of oxygen during the oxidation of uric acid that is catalyzed by the enzyme uricase. The enzyme is immobilized in a polyurethane hydrogel next to a probe whose luminescence is quenched by oxygen. Specifically, the metal organic probes ruthenium(II) tris(4,7-diphenyl-1,10-phenanthroline) or iridium(III) tris(2-phenylpyridine) were immobilized in an organically modified sol-gel. The consumption of oxygen as a result of the oxidation, catalyzed by the enzyme, was followed by measurement of changes of luminescence intensity or lifetime. Measurements were performed in a flow-through cell using air-saturated standard solutions of uric acid. Analytical ranges (0 to 2 mM), the response times (80 - 100 s), reproducibility and long term stability were investigated.

3.1. Introduction

The determination of uric acid (UA) plays an important role in clinical medicine. Uric acid (2,6,8-trihydroxypurine) is the end-product of the purine metabolism and is excreted by the kidneys and intestinal tract. The concentration of uric acid in urine of healthy humans is in the millimolar range whereas in blood serum it is in the micromolar range. Abnormally high concentrations of uric acid are symptoms of diseases like gout, hyperuricaemia and the Lesch-Nyhan syndrome.[1] Hence, several methods have been developed for the determination of uric acid. Many of them are based on enzymatic oxidation via the enzyme uricase which catalyzes the oxidation of uric acid to give allantoin and hydrogen peroxide (H_2O_2) according to the

following equation:

$$\text{uric acid} + O_2 \xrightarrow{\text{uricase}} \text{allantoin} + H_2O_2 \quad (1)$$

Uric acid can be determined by measurement of (a) the production of hydrogen peroxide, (b) the consumption of oxygen, or (c) the decrease in the absorbance of uric acid at 293 nm (where allantoin does not absorb). The common method for determination of UA is the uricase method which can be classified in the four types the direct equilibrium, the indirect equilibrium, the indirect kinetic, and the direct kinetic uricase methods. The application of the direct equilibrium or kinetic method for UA determination measures the decrease in absorbance of UA at 293 nm. The application of the indirect equilibrium or kinetic method quantifies the amount of H_2O_2 which is produced after completion of the uricase catalyzed oxidation. The various methods for determination of uric acid, and the potentially adverse effects of other xanthines on the precision of the methods due to various kinds of enzyme inhibition have been reviewed by Zhao et al..[2]

Numerous colorimetric methods have been developed for the determination of UA in biological samples like urine or serum by coupling the uricase reaction to a chromogenic product that is catalyzed by peroxidase and involving H_2O_2 as the oxidant.[3,4,5] The concentration of UA is proportional to the quantity of the chromophore formed. Based on this approach, an irreversible detection kit has been developed for fluorimetric and spectrophotometric assays.[6] Horseradish peroxidase assists in the oxidation of Amplex Red by H_2O_2 to give the red fluorescent resorufin. Other methods for the determination of UA are based on voltammetry, amperometry, capillary electrophoresis, or high performance liquid chromatography coupled to the detection by either UV absorbance or mass spectroscopy.

Electrochemical methods usually are reversible, whilst photometric or fluorimetric methods based on formation of a chromogenic or fluorescent product or not. Chu et al. have developed a method that is based on miniaturized capillary electrophoresis with amperometric detection.[7] The group of He has determined UA in the concentration range from 1 to 50 µM uric acid in the presence of ascorbic acid with a quercetin-modified wax-impregnated graphite electrode.[1] The voltammetric detection of UA can be carried out with a glassy carbon electrode modified with fullerene-C60. Determination of UA is enabled in the presence of ascorbic acid because the overlapping voltammetric responses of UA and ascorbic acid can be resolved into two well-defined voltammetric peaks.[8] An irreversible fiber optic biosensor for UA was made by immobilizing uricase and horseradish peroxidase to bovine albumin via glutaraldehyde.[9,10] Determination of UA is accomplished by measuring the hydrogen peroxide

produced. Using thiamine as non fluorescent substrate that is oxidized to a fluorescent product in presence of peroxidase and hydrogen peroxide.

Here we describe a sensitive, selective and fully reversible sensing scheme for UA in human blood serum. It is based on a single enzyme/probe sensing layer and exploits the consumption of oxygen as outlined in *scheme 1*.

3.2. Materials and Methods

3.2.1. Materials

Uricase (EC 1.7.3.3), from *Candida sp.* (recombinant, expressed in *Escherichia coli*, lyophilized powder ≥2 units/mg protein), uric acid, ruthenium(III) chloride hydrate, glutaraldehyde (50 wt % in H_2O) and 3-(trimethylsilyl)-1-propanesulfonic acid sodium salt (purity 97 %) were purchased from Sigma Aldrich (Steinheim, Germany; www.sigmaaldrich.com), 3-(N-morpholino) propanesulfonate sodium salt (MOPS sodium salt, 98 %) from ABCR (Karlsruhe, Germany; www.abcr.de), and the tris(2-phenylpyridyl) iridium(III) complex from Sensient Imaging Technologies GmbH (Wolfen, Germany; www.sensient-tech.com). The polyurethane hydrogel Hydromed D4 was obtained from Cardiotech (Wilmington, USA; www.cardiotech-inc.com), and the polyester support (Mylar) (product number 124-098-60) from Goodfellow (Bad Nauheim, Germany; www.goodfellow.de). The preparation of organically modified sol gel beads ("ormosil"), which are soluble in chloroform, was performed as reported before.[11] All chemicals and solvents were of analytical grade and used without further purification. Doubly distilled water was used for the preparation of the 13 mM MOPS buffer solution whose pH was adjusted to 7.5 with 1 M hydrochloric acid.

3.2.2. Preparation of Ruthenium-Based Oxygen Sensitive Beads (SB1)

The lipophilic fluorescent oxygen probe $Ru(dpp)_3TMS_2$ was prepared according to the procedure reported by Klimant et al.[12]. Then, 400 mg ormosil micro particles were dissolved, in 50 mL chloroform and 7 mg $Ru(dpp)_3TMS_2$ salt was added.[11] The resulting cocktail was

spread on a glass surface and dried at room temperature. After evaporation of the solvent, the orange colored film was mechanically ground and the particles washed several times with ethanol in order to remove $Ru(dpp)_3TMS_2$ that is bound to the surface once the solution remained colorless. The suspension of SB1 in ethanol was spread onto a glass surface, dried at room temperature, and mechanically ground again. The average size of the beads (SB1) is 5 µm as determined by microscope.

3.2.3. Preparation of Iridium-Based Oxygen Sensitive Beads (SB2)

Three mg of $Ir(ppy)_3$ and 200 mg of ormosil were dissolved in 250 mg chloroform and the solution was spread on a glass surface. After drying at room temperature, a yellow polymer film was formed, which was ground mechanically. The $Ir(ppy)_3$ beads (SB2) were washed several times with ethanol and separated by centrifugation. Thereafter the suspension of SB2 in ethanol was spread onto a glass surface and was dried at ambient air. After evaporation of ethanol, the yellow colored film was mechanically ground for a second time and treated as described above. The average diameter of the resulting SB2 beads is around 5 µm as determined by microscopy.

3.2.4. Crosslinking of Uricase with Glutaraldehyde

Crosslinking of uricase with glutaraldehyde is necessary for formation of a network structure to prevent the leaching out of the sensor membrane. Uricase (20.8 mg) was dissolved in 104 µL of MOPS buffer (13 mM; pH 7.5) and 26 µL of glutaraldehyde (0.5 wt % in H_2O) was added. The mixture was slightly shaken at room temperature for 2 h. Sensor membranes containing this modified uricase did not suffer from leaching out of the enzyme which is in contrast to sensor membranes containing uricase not crosslinked with glutaraldehyde.

3.2.5. Uric Acid Biosensor Membrane (BSM1)

Ten mg of the beads SB1 were dispersed in 500 µL of a 5 % wt solution of a hydrogel in ethanol/water (9:1, v:v). Then, 130 µL of a MOPS buffered uricase solution with an activity of 100 units (see *3.2.4*), crosslinked with glutaraldehyde as described above, was

added to the hydrogel, stirred and spread onto a dust-free polyester support by using a self made knife-coating device. The thickness of the wet sensor layer is 120 µm. After drying at ambient air for 1 h, the resulting sensor layer (referred to as BSM1) was either stored in MOPS buffer or placed in the flow through cell. The cross-section of the oxygen sensitive membrane is given in *Fig. 1*.

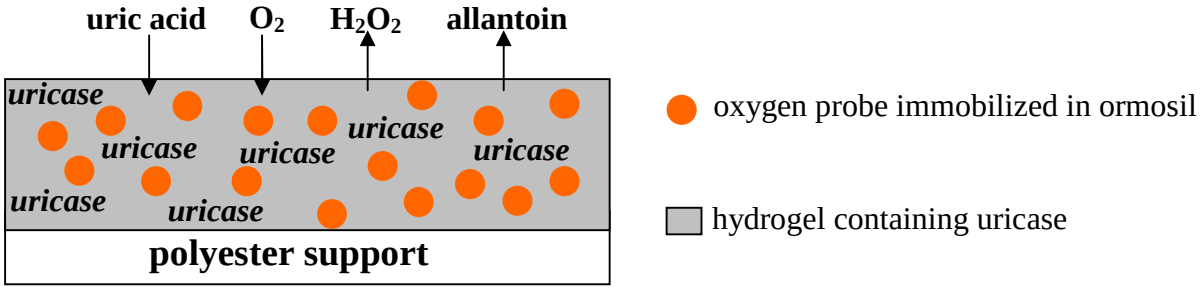

Fig. 1. *Cross section through the biosensor membrane for uric acid, and diffusional processes involved. The hydrogel layer contains the oxygen sensitive beads and the enzyme uricase. The thickness of the dried hydrogel layer typically is ~ 12 µm.*

3.2.6. Uric Acid Biosensor Membrane (BSM2)

Beads of type SB2 (25 mg) were dispersed in 500 µL of a 5 % wt solution of a hydrogel in ethanol/water (9:1, v:v). Then, 130 µL of a MOPS buffered uricase solution with an activity of 100 units (see 3.2.4.), crosslinked with glutaraldehyde as described above, was added to the hydrogel, stirred and spread onto a polyester support. The thickness of the wet sensor layer is 120 µm. After drying at room temperature for 1 h, BSM2 was either stored in MOPS buffer or placed in the flow through cell.

3.3. Instrumental and Measurements

3.3.1. Instrumental

Fluorescence excitation and emission spectra were acquired on an Aminco Bowman AB2 luminescence spectrometer (SLM Spectronic Unicam, www.spectronic.co.uk). The luminescence of sensor membrane BSM1 (containing the probe Ru) was excited at 468 nm and emission detected at 612 nm. The luminescence of sensor membrane BSM2 (containing the probe Ir) was excited at 398 nm and emission was detected at 507 nm.

pH was adjusted with a pH meter CG 842 from Schott (www.schottinstruments.com). Sensor films were prepared by a self made knife coating device (see *Fig. 2*). Calibration plots of the sensor films were done in a self made flow through cell (see *Fig. 3*).

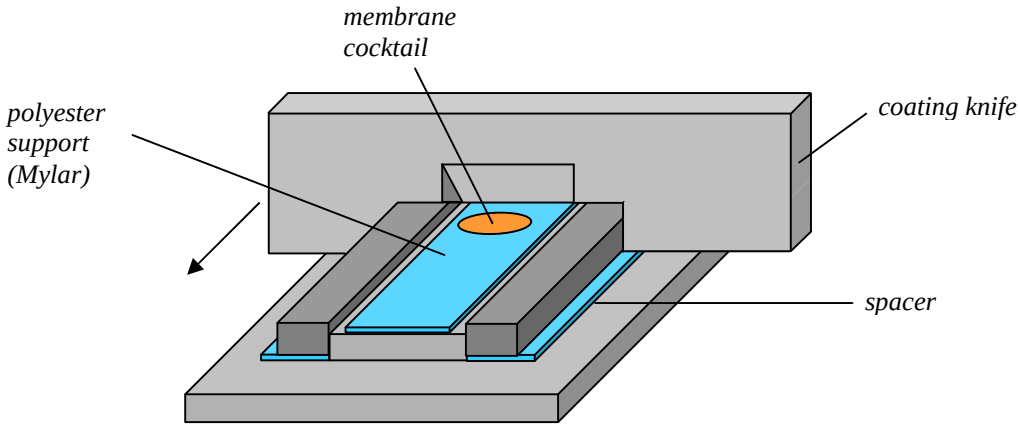

Fig. 2. *Self-made knife coating device*

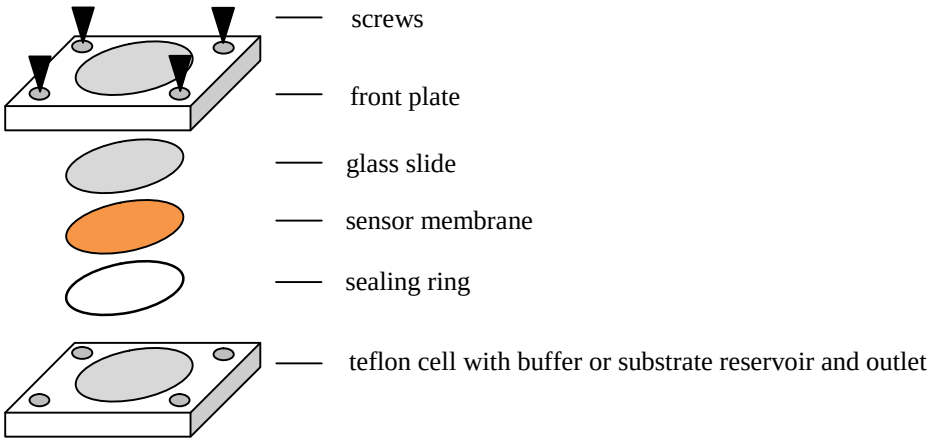

Fig. 3. *Schematic presentation of self-made flow through cell.*

3.3.2. Measurements of Luminescence Intensity or Lifetime for Characterization of BSM1

Response curves for BSM1 were recorded on a phase detection device (PDD-470) from Presens (www.presens.de) (see *Fig. 4*). Light of a 470-nm LED was focused to one branch of a bifurcated glass fiber bundle and directed onto the sensor membrane. Emitted light is guided back by the other branch of the fiber bundle and detected by a photodiode. Luminescence intensity or phase shift detection can be performed simultaneously with this instrument. The excitation light is sinusoidally modulated at a frequency of 49 kHz. The decay time can be calculated from the phase shifts via *equation 1* and the luminescence intensity is proportional to the amplitude (A) according to *equation 2*.

$$\tau = \frac{\tan \rho}{2\pi f} \qquad \textbf{Eq. 1.}$$

$$I \propto A^2 \qquad \textbf{Eq. 2.}$$

In *Eq. 1* f is the modulated frequency and ρ is the detected phase shift. At a flow rate of 0.3 mL per min the solutions were transported by a peristaltic pump (from ISMATEC, Germany, www.ismatec.de) via a tube of 0.25 mm average diameter from volumetric flasks containing uric acid solution of defined concentration (in buffer) through the cell.

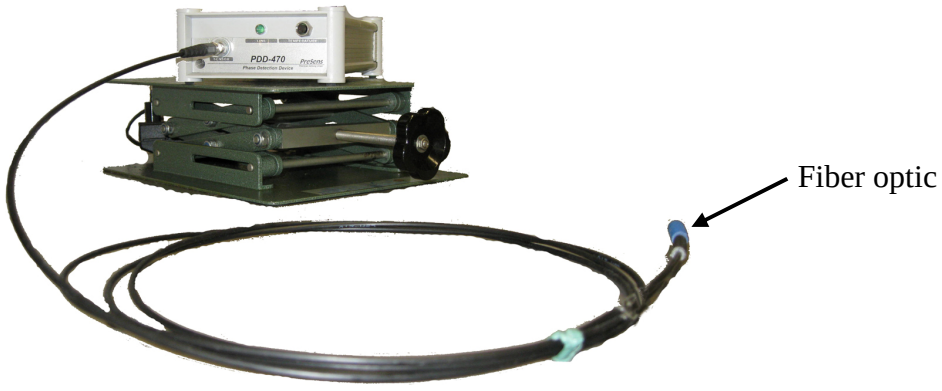

Fig. 4. *Phase detection device (PDD-470).*

3.3.3. Luminescence Measurements for Characterization of BSM2

The response of BSM2 was recorded on an Aminco Bowman AB2 luminescence spectrometer (SLM Spectronic Unicam, www.spectronic.co.uk), where the excitation light passed a monochromator and was focused into one branch of a bifurcated glass fiber bundle. The excitation light hits the sensor membrane placed in a self-made flow through cell. The emitted light was guided back by the other branch of the fiber bundle, passed a monochromator and was detected by a photomultiplier (*Fig. 5*). BSM2 was characterized by passing solutions of uric acid of various concentrations (0 to 2 mM) through the flow through cell at a rate of 0.7 mL per min. The solutions were transported by a Minipuls-3 peristaltic pump (Gilson, Villiers-le-Bel, France, www.gilson.com) via a tube of 0.25 mm diameter.

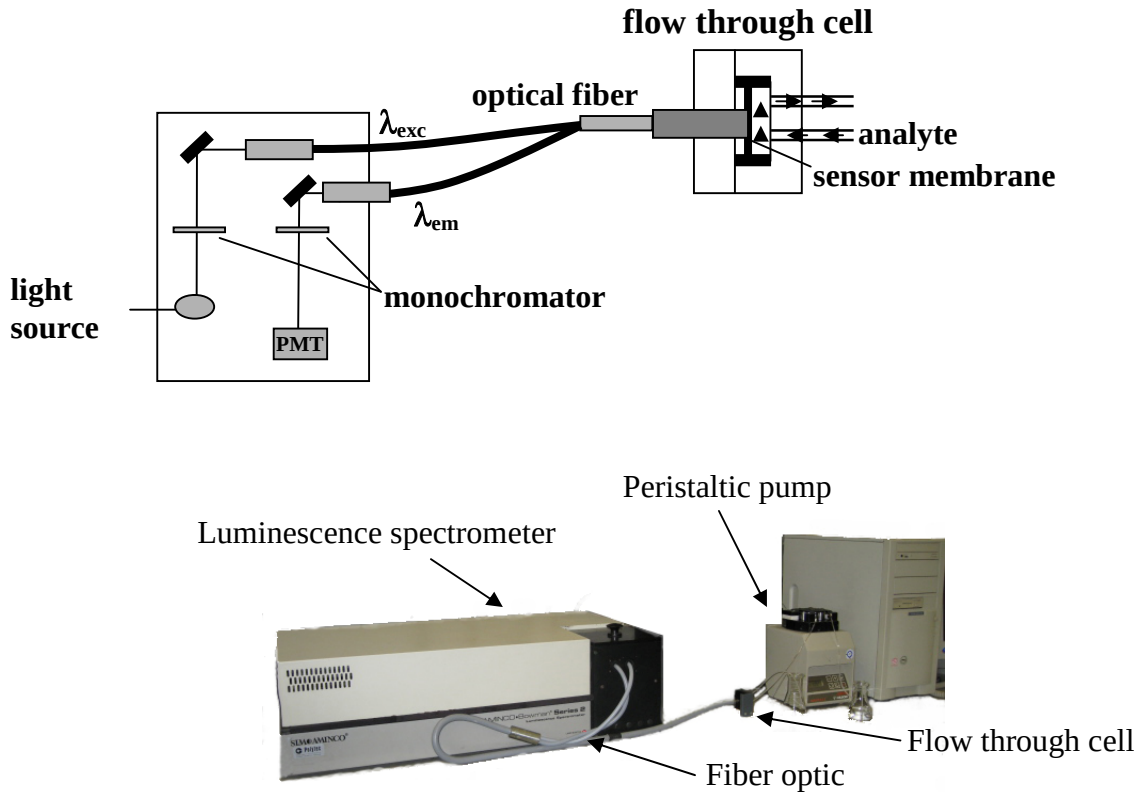

Fig. 5. *Schematic representation of the instrumental set up for recording the optical response of biosensor membrane BSM2.*

3.3.4. Blood Samples

Human blood serum samples were sourced from the university hospital of Regensburg. The frozen samples (0.8 mL) were thawed, thermostated to room temperature and diluted with MOPS buffer (pH 7.5) to 1.4 mL. The response curve for determination of

the UA content in the serum samples was recorded on a phase detection device (PDD-470) from Presens according to *chapter 3.3.2* The detected amplitude was converted into the intensity according to *equation 2* and all measurements were performed at room temperature.

3.4. Results

3.4.1. Selection of the Indicators

The $Ru(dpp)_3TMS_2$ probe (*Fig. 6*) was selected as an oxygen transducer because it has a strong absorption in the visible range of the spectrum (λ_{exc}: 468 nm), a large Stokes´ shift (λ_{em} 612 nm), a fairly high quantum yield (~ 30 %), a long decay time (approximately 4 µs in presence of nitrogen), and can be excited with a blue or blue-green LED.[13,14] If trimethylsilylpropane sulfonate is used as the counterion of the $Ru(dpp)_3$ complex, it is well lipophilic and soluble in ormosil.[11]

The second indicator for sensing oxygen $Ir(ppy)_3$ (*Fig. 6*) exhibits a broad absorption band with its maximum at 398 nm, a strong green luminescence (λ_{em} 507 nm) with a high quantum yield, and a long lifetime of < 2 µs.[15] It can be easily immobilized in ormosil due to its lipophilicity. Related iridium probes have been reported recently.[16] $Ir(ppy)_3$ is uncharged and well soluble in the ormosil matrix.

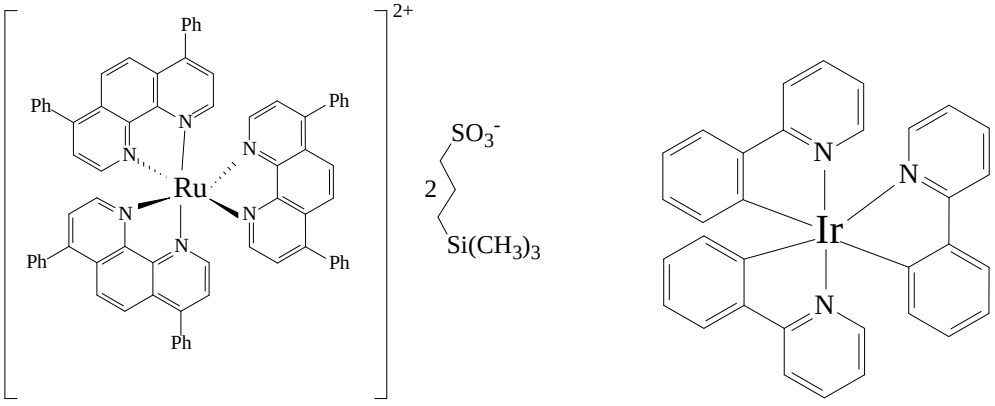

$Ru(dpp)_3TMS_2$ **$Ir(ppy)_3$**

Fig. 6*. Chemical structures of the oxygen probes $Ru(dpp)_3TMS_2$ and $Ir(ppy)_3$.*

3.4.2. Oxygen Sensing Capabilities of Sensor Beads SB1

The uncharged hydrogel Hydromed D4 is an ideal matrix for embedding the oxygen sensitive ormosil beads SB1. It is optically fully transparent, can be easily spread as a thin layer and displays good permeability for oxygen. *Fig. 7* shows the intensity based Stern-Volmer plot of the quenching of the luminescence of the ruthenium complex incorporated in ormosil (SB1) in the hydrogel layer at room temperature. The sensor membrane did not contain an enzyme. The Stern-Volmer plot is not linear. Such situations can be described by a modified equation that contains two quenching constants (see *equation 3*).

$$\frac{I_0}{I} = \left(\frac{f_1}{1 + K_{SV1} * pO_2} + \frac{f_2}{1 + K_{SV2} * pO_2} \right)^{-1} \qquad \textbf{Eq. 3.}$$

I and I_0, are the quenched and unquenched luminescence intensities of the sensor membrane respectively. K_{SV1} and K_{SV2} are the two Stern-Volmer constants, and f_1 and f_2 are the fractions of the total emission for each component, and pO_2 is the partial pressure of oxygen which causes the decrease of the luminescence intensity from I_0 (pO_2 zero) to I(pO_2>0). Equation 3 is the modified Stern-Volmer equation (the so-called two site model). It reflects the fact that polymer films have two different oxygen-accessible sites and each site shows different quenching constants.[17, 18]

3.4.3. Oxygen Sensing Properties of the Sensor Beads SB2

Fig. 7 shows the intensity based Stern-Volmer plot of the oxygen quenching of the iridium complex incorporated in ormosil (SB2) in the hydrogel matrix at room temperature. The sensor layer does not contain uricase. It follows the conventional Stern-Volmer equation

$$\frac{I_0}{I} = 1 + K_{SV} * pO_2 \qquad \textbf{Eq. 4.}$$

where I and I_0, are the quenched and unquenched luminescence intensities of the sensor membrane, and K_{SV} is the Stern-Volmer constant.

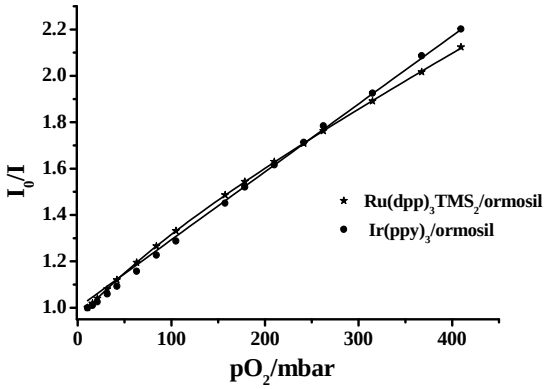

Fig. 7. *Stern-Volmer plots of the quenching of the luminescence intensity of $Ru(dpp)_3TMS_2$/ormosil beads (SB1) and $Ir(ppy)_3$/ormosil beads (SB2) in a hydrogel matrix in presence of oxygen at different pressures.*

Table 1

Stern-Volmer constants and weighing factors for the modified Stern-Volmer equation (eq. 2) for the quenching by oxygen of sensor beads SB1; and Stern-Volmer constant for sensor beads SB2; both incorporated in a hydrogel matrix.

	Sensor membrane of SB1 beads	Sensor membrane of SB2 beads
K_{SV1} in bar^{-1}	1.83	2.93
K_{SV2} in bar^{-1}	0.29	-
f_1	0.579	-
f_2	0.471	-

3.4.4. Selection of Material

The hydrogel is based on polyurethane which has been chosen as polymer matrix due to its good stability, the good permeability for uric acid, its impermeability for charged proteins, and its optical transparency. It is soluble in a 9:1 ethanol-water mixture and consists of hydrophilic and hydrophobic blocks which allow the embedding of lipophilic ormosil particles containing the oxygen sensitive dye $Ru(dpp)_3TMS_2$ or $Ir(ppy)_3$.[19] Furthermore the polymer is permeable to oxygen.

The oxygen probes were incorporated into an organically modified sol-gel (ormosil) that is hydrophobic. Hydrophobic sol-gels avoid the penetration of water into the matrix and are useful for sensing dissolved gases such as oxygen. The material is obtained by acid-

catalyzed condensation of phenyltrimethoxysilane and trimethylmethoxysilane in a molar ration of 18:1. It is soluble in chloroform, acetone and dichloromethane, contains much fewer silanol groups than usual ormosils and consequently is less densified over time which enhances the long-term and storage stability. Hydrophobic ormosils prevent the penetration of charged species into the matrix and enhance the selectivity for gas sensors.[11,20]

3.4.5. Spectral Properties of BSM1 and BSM2

The excitation and emission spectra of the oxygen probes incorporated in ormosil beads are shown in *Figure 8 (A, B)*. The beads of type SB1 show a broad excitation band with a maximum at around 468 nm, so that luminescence can be excited efficiently by a 470-nm LED. The red luminescence of the SB1 beads exhibits a strong maximum at 612 nm. The beads of type SB2 beads display an excitation peak at around 400 nm, and its green luminescence is best excited by a 405-nm diode laser or a purple LED.

The uricase in the sensor membrane catalyzes the oxidation of uric acid under consumption of oxygen, so that quenching of oxygen is partially suppressed and this causes an increase in the intensity (and lifetime) of the emission band of both probes.

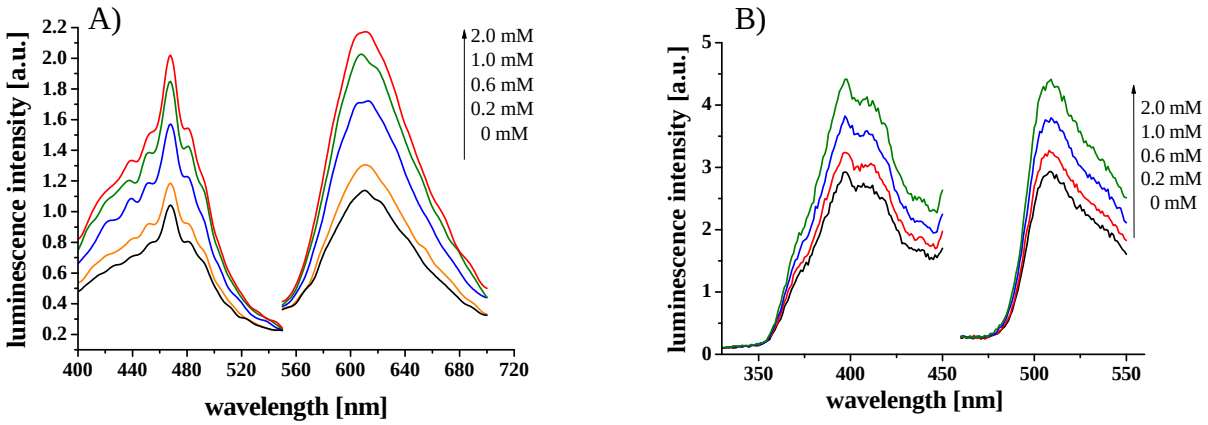

Fig. 8. *Excitation and emission spectra of biosensor membranes (A) BSM1, and (B) BSM2 in MOPS buffer (pH 7.5) at concentrations of uric acid increasing from 0 to 2.0 mM.*

3.4.6 Variation of Experimental Parameters

The effect of pH on the sensitivity of both biosensor membranes BSM1 and BSM2 were investigated. BSM1 and BSM2 were exposed to 1 mM uric acid in buffers of varying pHs (6.5-10.5). The results show that the response is slightly increasing from pH 6.5 to 8.0 and remains constant at higher pH. Further measurements were carried out at a pH of 7.5.

The enzyme uricase has to be crosslinked with glutaraldehyde before incorporation in the sensor membrane. Primary amino groups of uricase molecules react with the aldehyde groups of glutaraldehyde under formation of Schiff bases (see *Fig. 9*). Hence, uricase molecules form a network structure which avoids the effect of leaching out of uricase form the sensor membrane compared to non crosslinked uricase. Non crosslinked uricase molecules are smaller than the pore size of the sensor membrane and so leaching out of the membrane occurs. Crosslinking was performed at room temperature and in MOPS buffer of pH 7.5. Increasing concentrations of glutaraldehyde and long reaction times between glutaraldehyde and uricase cause an activity loss. Glutaraldehyde concentrations of 0.01 to 0.1 % and a crosslinking time 2 h cause no effect on the uricase activity. In the range from 0.15 to 0.4 % final glutaraldehyde concentration uricase activity is decreasing and upon 0.5 % and higher concentrations no activity is given. For the final concentrations 0.06 to 0.1 % no leaching out of uricase from the sensor membrane can be detected. Two hours crosslinking time was chosen because longer times cause an activity loss. Best results are achieved with a glutaraldehyde concentration of 0.1 % and a crosslinking time of 2 hours for both biosensor membranes.

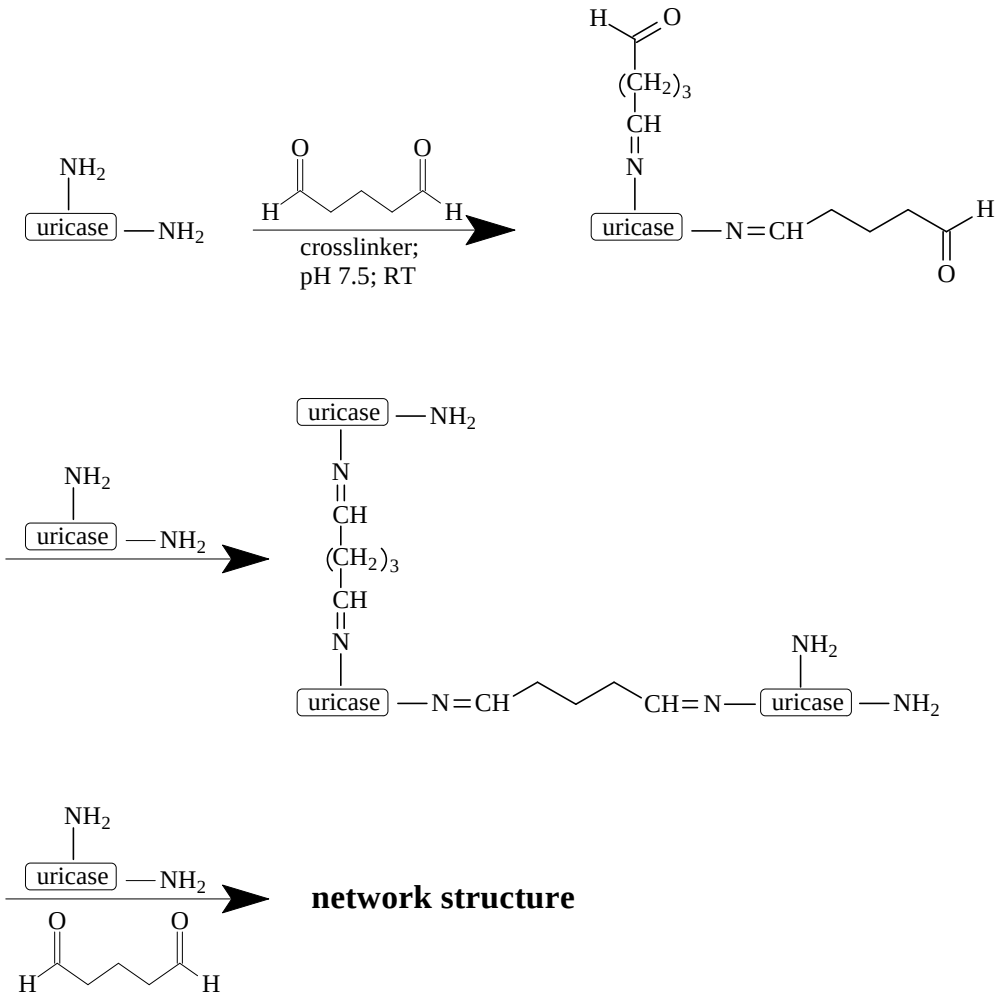

Fig. 9. *Scheme for crosslinking of uricase with glutaraldehyde at room temperature and pH 7.5.*

3.4.7. Response Curve of Biosensor Membrane BSM1 and BSM2

Biosensor membranes BSM1 and BSM2 respond to uric acid in the concentration range from 0.1 to 2.0 mM. The response curves for both biosensors are depicted in *Fig. 10 (A, B)*. Signal changes can be detected up to 2.0 mM. At higher concentrations there are no useful further signal changes.

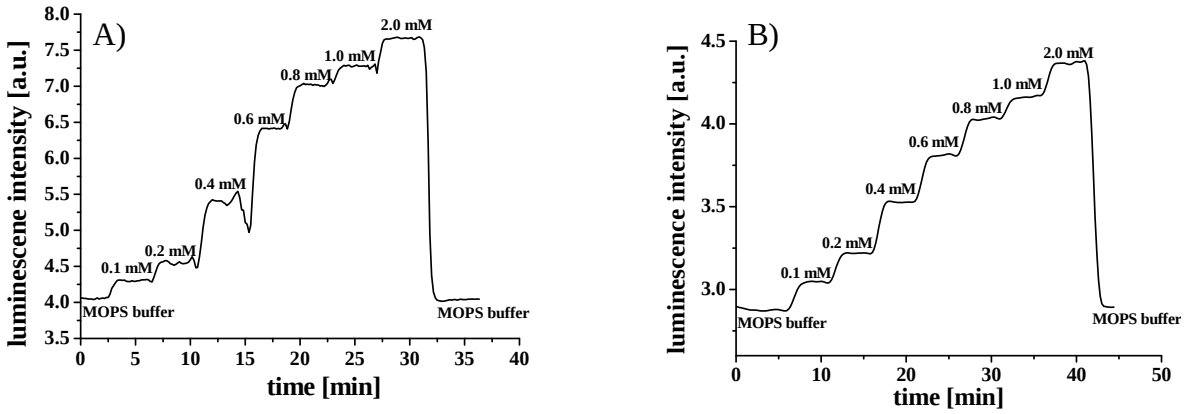

Fig. 10. *Typical response curve of uric acid biosensor (A) BSM1, and (B) BSM2 towards uric acid solutions passing at a flow rate of 0.3 mL/min for BSM1 and 0.7 mL/min for BSM2. All solutions are air saturated.*

The response times are approximately 1.2 min for BSM1, and for BSM2 1.3 min for a 90 % signal change (t_{90}). The return to the baseline by washing with MOPS buffer takes 1.9 min for both sensors. The response times are depending on the enzyme activity and the layer thickness of the sensor membrane. High enzyme activities result in shorter response time. The calculated layer thickness of BSM1 and BSM2 is approximately 12 µm. Thinner membranes could not be manufactured due to the size of the beads which is approximately 5 µm estimated via fluorescence microscope. Layer thicknesses of less than 12 µm cause an uneven layer surface whereas layer thicknesses of 20 and 25 µm prolong the response time of the sensors but without a change in the shape of the calibration curves.

The flow rate of the buffer and UA solutions in the flow system influences the signal changes. For biosensor membrane BSM1 flow rates of 0.1, 0.2, 0.3 and 0.7 mL/min were tested towards a 1 mM UA solution. The luminescence enhancement towards the 1 mM UA solution shows a decreasing effect with increasing flow rates. Low flow rates cause larger signal enhancements because more UA diffuses in the sensor membrane and is oxidized by uricase under oxygen consumption. A flow rate of 0.3 mL/min was chosen for all measurements. Similar results were obtained for biosensor membrane BSM2. Flow rates of 0.2, 0.3, 0.7 and 1.2 mL/min were tested. Best results were achieved applying a flow rate of 0.2 mL/min. No major differences in signal enhancement were obtained for the flow rates 0.3 and 0.7 mL/min. Higher flow rates show a decreasing effect of luminescence. A flow rate of 0.7 mL/min was chosen for further measurements.

3.4.8. Calibration Plot for BSM1 and BSM2

Fig. 11 (A, B) shows the calibration graphs for BSM1 and BSM2 obtained from the corresponding signal changes. The signal changes and the dynamic ranges are depending on the enzyme activity in the sensor layer. High uricase activities give larger signal changes. Saturation of the sensor is reached earlier because oxygen is consumed more rapidly. Consequently, the analytical range is narrower compared to low enzyme activities where the analytical range is wider. Best results for both biosensor membranes are obtained with a sensor cocktail (see 3.2.5. and 3.2.6.) containing uricase with an activity of 100 units. The calibration plots display with a dynamic range over around one order of magnitude (0.05 to 0.8 mM for BSM1 and 0.05 to 0.6 mM for BSM2). The limit of detection (LOD) at a signal to noise ratio of 3 is 50 µM for BSM1, and 20 µM for BSM2. This is obviously a result of the larger quenching constant of the probe $Ir(ppy)_3$ (see *Table 1*). The calibration curves were fitted by a Boltzmann fit according to *Eq. 5*.

$$\frac{I}{I_0} = A_2 + \frac{A_1 - A_2}{1 + \exp((x - x0))/dx} \qquad \textbf{Eq. 5}$$

I_0 is the luminescence intensity of MOPS buffer and I the luminescence intensity for different uric acid concentrations. A_1, A_2, x0 and dx are empirical parameters. The variable x is related to different UA concentrations.

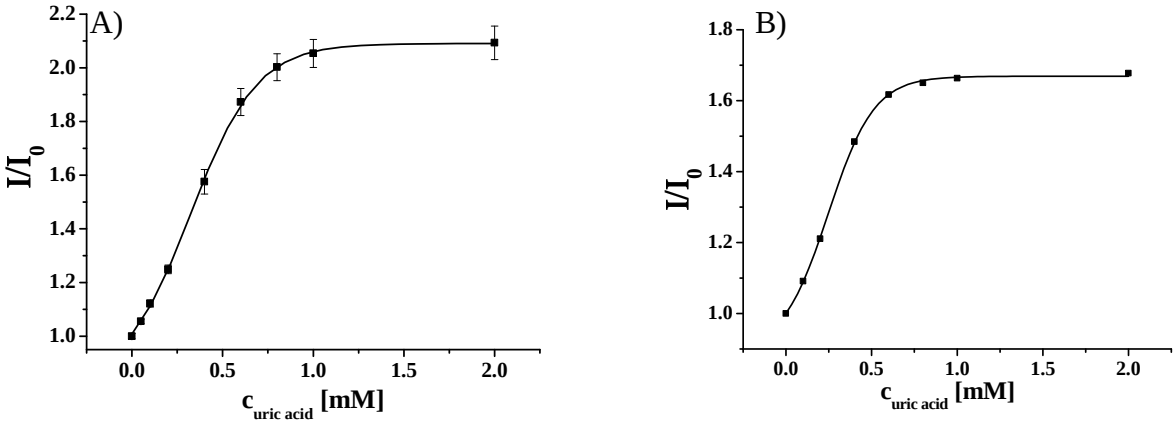

Fig. 11. *Calibration plot for (A) BSM1, and (B) BSM2. All measurements are performed in air saturated buffered uric acid standard solutions at pH 7.5 and room temperature.*

3.4.9. Stability and Reproducibility

The reproducibility of biosensor manufacturing, including sensor beads preparation, is given in *Fig. 12* by the calibration plots for two different BSM2 biosensor membranes. Both biosensors show similar behaviour. For getting reproducible results it is essential to follow the standard protocol for preparation of the biosensor membrane. Biosensor membranes BSM1 and BSM2 are stable for one month when stored in MOPS buffer at 4 °C, which was changed every week to avoid growth of micro-organisms. The response of BSM1 to a 1 mM solution of UA decreases during the first two days, probably enzyme molecules which are weakly crosslinked can be leaching out of the sensor membrane. Their network structure is smaller than the pore size of the sensor membrane. The activity remains stable during the next three weeks but for the ensuing time activity is further decreasing. The response of BSM2 into a 1 mM solution of UA shows a slight increase during the first five days and remains stable for the next three weeks followed by a decrease in activity.

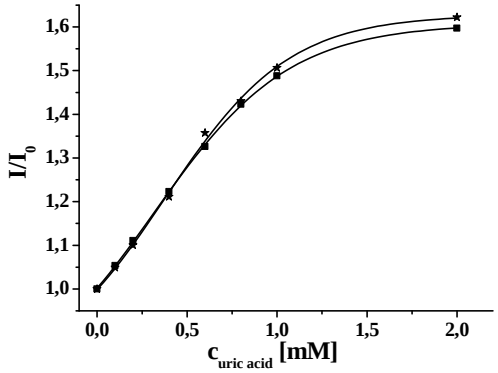

Fig. 12. *Reproducibility check for two different uric acid biosensor (BSM2). The two plots are obtained from the resulting response curves.*

3.3.10. Application of BSM1 for Detection of Uric Acid in Blood Serum

Biosensor membrane BSM1 was applied to analyze blood serum samples for UA whose concentration in blood serum is in the range from 0.12 to 0.45 mM.[1] The uric acid content of seven blood serum samples was determined. UA levels were determined by the spectrophotometric method in which UA is converted in allantoin and HP. Under the catalytic influence of peroxidase a quinone diimine dye is produced from HP, 4-aminophenanzone and TOOS ([N-ethyl-N-(2-hydroxy-3-sulfopropyl)-3-methyl aniline]). The produced quinine diimine dye is detected spectrophotometrically at 545 nm and its concentration is proportional to the sample UA concentration. Frozen serum samples were thawed (0.8 mL), thermostated

to room temperature and filled up to 1.4 mL with MOPS buffer of pH 7.5 to match the linear range. The biosensor membrane BSM1 was first calibrated with standard uric acid solutions ranging from 0 to 2 mM three times before determination of UA in serum samples was carried out. The calibration curve was smoothed via a Boltzmann fit according to *equation 5*. The UA concentrations were calculated from luminescence intensities using the Boltzmann fit. Specified levels and experimental data obtained by the biosensor BSM1 are listed in *Table 2*.

Table 2.

UA concentrations in blood serum as determined by the standard photometric method ("specified") and with biosensor BSM1.

Sample	Specified (mg/dL)[(a)]	Found (mg/dL)[(b)]	Recovery rate in %
1	10.11	9.06	89.6
2	10.93	10.06	92.0
3	7.55	6.69	88.6
4	10.15	9.07	89.4
5	9.05	9.07	100.2
6	11.00	9.27	84.3
7	10.62	9.28	87.4

[(a)] by photometry; [(b)] using the biosensor

3.4. Discussion

Two single-layer optical biosensors for determination of UA are simple, sensitive and highly specific. The dynamic range of biosensor membranes BSM1 and BSM2 is rather wide compared to the voltammetric and fluorometric methods.[10,21,24] Table 3 summarizes figures of merits of various methods. Most of the methods exhibit lower LODs. However, the fluorometric methods using Amplex Red or thiamine as substrates require the presence of peroxidase as an additional enzyme in order to convert the non fluorescent substrates into fluorescent products. The chemiluminescent method using luminol also requires peroxidase.[10,21,22,23]

Further features of the biosensor BSM1 and BSM2 are the application at room temperature and pH 7.5, whereas the chemiluminescent and the fluorimetric method using thiamine work best at pH 8.5.[10,22] The amperometric and the fluorometric methods using thiamine and Amplex Red as substrates require temperatures of > 30 °C.[10,21,25] Uricase exhibits maximum activity at temperatures between 25 °C and 37 °C but we prefer to work at room temperature.

The poor selectivity of amperometric uric acid sensors is problematic. Ascorbic acid (AA) heavily interferes as it can be oxidized at the potential applied for uric acid detection. To avoid this effect the electrodes have to be modified for distinct peak assignment of UA and AA.[24,25] The sensor beads SB1 and SB2, in contrast, are selective for oxygen. Their signal is not disturbed by ascorbic acid, human serum albumine, or cysteine.

The biosensors presented here consists of a single layer that contains the oxygen transducer beads and the enzyme in a bulk hydrogel matrix. Other matrices for immobilizing enzymes include sol-gels.[20,21,24] The application of sol-gels is very common because the activity of the enzyme can be retained over a long time.[9] Further on, enzymes are often covalently immobilized onto preactivated polyamide or poly(vinylidenedifluoride) membranes such as Immunodyne or Biodyne which results in preparation of two layer biosensors.[9]

Uric acid levels in blood serum are between 120 and 450 µM in healthy subjects whilst in pathological cases they can increase up to 500 µM.[1] For monitoring UA at normal levels in blood serum the samples have to be diluted with buffer. Advantageous is the pH of the samples because it can be kept constant during measurements. The results demonstrate that biosensor BSM1 can be applied to blood serum samples. BSM1 is the preferred sensor for UA determination because biosensor BSM2 suffers from photobleaching.

The determination of UA in blood by the method presented here requires the oxygen concentrations to be constant. As a result, all measurements are done with air saturated uric acid solutions. Otherwise a two sensor approach has to be developed. The first sensor detects the UA level via oxygen consumption which occurs as a consequence of enzymatic oxidation of uric acid. The second one, a reference oxygen sensor, is used for measuring oxygen of the sample.[20] The biosensors BSM1 and BSM2 display stability over four weeks, response times of around 1.5 min, good selectivity and reproducibility in manufacturing of the oxygen sensitive beads and the biosensor membranes. This scheme may be adapted to the determination of other substrates that are oxidized by an oxidase.

Table 3. *Overview of selected assays for UA*

Method	Substrate	Dynamic range / µM	LOD / µM	Remarks	Ref.
Fluorimetry	Thiamine	3-30	0.9	Fiber optic; immobilized uricase and peroxidase; irreversible	9
Fluorimetry	Amplex Red	0.02-1	-	Encapsulation of a coupled uricase-peroxidase system and amplex red in a sol-gel matrix; irreversible	19
Chemiluminescence	Luminol	5.9-595	0.59	Chemiluminescent biosensor on a chip coupled to a microfluidic system and a microreactor; irreversible	20

Fluorimetry	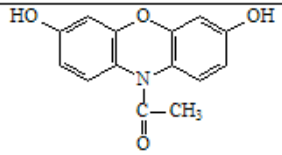 Amplex Red	10-1700	25	Sol-gel derived optical array biosensor; stable for 3 weeks; irreversible	21
Electrophoresis	-	0.25-500	0.025	Capillary electrophoresis with polarity reversal and electrochemical detection at carbon fiber microcylinder electrodes; detection of uric acid under 3 min; reversible	25
Voltametry	-	0.5-50	0.2	Application of a β-cyclodextrin-coated electrode with incorporated carbon nanotubes; reversible	26
Amperometry	-	100-800	10	Amperometric UA biosensor based on modified Ir-C electrode; reversible	27
Potentiometry	-	4-640	2	Fabricated from a uricase-immobilized eggshell membrane and an oxygen electrode; response time < 100 s; eggshell membrane stable for 3 months; reversible	28

Fluorimetry	*see 3.4.1*	15-600	15	$Ir(ppy)_3$ as oxygen probe; luminescent measurement; t_{90} value: 1.3 min; reversible	This work
Fluorimetry	*see 3.4.1*	15-800	15	$Ru(dpp)_3TMS_2$ as oxygen probe; luminescent measurement; t_{90}value: 1.2 min; reversible	This work

3.5. References

[1] He J. B., Jin G. P., Chen Q. Z., Wang Y., **A quercetin-modified biosensor for amperometric determination of uric acid in the presence of ascorbic acid** 2007. Anal. Chim. Acta 585, 337-343

[2] Zhao Y., Yang X., Lu W., Liao H., **The uricase methods for serum uric acid assay** 2008. Microchim. Acta, *in press*

[3] Fossati P., Prencipe L., Berti G., **Use of 3,5-dichloro-2-hydroxybenzenesulfonic acid/4-aminophenanzone chromogenic system in direct enzymic assay of uric acid in serum and urine** 1980. Clin. Chem. 26, 227-231

[4] Tamaoku K., Ueno K., Akiura K., Ohkura Y., **New water-soluble hydrogen donors for the enzymatic photometric determination of hydrogen peroxide. II. N-ethyl-N-(2-hydroxy-3-sulfopropyl) aniline derivatives** 1982. Chem. Pharm. Bull. 30, 2492-2497

[5] http://www.bioassaysys.com/DIUA.pdf

[6] Haugland R. P., **Handbook of fluorescent probes and research products** 2002; 9th ed., p.446

[7] Chu Q. C., Lin M., Geng C. H., Ye J. N., **Determination of uric acid in human saliva and urine using miniaturized capillary electrophoresis with amperometric detection** 2007. Chromatographia 65, 179-184

[8] Goyal R. N., Gupta V. K., Sangal, A., Bachheti, N., **Voltammetric determination of uric acid at a fullerene-C_{60}-modified glassy carbon electrode** 2005. Electroanalysis 17, 2217-2223

[9] Borisov S. M., Wolfbeis O. S., **Optical biosensors** 2007. Chem. Rev. 108, 423-461

[10] Gong Z., Zhang Z., **A fiber optic biosensor for uric acid based on immobilized enzymes** 1996. Anal. Lett. 29, 695-709

[11] Klimant I., Ruckruh F., Liebsch G., Stanglmayer A., Wolfbeis, O. S., **Fast response oxygen micro-optodes based on novel soluble ormosil glasses** 1999. Mikrochim. Acta 131, 35-46

[12] Klimant I., Wolfbeis O. S., **Oxygen-sensitive luminescent materials based on silicone-soluble ruthenium diimine complexes** 1995. Anal. Chem. 67, 3160-3166

[13] Cao Y., Koo Y. E. L., Kopelman R., **Poly(decyl methacrylate-)based fluorescent PEBBLE swarm nanosensors for measuring dissolved oxygen in biosamples** 2004. Analyst 129, 745-750

[14] Oter O., Ertekin K., Dayan O., Cetinkaya B., **Photocharacterization of novel ruthenium dyes and their utilities as oxygen sensing materials in presence of perfluorochemicals** 2008. J. Fluoresc. 18, 269-276

[15] Amao Y., Ishikawa Y., Okura I., **Green luminescent iridium(III) complex immobilized in fluoropolymer film as optical oxygen-sensing material** 2001. Anal. Chim. Acta 445, 177-182

[16] Borisov S. M., Klimant I., **Ultrabrigth oxygen optodes based on cyclometalated iridium(III) coumarin complexes** 2007. Anal. Chem. 79, 7501-7509

[17] Demas J. N., DeGraff B. A., Xu W., **Modeling of luminescence quenching-based sensors: comparison of multisite and nonlinear gas solubility Models** 1995. Anal. Chem. 67, 1377-1380

[18] Carraway E. R:, Demas J. N., DeGraff B. A., Bacon J. R., **Photophysics and photochemistry of oxygen sensors based on luminescent transition-metal complexes** 1991. Anal. Chem. 63, 337- 342

[19] Schroeder C. R., Weidgans B. M., Klimant I., **pH fluorosensors for use in marine systems** 2005. Analyst 130, 907-916

[20] Wolfbeis O. S., Oehme I., Papkovskaya N., Klimant I., **Sol-gel based glucose biosensors employing optical oxygen transducers, and a method for compensating for variable oxygen background** 2000. Biosens. Bioelectron. 15, 69-76

[21] Martinez-Pérez D., Ferrer M. L., Mateo C. R., **A reagent less fluorescent sol-gel biosensor for uric acid detection in biological fluids** 2003. Anal. Biochem. 322, 238-242

[22] Lv Y., Zhang Z., Chen F., **Chemiluminescence biosensor chip based on a microreactor using carrier air flow for determination of uric acid in human serum** 2002. Analyst 127, 1176-1179

[23] Tsai H. C., Doong R. A., **Simultaneous determination of renal clinical analytes in serum using hydrolase- and oxidase-encapsulated optical array biosensors** 2004. Anal. Biochem. 334, 183-192

[24] Wolfbeis O. S., Reisfeld R., Oehme I., **Sol-gels and chemical sensors** 1996. Structure & Bonding 85, 51-98

[25] Boughton J. L., Robinson B. W., Strein T. G., **Determination of uric acid in human serum by capillary electrophoresis with polarity reversal and electrochemical detection** 2002. Electrophoresis 23, 3705-3710

[26] Wang Z., Wang Y., Luo G., **A selective voltammetric method for uric acid detection at β-cyclodextrin modified electrode incorporating carbon nanotubes** 2002. Analyst 127, 1353-1358

[27] Luo Y. C., Do J. S., Liu C. C., **An amperometric uric acid biosensor based on modified Ir–C electrode** 2006. Biosens. Bioelectron. 22, 482-488

[28] Zhang Y., Wen G., Zhou Y., Shuang S., Dong C., Choi M. M. F., **Development and analytical application of an uric acid biosensor using an uricase-immobilized eggshell membrane** 2007. Biosens. Bioelectron. 22, 1791-1797

Chapter 4

Optical Glucose Biosensors Using Oxygen Transduction or pH Transduction

An optical one layer biosensor for monitoring glucose is presented. The scheme is based on the measurement of the oxygen consumption during the oxidation which is catalyzed by the enzyme glucose oxidase (GOx). GOx is incorporated in a hydrogel on polyurethane basis next to a probe whose luminescence is dynamically quenched by oxygen. The ruthenium (II) complex ruthenium(II) tris (4,7-diphenyl-1,10-phenanthroline) is applied as oxygen transducer which is immobilized in ormosil (organically modified sol-gel). As a result of the oxidation, catalyzed by GOx, the oxygen consumptions can be followed by changes in luminescence intensity. The measurements are performed in a flow-through cell applying air saturated standard glucose solutions. The analytical range (0 to 3.0 mM), the response times, reproducibility and long term stability were investigated. In view of development a dual sensor for determination of glucose via an oxygen and pH transducer, glucose was determined via pH changes. GOx catalyzes the oxidation of glucose to gluconic acid, which lowers the pH in the microenvironment of the biosensor. The enzymatic reaction is monitored by following the changes in luminescence of a pH probe. The analytical range and the response time are given in this work. The combination of oxygen and pH transducer for glucose determination is described in detail.

4.1. Introduction

Determination of glucose is very important in clinical analysis, biotechnology, agricultural and food industry.[1] In food industry it is significant for process controlling and in clinical analysis for diagnosis of diabetes and the following treatment.[2,3] Diabetics is very popular and a metabolic disorder resulted from insulin deficiency and hyperglycemia. Hence, glucose concentrations in blood varies very intense than in the normal status. On this account a variety of methods for glucose sensing are developed based on amperometry, potentiometry, chemilumimetry, spectrometry and fluorimetry.[4,5,6,7] Most of these methods are based on following the oxidation of glucose catalyzed by GOx according to *scheme 1*. GOx catalyzes the oxidation of β-D-glucose in presence of molecular oxygen to glucono-δ-lactone, which hydrolyzes spontaneously to gluconic acid. FAD (flavin-adenine dinucleotide), a cofactor is also involved in this process which reacts with glucose to $FADH_2$ and then it is retrieved by oxygen.

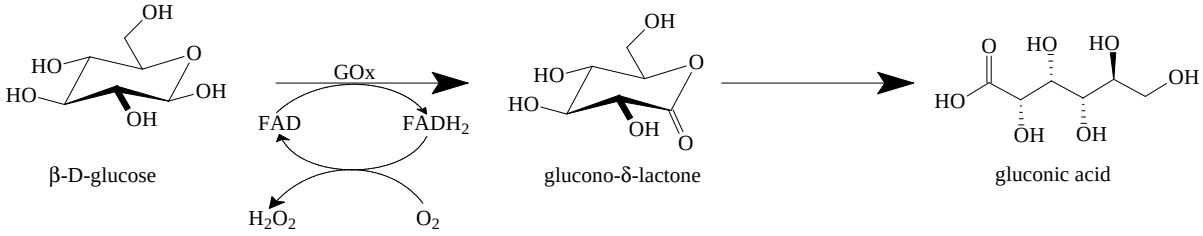

Scheme 1. *GOx catalyzed oxidation of β-D-glucose.*

Corresponding to *scheme 1* glucose can be determined by (1) measuring the consumption of oxygen during the oxidation, (2) the production of hydrogen peroxide (HP) or (3) the production of D-gluconic acid which lowers the pH of the solution.

Many colorimetric methods are developed for the determination of glucose by coupling the GOx reaction with the oxidation of a chromophore catalyzed by peroxidase under hydrogen peroxide consumption. Guilbault et al. presented at the end of the sixties new substrates for glucose detection. A very popular substrate is homovanillic acid (HVA). In presence of peroxidase and hydrogen peroxide the nonfluorescent HVA is converted in the highly fluorescent product, which can be detected fluorimetrically.[8,9] Further applied substrates are rhodamine B hydrazide, Amplex Red or p-aminophenanzone. The non fluorescent rhodamine B hydrazide is oxidized by hydrogen peroxide to the highly fluorescent rhodamine catalyzed by iron(III)-tetrasulfonatophthalocyanine.[10] Amplex Red is the state of the art substrate for glucose detection, which is the basis of a commercial available detection kit. The colorless and nonfluorescent Amplex Red is oxidized by HP catalyzed by peroxidase

to the brightly fluorescent resorufin.[11] p-Aminophenanzone is applied as substrate in the commercial available test strips where it is oxidized to a highly fluorescent dye. The colour of the formed dye can be estimated visually or with a reflectometer whose light source is a green LED.[12]

The first biosensor for glucose sensing was developed by Clark and Lyons in 1962. GOx was immobilized on a semipermeable dialysis membrane over an oxygen electrode. Glucose sensing was performed by measurement of the consumed oxygen during the enzyme–catalyzed reaction according to *scheme 1*. A negative potential was applied to a platinum cathode for the reductive detection of the consumed oxygen.[13] This technology was assigned to Yellow Spring Instruments Company which developed the first analyzer for direct measurement of glucose in 25 µL blood serum samples. Updike and Hicks improved this system by using two oxygen working electrodes for removing interferences due to variations in oxygen levels.[2,13] Nowadays electrochemical biosensors consists of various nanomaterials like carbon nanotubes (CNT) which are used as electrical connectors between the electrode and the redox center of GOx.[13,14]

Further on, a variety of optical biosensors are developed. One of the first optical biosensors based on the measurement of the oxygen partial pressure was developed by Uwira in 1984.[15] Further groups continued the research on the basis of the principle of Uwira. Choi et al.[1,16] developed diverse reversible optical biosensors based on the same sensing scheme and biosensor preparation. One two-layer sensor was made by immobilization of GOx on a bamboo inner shell membrane crosslinked with glutaraldehyde, which was brought up to the surface of an oxygen-sensitive optode membrane.[17] At the beginning of the nineties, fiber-optic glucose biosensors with an oxygen optode as transducer were developed. Here, the oxygen consumption was measured via dynamic quenching of the fluorescence of an indicator by molecular oxygen.[6,18] Pasic and co-workers developed a miniaturized fiber-optic hybrid sensor for continuous glucose monitoring in subcutaneous tissue. The biosensor consists of two oxygen optodes. One optode implies just the oxygen sensitive coating and the second optode contains the oxygen sensitive coating and the immobilized GOx. Simultaneous measurements of the local oxygen tension and the oxygen level which is achieved after oxidation of glucose catalyzed by GOx under oxygen consumption are feasible.[19]

In this work, reversible one-layer biosensors for determination of glucose via an oxygen or pH transducer are described. The polymer layer contains the oxygen or pH sensitive dye incorporated in particles next to the enzyme glucose oxidase. Glucose detection via oxygen transduction is simple, sensitive and selective. The detection principle is based on

using an oxygen transducer which is coupled to an enzymatic reaction according to *scheme 1*. Determination of glucose via pH transduction is hardly applicable and does not show the desirable results.

4.2. Materials and Methods

4.2.1. Material

Glucose oxidase (EC 1.1.3.4) from *Aspergillus niger* (lyophilized, powder, 211 unit/mg), glutaraldehyde solution (50 wt % in H_2O), ruthenium (III) chloride hydrate, 3-(trimethylsilyl)-1-propanesulfonic acid sodium salt (purity 97 %) were purchased from Sigma Aldrich (Steinheim, Germany; www.sigmaaldrich.com). 3-(morpholino) propanesulfonate sodium salt (MOPS sodium salt, 98 %) from ABCR (Karlsruhe, Germany; www.abcr.de). pH-sensitive micro beads consisted of 8-hydroxy-pyrene-1,3,6-trisulfonate (HPTS) which are covalently linked to amino-modified poly(hydroxyethyl methacrylate) (p-HEMA that was copolymerized with N-aminoethylacrylamide) was obtained from Presens (Regensburg, Germany, www.presens.de). D-glucose was provided from Merck (Darmstadt, Germany; www. Merck.de). The polyurethane hydrogel Hydromed D4 was obtained from Cardiotech (Wilmington, USA; www.cardiotech-inc.com). The polyester support (Mylar) (product number 124-098-60) was purchased from Goodfellow (Bad Nauheim, Germany; www.goodfellow.de) and ormosil was synthesized according to Klimant et al..[20] All chemicals and solvents were of analytical grade and are used without further purification. Doubly distilled water was used for preparation of MOPS buffer which was adjusted to pH 7.5 with hydrochloric acid. Glucose solutions were daily prepared.

4.2.2. Preparation of Ruthenium-Based Oxygen Sensitive Beads (SB)

The preparation of ruthenium-based oxygen sensitive beads (SB) was performed according to *chapter 3.2.2*.

4.2.3. Crosslinking of Glucose Oxidase with Glutaraldehyde

Crosslinking of GOx with glutaraldehyde is necessary for formation of a network structure which avoids the effect of leaching out from the sensor membrane after immobilization compared to single GOx molecules. GOx (2.8 mg) were dissolved in 117 µL MOPS buffer (13 mM; pH 7.0) and 13 µL glutaraldehyde (0.5 wt % in H_2O) was added. The mixture was slightly shaken at room temperature for 1 hour.

4.2.4. Manufacturing of Biosensor Membrane BSM3

For preparation of biosensor membrane (BSM3), 10 mg of the oxygen sensitive beads SB were suspended in 500 µL of a 5 % wt solution consisting of a hydrogel in ethanol/water (9:1 v:v) solution. 130 µL of MOPS buffered glucose oxidase solution crosslinked with glutaraldehyde, was added to the hydrogel, stirred and spread on a dust-free polyester (Mylar) support using a self-made knife-coating device. The thickness of the wet sensor layer is 120 µm. After drying at ambient air for 1 h BSM3 was stored in MOPS buffer or placed in a flow through cell. In *Fig. 1* the cross-section through the biosensor membrane is given.

4.2.5. Manufacturing of Biosensor Membrane BSM4

Manufacturing of biosensor membrane BSM4 was carried out according to *chapter 4.2.4.* Instead of oxygen sensitive beads 14 mg of pH sensitive beads (HPTS linked to amino-modified poly(hydroxyethyl methacrylate) were added to the hydrogel (see *Fig. 1*).

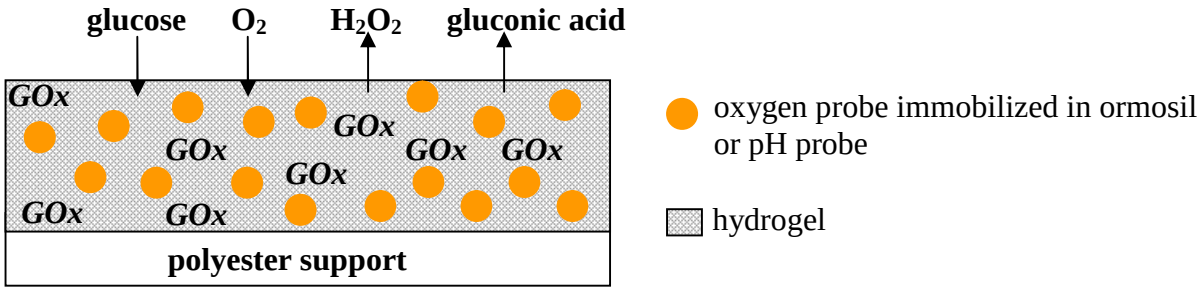

Fig. 1. *Cross section through the biosensor membrane. The hydrogel layer contains the oxygen sensitive beads or the pH sensitive beads and the enzyme glucose oxidase.*

4.2.6. Instrumental

Excitation and emission spectra were acquired on an Aminco Bowman AB2 luminescence spectrometer (from SLM Spectronic Unicam). Luminescence was excited at 468 nm and emission was detected at 612 nm for the oxygen probe or at 540 nm for the pH probe. pH was adjusted with a pH meter CG 842 from Schott (www.schottinstruments.com). Sensor foils were prepared by a self made knife coating device. Calibration plots of prepared sensor films were done in a self made flow through cell.

4.2.7. Luminescence Measurements for Characterization of Biosensor Membranes BSM3 and BSM4

Response curves for BSM3 and BSM4 were recorded with an Aminco Bowman AB2 luminescence spectrometer (from SLM Spectronic Unicam) (see *chapter 3.3.3*), where the excitation light is passed through a monochromator and was focused to one bunch of a bifurcated glass fiber bundle. The excitation light launches in the sensor membrane, which is fixed in a self-made flow through cell. The emitted light was guided back by the other bunch of the fiber bundle through a monochromator and the photomultiplier inside the spectrometer. The biosensor membranes were characterized by passing glucose solutions of varying concentrations (for BSM3 0 to 3 mM, and for BSM4 0 to 1.5 M) through a Minipuls-3-peristaltic pump (Gilson, Villiers-le-Bel, France) via a tube of 0.25 mm average from volumetric flasks containing glucose solutions of defined concentration (in buffer) through the cell.

4.3. Results and Discussion for Determination of Glucose via an Oxygen Transducer

4.3.1. Choice of Indicator

Transition metal complexes, particularly Ru (II), Os (II) or Re (II), are widely applied as oxygen sensitive material in analytical chemistry.[21,22] For this reason the $Ru(dpp)_3TMS_2$ complex (see *Fig. 2*) was chosen as an oxygen transducer, due to its strong visible absorption (λ_{exc} 468 nm) with an emission at 612 nm, the large Stokes´ shift at around 144 nm, the long

luminescence lifetime (approximately 2 µs in presence of oxygen) and as well the high quantum yield. The excitation can be carried out by a green or blue-green LED. The application of trimethylsilylpropane as counterion of the $Ru(dpp)_3TMS_2$ complex, intensifies its lipophilic properties and the solubility in ormosil is much better.[20] In view of preparation of a dual sensor which contains an oxygen and a pH transducer, the $Ru(dpp)_3TMS_2$ complex was selected as oxygen transducer and HPTS (8-hydroxypyrene-1, 3, 6-trisulfonate) immobilized on amino-modified ploy(hydroxyethyl methacrylate) (p-HEMA) will be used as pH transducer. HPTS exhibits a pH depended absorption shift allowing ratiometric measurements using an excitation ratio of 450/405 nm and its emission can be detected at ~ 510 nm. [23] The dual sensing oxygen and pH transducer can be excited at the same wavelength of ~ 460 nm. Their emissions can be clearly separated because emission of HPTS is at ~ 510 nm and of the $Ru(dpp)_3TMS_2$ complex at ~ 612 nm.

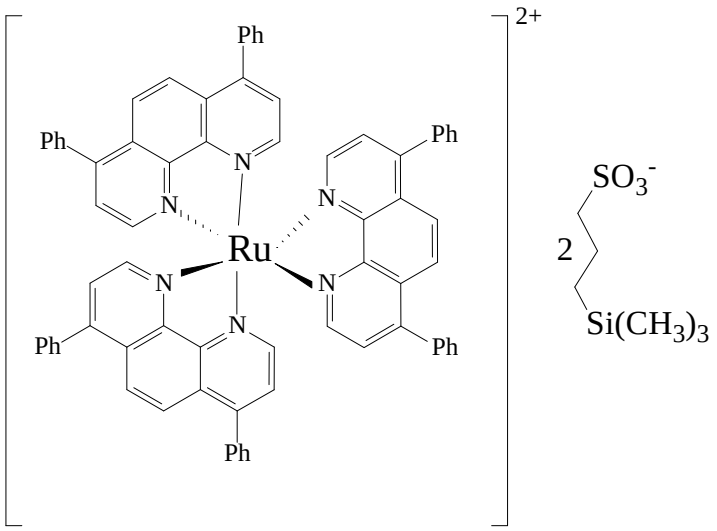

Fig. 2. *Chemical structure of the oxygen probe $Ru(dpp)_3TMS_2$*

4.3.2. Choice of Hydrogel and Ormosil

As polymer matrix the hydrogel Hydromed D4 on polyurethane basis was chosen due to its good stability. Its solubility is given in an ethanol-water mixture (90:10 v/v) and consists of hydrophilic and hydrophobic blocks which allow the embedding of lipophilic ormosil particles containing the oxygen sensitive dye $Ru(dpp)_3TMS_2$. Further on, the polymer shows best permeability for oxygen, glucose and protons.

Embedding of the oxygen sensitive dye occurred in ormosil an organically modified sol-gel which is composed of phenyltrimethoxysilane and trimethylmethoxysilane.

Hydrophobic sol-gels avoid the penetration of water into the matrix and are useful for gaseous sensing. They contain fewer silanol groups and consequently will be less densified over time which enhance the long-term and storage stability. Hydrophobic ormosils avoid the penetration of charged species into the matrix and enhance the selectivity of gas sensors.[20]

4.3.3. Oxygen Sensing Properties of the Sensor Beads SB

Oxygen sensing is based on the quenching of a photoexcited luminophore immobilized in ormosil and incorporated in a polymer matrix. A variety of luminescent species can be used as indicators. In this work ruthenium(II) tris (4,7-diphenyl-1,10-phenantholine) was used. The quenching process can be described by the modified Stern-Volmer equation (two site model):

$$\frac{I_0}{I} = \left(\frac{f_1}{1 + K_{SV1} \times pO_2} + \frac{f_2}{1 + K_{SV2} \times pO_2} \right)^{-1} \qquad \textbf{Eq. 1}$$

where I and I_0 are the luminescent intensities in the presence and absence of the quencher, K_{SV1} and K_{SV2} are the Stern-Volmer constants for two different microenvironments, f_1 and f_2 are the fractions of the total emission for each component. pO_2 is the air pressure. Normally, luminophores embedded in a polymer matrix show a non-linear behaviour which can be depicted by the modified Stern-Volmer equation. In *Fig. 3* the Stern-Volmer plot is shown. K_{SV1} is 0.0018 $mbar^{-1}$, K_{SV2} 0.0003 $mbar^{-1}$, f_1 0.4712 and f_2 0.5792.

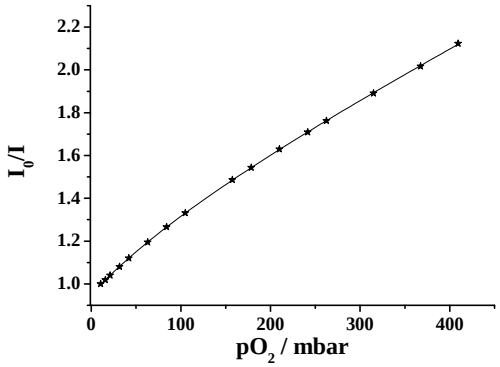

Fig. 3. *Stern-Volmer plot of the quenching of the luminescence intensity of the excited state of oxygen sensitive beads SB embedded in a hydrogel matrix.*

4.3.4. Spectral Properties of BSM3

The fluorescent beads SB display a broad excitation band with its maximum around 468 nm. The SB beads can be excited efficiently at wavelengths between 460 nm and 470 nm, for example using a 470 nm LED. The luminescence emission spectrum exhibits its maximum at 468 nm. The excitation and emission spectrum is shown in *Fig. 4*. An increase of luminescence intensity at 612 nm is given during the oxidation of glucose catalyzed by GOx due to oxygen consumption. GOx is immobilized in the sensor matrix. In *Fig. 4* the excitation and emission spectra of BSM3 are given in presence of MOPS buffer and varying concentrations (0.2 to 2.0 mM) of glucose.

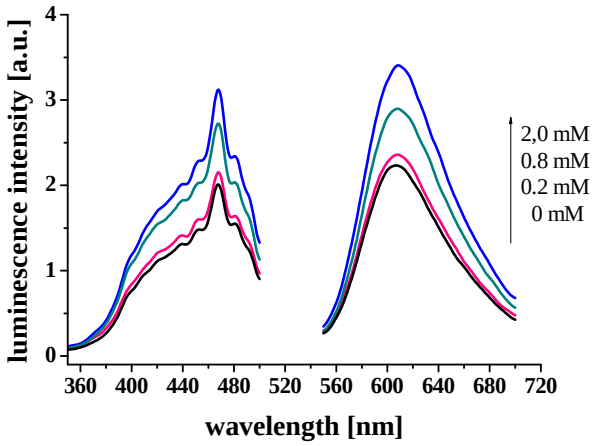

Fig. 4. *Excitation (left) and emission (right) spectra of biosensor membrane BSM3 containing the Ru-complex in MOPS buffer solution (pH 7.5) at glucose concentrations of 0 to 2.0 mM.*

4.3.5. Effect of pH on BSM3

The activity of GOx is pH dependent. The maximum activity of GOx in solution is given at pH 5.1 and 35 °C.[24] The pH dependency of the luminescence change was investigated by exposing BSM3 to a 1 mM glucose solution which is shown in *Fig. 5*. A broad pH maximum is observed in the range from 5.5 to 7.5. For pH 4.0 to 5.5 luminescence changes are strongly pH dependent. Due to crosslinking of GOx with glutaraldehyde and immobilization in the sensor matrix the pH optimum is shifted to neutral pH. For all further measurements a pH at 7.0 was chosen.

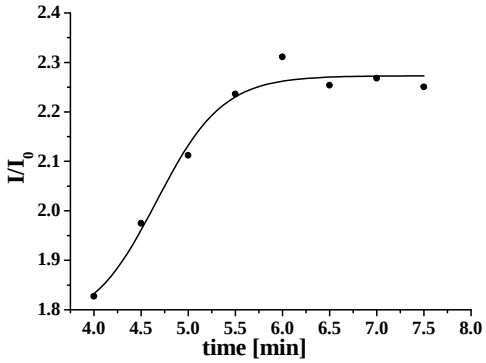

Fig. 5. *Effect of pH on luminescence change of biosensor BSM3 upon exposure to 1.0 mM glucose at various pH´s.*

4.3.6. Effect of Crosslinking and Immobilization in the Sensor Matrix

The enzyme glucose oxidase has to be crosslinked with glutaraldehyde before its immobilization in the sensor membrane. Glucose oxidase from *Aspergillus niger* is a dimer which consists of 2 equal subunits. Each unit contains one flavin adenine dinucleotide moiety and one iron. GOx is a glucoprotein which contains neutral sugars, amino sugars, 3 cysteine residues and 8 potential sites for N-linked glycosylation.[24] The glutaraldehyde crosslinking is carried out according to *chapter 3.4.6*. A network structure is formed and hence, the effect of leaching out from the sensor membrane is avoided compared to single GOx molecules. The reaction is performed at room temperature and pH 7.0. Increasing concentrations of glutaraldehyde and reaction times between glutaraldehyde and GOx reduce the GOx activity. A crosslinking time of 1 h and a glutaraldehyde concentration of 0.05 % are sufficient. Higher glutaraldehyde concentrations affect the GOx activity dramatically.

4.3.7. Response of Biosensor BSM3

Glucose oxidase catalyzes the oxidation of glucose into gluconic acid and hydrogen peroxide accompanied by the simultaneous consumption of dissolved oxygen. The oxygen consumption can be measured by the effect of luminescence increase of the oxygen transducer $Ru(dpp)_3TMS_2$. The increase in luminescence intensity can be detected as analytical signal. *Fig. 6* shows the typical response curve for the glucose biosensor membrane BSM3. Increasing concentrations of glucose cause an increase in luminescence intensity of the oxygen transducer. Biosensor membrane BSM3 is sensitive to glucose in the concentration

range from 0.2 to 3.0 mM. Highest signal changes can be detected in the concentration range from 0.2 to 1.0 mM. At higher concentrations no further changes in luminescence intensity can be detected.

The response time for biosensor membrane BSM3 is approximately 0.9 min for a signal change of 90 % (t_{90}). The time for returning back to the baseline by washing with MOPS buffer (13 mM; pH 7.0) takes around 2.1 min. Further on, the response time is depending on the GOx activity which is immobilized in the sensor membrane and the layer thickness. The layer thickness of biosensor membrane BSM3 is 120 µm under wet conditions and after drying approximately 12 µm. Increasing layer thicknesses prolong the response time but not the shape of the calibration plot. The application of thinner layer thicknesses is not feasible due to the bead size of SB. Their size is around 5 µm estimated via a fluorescence microscopy. Layer thicknesses lower than 5 µm cause an uneven layer surface where the oxygen sensitive beads are poorly fixed in the sensor membrane.

The flow rate affects the response of the glucose biosensor. Biosensor membrane BSM3 was exposed to a 0.8 mM glucose solution at varying flow rates. The luminescence change is decreasing with increasing flow rates. The oxygen consumption during the reaction causes a decrease in the oxygen concentration in the membrane. Hence, a kinetic equilibrium is adjusted which is dependent on the rates of oxygen consumption and supply.[25] Therefore, the oxygen transport is controlled by the flow rate.[25] Flow rates of 2 mL/min or higher cause low luminescence changes, but the response times (t_{90}) are faster. Lower flow rates are favourable to the enzymatic oxidation of glucose which results in a larger luminescence change. The agreement between luminescence change and the response was a flow rate of 0.7 mL/min which was applied to all further measurements.

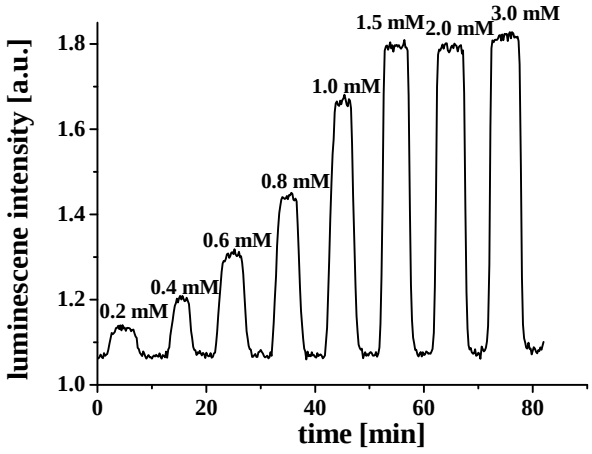

Fig. 6. *Response curve of glucose biosensor membrane BSM3 towards glucose solutions passing at a flow rate of 0.7 mL/min.*

4.3.8. Calibration Plot for BSM3

Fig. 7 shows the calibration plot for biosensor BSM3 obtained from the corresponding response curve. Immobilization of varying quantities of GOx in the sensor matrix cause different calibration curves. The dynamic range and the signal changes depends on the activity of GOx immobilized in the biosensor membrane BSM3. High enzyme activities are responsible for a large oxygen gradient along the biosensor membrane. Therefore, large luminescence changes are obtained. The analytical range decreases with increasing enzyme activities due to fast oxygen consumption in the sensor membrane whereas small amounts of GOx enlarge the analytical ranges. Best results are received at a GOx activity of 600 units immobilized in the biosensor membrane. The calibration plot shows a sigmoidal progression with a dynamic range from 0.2 to 1.0 mM. The limit of detection at a signal-to-noise ratio of 3 is 0.2 mM.

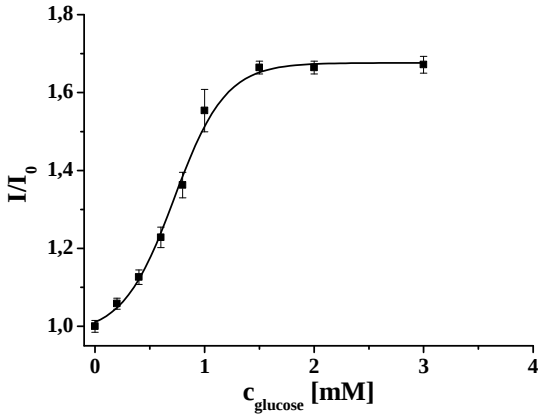

Fig. 7. *Calibration plot for biosensor membrane BSM3.*

4.3.9. Repeatability and Stability of Biosensor BSM3

For investigation of the repeatability of the glucose biosensor membrane BSM3, it was 5 times alternating exposed to a 0.8 mM glucose and MOPS buffer (13 mM; pH 7.0) solution during a period of 7 hours. The biosensor offers good repeatability with a standard deviation of 0.95. The stable response assumes on the one hand the enzyme GOx is not leaching out of the sensor membrane and on the other hand the oxygen sensitive dye is photostable.

The stability of biosensor BSM3 was analyzed in a period of three weeks. BSM3 is stable when it is stored in MOPS buffer (13 mM; pH 7.0) at 4 °C. MOPS buffer have to be changed every week for avoiding the growth of micro-organisms. The response towards a 0.8 mM glucose solution is stable in this time period.

4.3.10. Interferences

The disadvantage of amperometric glucose sensors is the poor electrochemical selectivity. The main interferences are the electroactive compounds ascorbic acid, uric acid or acetaminophen which can be oxidized at the applied potential and can manipulate the current signal.[26] Usually, ascorbic acid, uric acid and acetaminophen after oral taking are present in physiological samples like blood. Consequently, wrong glucose concentrations are measured and hyper-or hypoglycaemia cannot be detected. For avoiding this effect the electrodes are coated with Nafion which is applied as a permselective barrier to retard the entry of anionic biological interferences.[5,27]

The interferences ascorbic acid, uric acid, citric acid and acetaminophen were evaluated. The response of the biosensor BSM3 was determined by exposing to these acids in presence of 0.8 mM glucose. Fructose and sucrose were tested as well in presence of 0.8 mM glucose. The results are summarized in *Table 1*.

Table 1. *Effect of interferences to 0.8 mM glucose*

Interference	Test concentration mg/dL	Interference effect at 0.8 mM glucose
Ascorbic acid	0.3	<0.02
	1.3	<0.01
	6.3	<0.01
Citric acid	8.4	<0.02
	21	<0.02
Uric acid	0.6	<0.06
	2.9	<0.06
	5.8	<0.06
Acetaminophen	1	<0.02
	10	<0.02
Fructose	1.8	<0.01
	18.0	<0.01
	180	<0.01
Sucrose	3.4	<0.02
	34.2	<0.02
	342	<0.02

4.4. Results and Discussion for Determination of Glucose via pH Transduction

In this chapter the determination of glucose via a pH transducer is shown. The main idea described in this chapter was the development of a dual sensor for glucose. Glucose can be determined via oxygen and pH transduction. In *chapter 4.3* glucose was determined via an oxygen transducer which achieved good results. The principle of the dual sensor is based on the glucose determination simultaneously via oxygen and pH transducers which are excited at the same wavelength. Favourably is the photoexcitation can be carried out for example with one LED. The emissions of both transducers can be detected at different wavelengths and therefore no overlap is given.

8-Hydroxy-pyrene-1,3,6,-trisulfonate (HPTS) was applied as pH transducer which was immobilized to two different kinds of particles. First, it was covalently linked to an amino-modified poly(hydroxyethyl methacrylate) (p-HEMA) (bead size ~ 5 µm) and secondly it was immobilized by electrostatic attraction to polymer beads which have quaternary amino groups on the surface. These particles (PLSAX) are a combination of the rigid macroporous polystyrene/divinyl benzene polymer matrix and the chemically stable quaternized polyethylimine with a bead size of 10 µm. The absorption band of HPTS in a alkaline solution is at around 460 nm, which disappears when the solution becomes acidic. The more the solution becomes acidic the less the light will be absorbed and consequently emitted at a wavelength of ~ 510 nm. In acidic solutions the absorption band is shifted from ~ 460 nm to 405 nm, but emission occurs always at the same wavelength (~ 510 nm). Hence, the luminescence of HPTS increases with the pH when excited at 460 nm.[28] In this work the beads HPTS/p-HEMA or HPTS/(PLSAX) are embedded in a polyurethane hydrogel matrix whose properties are explained in *chapter 4.3.2*. Both kinds of HPTS-beads were calibrated with Robinson-Britton buffer solutions (10 mM) in the pH range from 2 to 11. In *Fig. 8* the calibration plots are shown. The pK_a for HPTS/pHEMA is 8.4 and for HPTS/PLSAX 4.9. pH changes can be detected by HPTS/pHEMA beads in the pH range from 7 to 9 and for HPTS/PLSAX beads from 4 to 6.

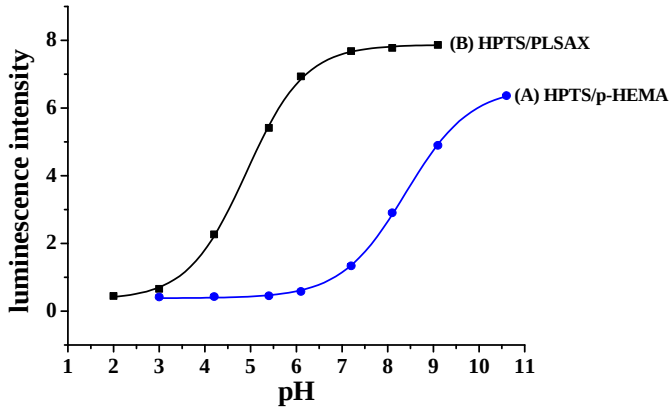

Fig. 8. *pH dependency of the luminescence intensity of HPTS immobilized on (A) p-HEMA, (B) PLSAX and embedded in a hydrogel matrix. Excitation wavelength was 468 nm.*

In view of application of the biosensor near neutral pH HPTS covalently linked to p-HEMA is the best alternative. Preparation of biosensor BSM4 was performed according to *chapter 4.2.3 and 4.2.5*. All measurements were done in a self-made flow through cell according to *chapter 4.2.6* and *4.2.7* and carried out in Robinson-Britton buffer (0.1 mM; pH 8.4) at room temperature.

The enzyme GOx catalyzes the oxidation of glucose into hydrogen peroxide and gluconic acid under oxygen consumption. The product gluconic acid dissociates and a pH change in the microenvironment of the biosensor membrane was generated. The pH shift is measured by the effect of luminescence decrease of the pH indicator. The typical response curve for this biosensor membrane BSM4 is given in *Fig. 9 (A)*. High signal changes are obtained using a 0.1 mM buffer solution, at higher concentrations no significant change in luminescence can be detected. Probably the amount of the produced gluconic acid is sufficiently compensated by the buffer capacity. Biosensor membrane BSM4 is sensitive to glucose in the concentration range from 0 to 1.5 M which is shown in *Fig. 9 (B)*.

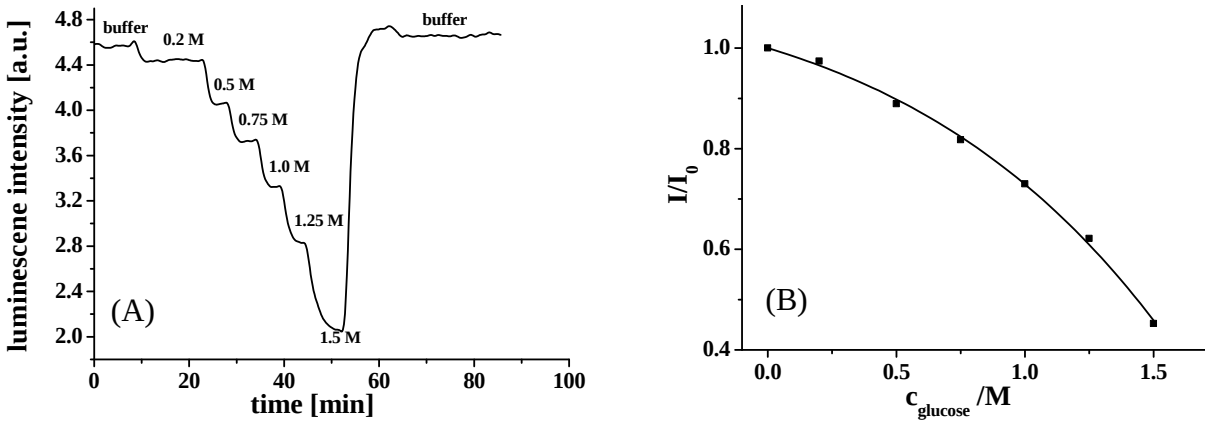

Fig. 9. *(A) Response curve of biosensor membrane BSM4 for determination of glucose via pH transduction; (B) Calibration plot for glucose from the resulting response curve.*

The determination of glucose in the millimolar range would be preferable but no signal changes could be detected. Compared to biosensor membrane BSM3 glucose is detected in the millimolar range. On this account the combination of pH and oxygen transduction for glucose monitoring is not realizable. Further on, the reproducibility of this result is low and the calibration plots are varying.

HPTS was replaced by the commonly used pH transducer carboxyfluorescein (CF) which was covalently linked to an amino-modified hydrogel and the bead size was around 5 µm. The excitation maximum is located at 492 nm, but excitation at 468 nm is also possible due to a broad excitation band, emission can be detected at 530 nm. The pK_a of the CF beads is 6.8. Once a time glucose could be determined in the millimolar concentration range using 0.1 mM buffer solutions of pH 7 but the response time for each concentration takes more than 30 min and no steady state was obtained. Further on, the return back to the baseline is very time consuming and due to its bad photostability the baseline cannot be reached again. In this work glucose monitoring via pH transduction was not realizable.

4.5. Conclusion

In the first part of this chapter, a luminescent glucose biosensor was developed by incorporation of the enzyme glucose oxidase and the oxygen probe in a hydrogel matrix on basis of polyurethane. The principle of this biosensor is based on the detection of glucose via an oxygen transducer. The influence of the parameters pH, flow rate and common

interferences has been investigated. The foremost advantage of this sensor is, it consists of one layer which contains the oxygen probe and the enzyme glucose oxidase compared to two layer optical biosensors.[1,17] Further advantages are compared to other optical biosensors which are described in literature are (1) excitation and emission occurs in the visible range, and (2) the large Stokes´ shift which allows the separation of the luminescence from the stray light. The dynamic concentration range of the biosensor for determination of glucose is between 0 and 1 mM. Normal glucose levels are in the range 4.4 to 6.6 mM.[29] For the determination of glucose in blood serum, serum samples have to be diluted with buffer before application. The advantage of dilution is also that the effect of interfering species will be reduced and the pH will be kept constant during the measurements.

In the second part a luminescent glucose biosensor was developed based on the principle of pH sensing. The main idea in this chapter was the development of a dual sensor for determination of glucose via oxygen and pH transduction. Initially, two single biosensors should be prepared and then combined for simultaneous sensing. The product gluconic acid which is produced during the oxidation process of glucose catalyzed by GOx dissociates and the pH in the microenvironment of the biosensor changes. This can be detected by the luminescence decrease of the pH indicator. Disadvantageous of this biosensor is that the results are not reproducible and the dynamic range is in the molar range which does not allow the preparation of a dual sensor for glucose monitoring.

4.6. References

[1] Zhou Z., Qiao L., Zhang P., Xiao D., Choi M. F. F., **An optical glucose biosensor based on glucose oxidase immobilized on a swim bladder membrane** 2005. Anal. Bioanal. Chem. 383, 673-679

[2] Trettnak W., Leiner M. J. P., Wolfbeis O. S., **Optical sensors. Part 34. Fibre optic glucose biosensor with an oxygen optrode as the transducer** 1988. Analyst 113, 1519-1523

[3] Wu B., Zhang G., Zhang Y., Shuang S., Choi M. M. F., **Measurement of glucose concentrations in human plasma using a glucose biosensor** 2005. Anal. Biochem. 340, 181-183

[4] Yan W., Feng X., Chen X., Hou W., Zhu J. J., **A super highly sensitive glucose biosensor based on Au nanoparticles–AgCl@polyaniline hybrid material** 2008. Biosen. Bioelectron. 23, 925-931

[5] Zou Y., Xiang C., Sun L. X., Xu F., **Glucose biosensor based on electrodeposition of platinum nanoparticles onto carbon nanotubes and immobilizing enzyme with chitosan-SiO_2 sol-gel** 2008. Biosens. Bioelectron. 23, 1010-1016

[6] Moreno-Bondi M. C., Wolfbeis O. S., Leiner M. J., Schaffar B. P., **Oxygen optrode for use in a fiber-optic glucose biosensor** 1990. Anal. Chem. 62, 2377-2380

[7] Gorton L., Bhatti K. M., **Potentiometric determination of glucose by enzymic oxidation in a flow system** 1979. Anal. Chim. Acta 105, 43-52

[8] Guilbault G. G., Brignac P. J., Juneau M., **New substrates for the fluorimetric determination of oxidative enzymes** 1968. Anal. Chem. 40, 12561-263

[9] Guilbault G. G., Brignac P., Zimmer M., **Homovanillic acid as a fluorimetric substrate for oxidative enzymes. Analytical applications of the peroxidase, glucose oxidase, and xanthine oxidase systems** 1968. Anal. Chem. 40, 190-196

[10] Chen X., Zou J., **Application of rhodamine B hydrazide as a new fluorogenic indicator in the highly sensitive determination of hydrogen peroxide and glucose based on the catalytic effect of iron(III)-tetrasulfonatephthalocyanine** 2007. Microchim. Acta 157, 133-138

[11] Haugland R. P., **Handbook of fluorescent probes and research products** 2002, 9th ed., p. 443

[12] Phillips K. J., Cole G. W., **Test strip for blood glucose determination** 2003. U.S. Patent

[13] Wang J., **Electrochemical glucose biosensors** 2008. Chem. Rev. 108, 814-825

[14] Sato N., Okuma H., **Development of single-wall carbon nanotubes modified screen-printed electrode using a ferrocence-modified cationic surfactant for amperometric glucose applications** 2008. Sens. Actuators B 129, 188-194

[15] Uwira N., Opitz N., Luebbers D. W. **Influence of enzyme concentration and thickness of the enzyme layer on the calibration curve of the continuously measuring glucose optode** 1984. Adv. Exp. Med. Biol. 169, 913-921

[16] Wu X. J., Choi M. M. F., **An optical glucose biosensor based on entrapped-glucose oxidase in silicate xerogel hybridised with hydroxyethyl carboxymethyl cellulose** 2004. Anal. Chim. Acta 514, 219-226

[17] Yang X., Zhou Z., Xiao D., Choi M. M. F., **A fluorescent glucose biosensor based on immobilized glucose oxidase on bamboo inner shell membrane** 2006. Biosens. Bioelectron. 21, 1613-1620

[18] Schaffar B. P. H., Wolfbeis O. S., **A fast responding fiber optic glucose biosensor based on an oxygen optrode** 1990. Biosens. Bioelectron. 5, 137-148

[19] Pasic A., Koehler H., Klimant I., Schaupp L., **Miniaturized fiber-optic hybrid sensor for continuous glucose monitoring in subcutaneous tissue** 2007. Sens. Actuators B 122, 60-68

[20] Klimant I., Ruckruh F., Liebsch G., Stangelmayer A., Wolfbeis O. S., **Fast response oxygen micro-optodes based on novel soluble ormosil glasses** 1999. Mikrochim. Acta 131, 35-46

[21] Lee S. K., Shin Y. B., Pyo H. B., Park S. H., **Highly sensitive optical sensing material: thin silica xerogel doped with tris(4,7-diphenyl-1, 10-phenanthroline) ruthenium** 2001. Chem. Lett. 4, 310-311

[22] Draxler S., Lippitsch M. E., Klimant I., Kraus H., Wolfbeis O. S., **Effects of polymer matrixes on the time-resolved luminescence of a ruthenium complex quenched by oxygen** 1995. J. Phys. Chem. 99, 3162-3167

[23] Haugland R. P., **Handbook of fluorescent probes and research products** 9th ed. 2002. 836-837

[24] www.sigmaaldrich.com/catalog/search/Product/Detail/Fluka/49180

[25] Wolfbeis O. S., Oehme I., Papkovskaya N., Klimant I., **Sol-gel based glucose biosensors employing optical oxygen transducers, and a method for compensating for variable oxygen background** 2000. Biosens. Bioelectron. 15, 69-76

[26] Pasic A., Koehler H., Schaupp L., Pieber T. R., Klimant I., **Fiber-optic flow-through sensor for online monitoring of glucose** 2006. Anal. Bioanl. Chem. 386, 1293-1302

[27] Yu J., Yu D., Zhao T., Zeng B., **Development of amperometric glucose biosensor through immobilizing enzyme in a Pt nanoparticles/mesoporous carbon matrix** 2008. Talanta 74, 1586-1591

[28] Wolfbeis O. S., Fuerlinger E., Kroneis H., Marsoner H., **Fluorimetric analysis: 1. A study on fluorescent indicators for measuring near neutral ("physiological") pH-values** 1983. Freseniuns Z. Anal. Chem. 314, 119-124

[29] Wilkins E., Atanasov P., **Glucose monitoring: state of the art and future possibilities** 1996. Med. Eng. Phy. 18, 273-288

Chapter 5

Simultaneous Sensing of Glucose via an Oxygen and pH Transducer besides Monitoring of the Temperature

A triple biosensor for luminescent determination of oxygen, pH and temperature is applied for glucose sensing. The oxygen, pH and temperature transducers are incorporated in particles, which are embedded next to the enzyme glucose oxidase in a hydrogel matrix based on polyurethane. Glucose sensing can be carried out via oxygen or pH transduction. Glucose is enzymatically converted to gluconic acid and hydrogen peroxide under oxygen consumption catalyzed by the enzyme glucose oxidase (GOx). The luminescence lifetime of the oxygen probe Pt(II)-5,10,15,20-tetrakis-(2,3,4,5,6-pentafluorophenyl) porpholactone (PtTFPL) is quenched dynamically by oxygen. Gluconic acid, one of the end-products, is dissociated to gluconate and protons which lowers the pH in the microenvironment of the biosensor. This can be detected by the pH indicator 8-hydroxypyrene-1,3,6-trisulfonate (HPTS). Both the luminescence of PtTFPL and the activity of GOx are temperature dependent. Therefore a temperature transducer, the europium complex Eu(III)-tris(thenoyltrifluoroacetonato)-(2-(4-(diethylaminophenyl)-4,6-bis(3,5-dimethylpyrazol-1-yl)-1,3,5-triazine ($Eu(tta)_3(dpbt)$), is applied. PtTFPL was incorporated in the copolymer poly(styrene-co-acrylonitrile), $Eu(tta)_3(dpbt)$ was dissolved in poly(vinyl chloride), and HPTS covalently linked to an amino-modified poly(hydroxyethyl methacrylate). The measurements were performed in a microtiter plate using air saturated standard glucose solutions. The biosensor was applied for sensing of glucose via oxygen or pH transductions and for monitoring the temperature during analysis.

5.1. Introduction

Sensing of oxygen, temperature and pH is very important in many fields of technology and research like in marine research, food industry and biotechnology.[1,2,3,4] Monitoring of oxygen and pH are essential in clinical analysis. pH values higher than 7.45 results in alkalosis and lower than 7.35 in acidosis. Temperature sensing is necessary in optical sensing of oxygen because quenching is highly temperature dependent.[5] Optical methods for temperature sensing can be classified into two groups. One group is based on the temperature dependence of the absorption or reflection of defined materials, the other one on luminescence temperature dependency which can be detected by changes in wavelength, decay time or intensity.[6] Common luminescent temperature probes include inorganic phosphors, lanthanum oxysulfides and organic molecules.[6]

Simultaneous sensing of oxygen and pH or oxygen and temperature is a great progress in many areas of research and technology. In the last years many reports about dual sensing of oxygen and pH or oxygen and temperature were published.[7,8,9,10,11] The application of optical sensors displays some advantages compared to electrochemical sensors. The main advantages are that no reference element is required and the application for non-invasive measurements is feasible.[4,5]

In the last 25 years research groups sparked their interest on dual sensing of oxygen and carbon dioxide, pressure and temperature, oxygen and temperature or oxygen and pH. In the late eighties Wolfbeis et al. [12] developed a fiber-optic fluorosensor for oxygen and carbon dioxide. This dual sensor is based on a double layer design. Both indicators can be excited at the same wavelength and display different emission maxima. The emission band can be separated by interference filters. Borisov et al. [13] reported about a pCO_2/pO_2 dual sensor based on double layer design where oxygen was sensed via changes in the decay time (measured by phase fluorometry) based on a quenching process and carbon dioxide via changes in pH. Sol-gel derived films for luminescence-based oxygen and pH sensing were developed by Wencel and coworkers. [14] Oxygen sensing is performed on the basis of luminescence quenching of a ruthenium complex which is detected by phase fluorimetry and pH sensing by application of excitation ratiometric detection of the fluorescence of the pH sensitive dye. An alternative strategy for oxygen and pH sensing was the application of the DLR method. Kocincová et al. [5] reported on a fiber-optic microsensor for simultaneous sensing of oxygen and pH, or of oxygen and temperature. Here, the tip of an optical fiber was covered with the sensing material which contains both transducers.

Corresponding to *scheme 1* in *chapter 4.1* glucose can be determined by (1) measuring the consumption of oxygen during the oxidation, (2) the production of hydrogen peroxide (HP) or (3) the production of D-gluconic acid which lowers the pH of the solution. The resolution of the signal of one analyte by applying multianalyte sensing can be divided spectrally, using different excitation/emission filters or excitation light sources, or temporally, using the advantageous of different lifetimes of the applied indicators. Hence, simultaneous sensing of glucose via an oxygen and pH transducer is feasible. In this work a one layer triple sensor containing an oxygen, pH and temperature transducer is applied for the detection of glucose via oxygen and pH transduction while monitoring temperature of the environment. The biosensor preparation is simple and the application to glucose determination via the oxygen transducer is highly sensitive and selective. The oxygen, pH and temperature transducers are incorporated in particles, embedded in one layer. Sensing of glucose via an oxygen transducer occurs via detecting changes in lifetime of the oxygen probe, which is based on dynamic quenching. Monitoring of temperature is carried out by detection of the lifetime of the temperature probe. Luminescence lifetime detection is done by application of the RLD (rapid lifetime determination) method. Glucose sensing via pH is performed by detecting the changes in luminescence intensity of the pH sensitive dye. All indicators are excited at the same wavelength, but emission takes place at different wavelengths which can be detected by using suitable emission filters.

5.2. Materials and Methods

5.2.1. Material

Glucose oxidase (EC 1.1.3.4) from *Aspergillus Niger* (lyophilized, powder, 211 unit/mg), glutaraldehyde solution (50 wt % in H_2O), poly(vinyl chloride) (PVC) and poly(styrene-co-acrylonitrile) (30 wt % acrylonitrile) (PSAN) were purchased from Sigma Aldrich (Steinheim, Germany; www.sigmaaldrich.com). D-glucose, acetic acid (100 %), phosphoric acid (85 %) and boronic acid were provided by Merck (Darmstadt, Germany; www.merck.de). The pH sensitive beads consisting of 8-hydroxy-pyrene-1,3,6-trisulfonate (HPTS) covalently linked to amino-modified poly(hydroxyethyl methacrylate) (p-HEMA) which was copolymerized with N-aminoethylacrylamide was obtained from Presens

(Regensburg, Germany; www.presens.de). Pt(II)-5,10,15,20-tetrakis-(2,3,4,5,6-pentafluorophenyl) porpholactone (PtTFPL) was purchased from Frontier Scientific Europe (Cranforth, United Kingdom; www.frontiersci.com). Eu(III)-tris(thenoyltrifluoroacetonato)-(2-(4-diethylaminophenyl)-4,6-bis(3,5-dimethylpyrazol-1-yl)-1,3,5-triazine) was synthesized according to Yang et al..[15] The polyurethane hydrogel Hydromed D4 was obtained from Cardiotech (Wilmington, USA; www.cardiotech-inc.com), the polyester support (Mylar) (product number 124-098-60) from Goodfellow (Bad Nauheim, Germany; www.goodfellow.de). All chemicals and solvents were of analytical grade and were used without further purification. Doubly distilled water was used for preparation of Robinson Britton buffer which was adjusted to pH 8.5 with 1 mM sodium hydroxide. Glucose solutions were daily prepared in 0.01 mM Robinson-Britton buffer (pH 8.5) containing 0.1 M NaCl.

The syntheses of the platinum-based oxygen sensitive particles PtTFPL/PSAN and europium-based temperature sensitive particles $Eu(tta)_3(dpbt)$/PVC were prepared by Stich et. al. as reported before.[16]

5.2.2. Buffer Preparation

Doubly distilled water was used for the preparation of the buffer solution. A stock solution of Robinson-Britton buffer was prepared by dissolving 247 mg boronic acid, 228 µL acetic acid (100 %) and 229 µL phosphoric acid (85 %) in 100 mL of water. 2.5 mL of the stock solution and 5.8 g NaCl as background electrolyte were added to 970 mL of doubly distilled water, adjusted to pH 8.5 with sodium hydroxide (1 M) and filled up to 1000 mL.

5.2.3. Crosslinking of Glucose Oxidase with Glutaraldehyde

GOx is crosslinked with glutaraldehyde to obtain a network structure which avoids leaching out of the sensor membrane after immobilization compared to single GOx molecules. GOx (3.6 mg) was dissolved in 117 µL MOPS buffer (13 mM; pH 7.5) and 13 µL glutaraldehyde (0.5 wt % in H_2O) was added. The mixture was slightly shaken at room temperature for 1 hour.

5.2.4. Manufacturing of Triple Biosensor Membrane BSM5

Specifically, 11 mg $Eu(tta)_3(dpbt)$/PVC particles synthesized by Stich et al.[16], 36.0 mg HPTS/p-HEMA particles and 23.5 mg PtTFPL/PSAN particles, synthesized by Stich et al.[16], were dispersed in 2 g of a 5 % wt solution of hydrogel in ethanol/water (9:1, v:v) and stirred over night to get a homogeneous distribution of the particles. From this cocktail, containing oxygen, pH and temperature sensitive particles, 500 µL were taken, and 130 µL glucose oxidase solution (activity 770 units) crosslinked with glutaraldehyde *according to 4.2.3* was added, stirred and spread onto a polyester support using a self made knife coating device. The thickness of the wet biosensor layer was 120 µm. After drying at room temperature for 1 h BSM5 was stored in MOPS buffer (13 mM, pH 7.0). *Fig. 1* shows the cross-section through biosensor membrane BSM5.

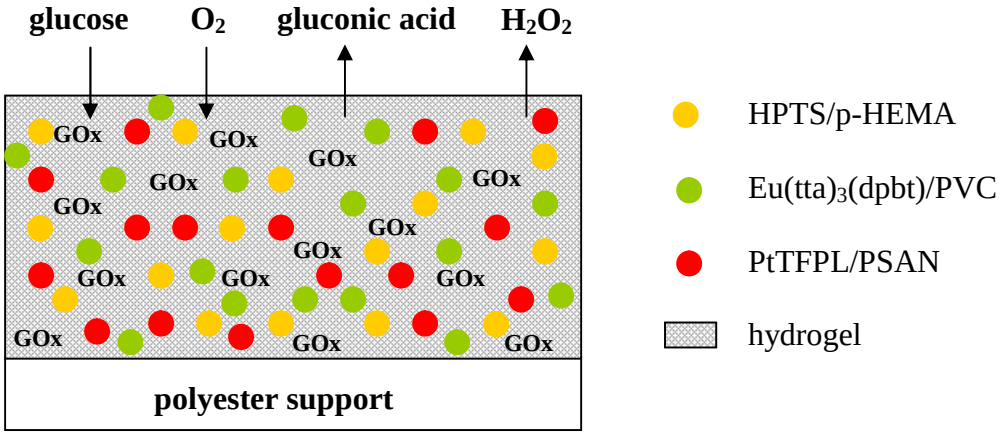

Fig. 1. *Cross-section through biosensor membrane BSM5. The hydrogel layer contains the probes for oxygen, pH, and temperature, and the enzyme glucose oxidase.*

5.3. Instrumental and Measurements

5.3.1. Instrumental

Excitation and emission spectra were acquired on an Aminco Bowman AB2 luminescence spectrometer (from SLM Spectronic Unicam). Luminescence intensity was excited at 400 nm and emission was detected at 610 nm for the temperature sensitive europium dye, at 750 nm for the oxygen sensitive platinum dye and at 510 nm for the pH sensitive dye. pH was adjusted with a pH meter (CG 842 from Schott;

www.schottinstruments.com). Sensor films were prepared by a self made knife coating device (see *chapter 3.3.1*).

5.3.2. Lifetime Measurements for Characterization of BSM5

The lifetimes of the oxygen and temperature probes were measured with an imaging set up shown in *Fig. 2*. Sensor spots of an average diameter of 0.5 cm were placed in the wells of a microtiter plate. The wells were filled with 100 µL glucose solutions of varying concentrations (0 to 3.0 mM) and covered with 100 µL paraffin oil for avoiding oxygen penetration. For every glucose concentration the lifetime of the oxygen probe was determined in three replicates. The spots were excited with a 96-LED array and the light of a pulsed LED array passes an excitation filter which hits the spots in the wells. The emission of the oxygen and temperature probe is separated by emission filters and detected by a CCD camera. Subsequently, the lifetimes were calculated according to *equation 1* in *chapter 5.4.2.*

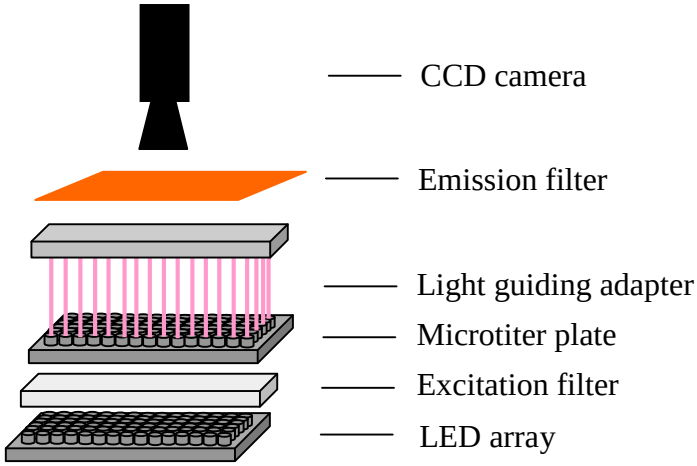

Fig. 2. *Scheme of imaging set up.*

5.3.3. Luminescence Measurements for Characterization of BSM5

The luminescence intensity of the pH indicator HPTS was carried out with an imaging set up which is depicted in *Fig. 3*. HPTS is excited by a 405 nm LED. Light with a wavelength of 405 nm hits to the sensor membrane, where HPTS was excited, and the emission light was filtered by an emission filter and detected by a CCD camera.

The instrumental set up in *Fig. 3* was applied for testing the response of BSM5 to various pH-values ranging from 3 to 11.5. Here, 2 mL of a Robinson-Britton buffer solution

of varying pH was filled into the glass vessel. Luminescence intensity was measured after 15 min. Afterwards BSM5 was washed with doubly distilled water and the next pH solution was added.

For determination of glucose with BSM5 2 mL of a glucose solution (prepared in 0.01 mM Robinson Britton pH 8.5) ranging from 0 to 3 mM were filled into the glass vessel. The luminescence intensity was measured after 45 minutes. Afterwards the glucose solution was replaced by a higher concentrated glucose solution and luminescence intensity was measured again after 45 minutes.

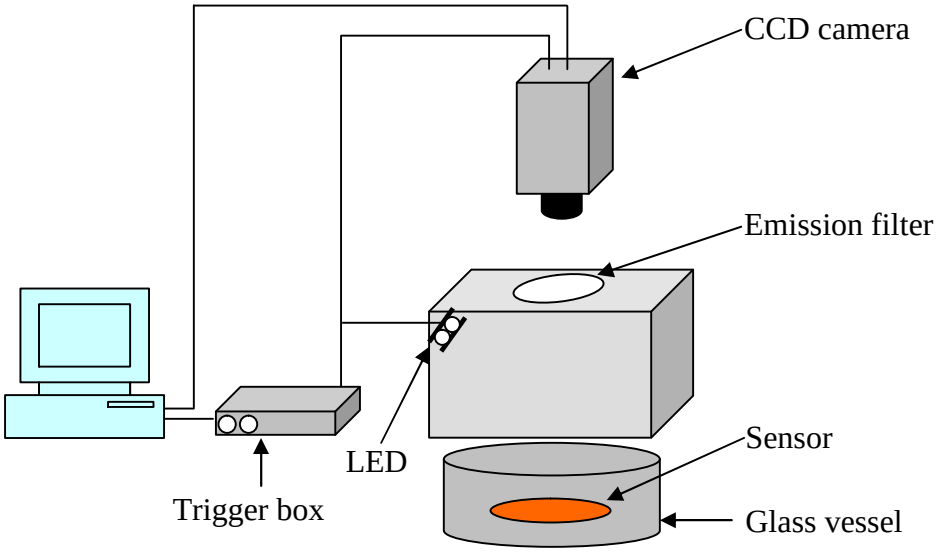

Fig. 3. *Imaging set up for determination of luminescence intensity of HPTS.*

5.4. Results and Discussion

5.4.1. Choice of Indicators

Pt(II) or Pd(II) complexes are widely applied as oxygen sensitive materials. Most work was done with ruthenium complexes such as Ru(II)-tris(4,7-diphenyl-1,10-phenanthroline)$^{2+}$ which displays a long lifetime, high quantum yield and a large Stokes´ shift.[17] Phosphorescent complexes of Pt(II) have much longer lifetimes, larger Stokes´ shifts, and higher luminescent quantum yields.[18] Due to these properties, Pt(II)-5,10,15,20-tetrakis-(2,3,4,5,6-pentafluorophenyl) porpholactone (PtTFPL) was applied as the oxygen probe. PtTFPL shows a strong absorption band around 390 nm, a large Stokes´ shift (~360 nm) and

long lifetimes (7 - 42 µs).[19] In *Fig. 4* the chemical structure and the absorption and emission spectra of PtTFPL are given. PtTFPL was incorporated into the copolymer poly(styrene-co-acrylonitrile) (PSAN) for increasing the dynamic range of the oxygen determination. PSAN is moderate gas permeable (its oxygen permeability coefficient *P* $3.5 \cdot 10^{-14}$ cm^2 Pa s^{-1}) which reduces the fast dynamically quenching of the luminescence intensity of PtTFPL.[20]

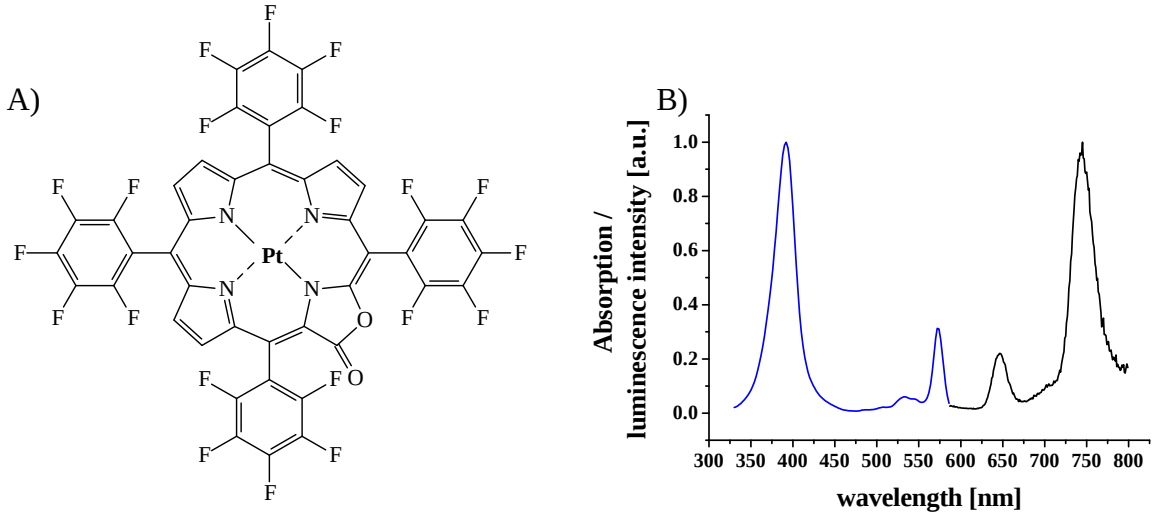

Fig. 4. *(A) Chemical structure of PtTFPL; (B) Absorption (blue) and emission (black) spectra of PtTFPL in toluene.*

Generally, europium(III) complexes exhibit long luminescence decay times (0.1 to 1 ms) and emit in a narrow optical window. [21,22,23] The probe $Eu(tta)_3(dpbt)$ was chosen as the temperature sensitive indicator due to its strong absorption around 400 nm, the large Stokes´ shift (~ 214 nm), the high quantum yield (~ 0.39) and the long luminescence lifetime (480 µs at 25 °C).[24] The lifetime is increasing with decreasing temperature. At 1 °C the lifetime raises up to 620 µs.[24] Light is absorbed by the organic ligand of europium complexes and the energy is transferred through intersystem crossing and intramoleculary energy transfer to the Eu^{3+} ion which emits the luminescence.[25,26] The temperature sensitivity is depending on the efficiency of thermal quenching. The largest contribution comes from the thermal deactivation of $^5D_1$ and $^5D_0$ europium energy levels. In this process the electronic energy level is coupled to the environment through molecular vibration energy levels.[6] Therefore, temperature affects the efficiency of the energy transfer from antenna ligand to the Eu^{3+}-ion. The chemical structure and the absorption and emission spectra of $Eu(tta)_3(dpbt)$ are shown in *Fig. 5*.

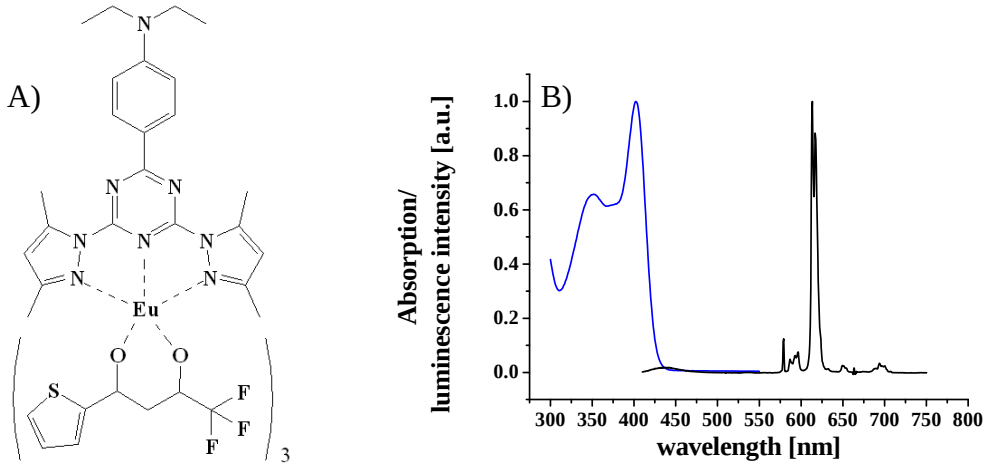

Fig. 5. *(A) Chemical structure of Eu(tta)$_3$(dpbt); (B) Absorption (blue) and emission (black) spectra of Eu(tta)$_3$(dpbt) in toluene.*

8-hydroxypyrene-1,3,6-trisulfonate displays a strong pH dependency of its luminescence intensity. It also exhibits a pH dependent absorption which allow ratiometric measurements using the excitation ratio at 450/405 nm.[27] The emission is detected at 520 ± 10 nm. HPTS is an ideal indicator for sensing physiological pH (pK_a ~ 7.3 in aqueous buffer solutions).[27] The immobilization of HPTS covalently to p-HEMA and the incorporation in a hydrogel shift the pK_a to higher values. The chemical structure and the excitation and emission spectra of HPTS are shown in *Fig. 6*.

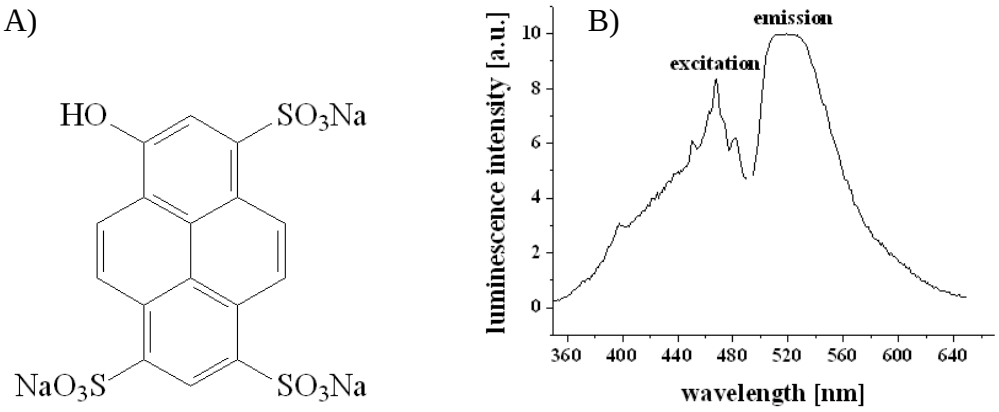

Fig. 6. *(A) Chemical structure of HPTS; (B) Excitation and emission spectra of HPTS covalently linked to p-HEMA and incorporated in a hydrogel membrane. Measurements are done at pH 9 and room temperature.*

The hydrogel Hydromed D4 is polyurethane based and was chosen as the polymer matrix because it is uncharged, highly proton permeable and very stable. It has a water uptake

capacity of more than 50 % and contains hydrophilic regions and hydrophobic blocks which allows the embedding of the HPTS/p-HEMA, the $Eu(tta)_3(dpbt)$/PVC and the PtTFPL/PSAN particles.[28]

5.4.2. Rapid Lifetime Determination (RLD)

Luminescence lifetime determination is a pleasant parameter in optical chemical sensing. It is neither influenced by fluctuations of the overall intensity, nor by variations of the optical properties of the samples including turbidity, coloration and refractive index.[29] The rapid lifetime determination (RLD) is a time domain method for lifetime based imaging. Generally, lifetime can be detected in the time domain or the frequency domain modus.[30] After excitation with a square wave-pulsed light source, luminescence is detected in two different gates (A_1 and A_2) which are located in the emission phase (see *Fig. 7*). For recording the intensities a CCD camera is used. The ratio (A_1/A_2) of the two intensity data matrices is related to the lifetime of the indicator luminescence in the sensor membrane and is independent from the whole signal intensity.[29] The lifetime τ can be calculated according to *equation 1* in the case of monoexponential decay and a constant time for each gate.

$$\tau = \frac{t_2 - t_1}{\ln \frac{A_1}{A_2}} \qquad \textbf{Eq. 1}$$

A_1 and A_2 are the intensities of both gates in the emission phase and t_1 and t_2 are the times when the first and the second gate are opened.

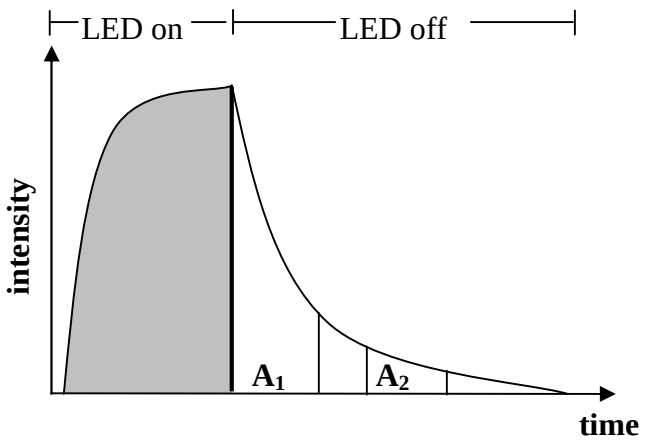

Fig. 7. *Schematic of rapid lifetime determination (RLD) method.*

Generally, the first gate is opened after a time period of 100 ns after switching off the LED. With that delay the background fluorescence e.g. from the sample has fully decayed and interferences of backscattered excitation light is also eliminated.[29] In this work the first gate was opened immediately after switching off the LED because there are no differences in the results. Biosensor membrane BSM5 was imaged and calibrated by this method. After excitation with a square wave-pulsed light of a LED (405 nm) two images (for every gate) were taken during the luminescence lifetime period of the luminophore mixture (Pt(TFPL) and $Eu(tta)_3(dpbt)$) (see *table 1*).

Table 1. *Parameters applied for calibration of the triple sensor material.*

	Pt(TFPL) (O_2)		**$Eu(tta)_3(dpbt)$ (T)**	
Excitation period	160 µs		2000 µs	
	A_1	A_2	A_1	A_2
delay/µs	0	20	0	100
gate	50	50	400	400

5.4.3. Spectral Properties

The spectra of the oxygen-, temperature- and pH-transducers are shown in *chapter 5.4.1*. An important characteristic for the choice of these indicators is the excitation by one light source. Pt(TFPL) and $Eu(tta)_3(dpbt)$ display strong absorption at 400 nm. However, HPTS exhibits its absorption maximum at 405 or 470 nm depending on the pH. The maximum absorption is at 470 nm at pH > 8, whereas at < 6 the maximum is at 405 nm. Hence, all fluorophores can be excited at 405 nm using a violet LED or a 405 nm diode laser. The excitation light passes a BG12 longpass filter for removing any LED stray light.

The emission of Pt(TFPL) can be imaged applying the long pass emission filter RG 695, the emission of $Eu(tta)_3(dpbt)$ applying the bandpass filter D610/60 and for HPTS applying the bandpass filter D530/50. The emission spectra of the transducer and the transmission spectra of the optical filters are shown in *Fig. 8*.

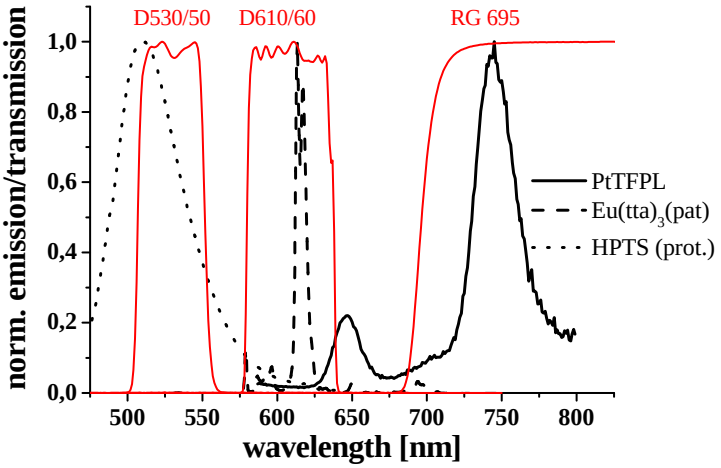

Fig. 8. *Emission spectra of pH, oxygen and temperature probe combined with the transmission spectra of the emission filters.*

5.4.4. Oxygen Sensing Properties of the PtTFPL/PSAN Particles

Luminescent probe materials embedded in polymer matrices show different microenvironments resulting in multiple sites where quenching can happen. Hence, the steady state Stern-Volmer shows non-linear characteristics. [31] Various quenching mechanisms are suggested in literature such as the two exponential/two-site model, the log-Gaussian model and the three parameter model.[32] The most often applied model is the two site model which is expressed in *equation 2*. It is simple and results in a reasonable approximation to the sensor response.[32]

$$\frac{\tau_0}{\tau} = \left(\frac{f_1}{1 + K_{SV1} * pO_2} + \frac{f_2}{1 + K_{SV2} * pO_2} \right)^{-1} \qquad \textbf{Eq. 2.}$$

τ_0 and τ are the unquenched and quenched lifetimes of the oxygen probe, K_{SV1} and K_{SV2} are the Stern-Volmer constants for the two microenvironments, and f_1 and f_2 are the fractions of the total emission for each component, pO_2 is the partial pressure of oxygen which causes the decrease of the luminescence intensity. The Stern-Volmer plot is shown in *Fig. 9* and the Stern-Volmer constants K_{SV1} and K_{SV2} with the parameters f_1 and f_2 are given in *table 2*. The application of air-saturated standard glucose solutions for calibration of BSM5 is adequate due to the strong quenching effect at 213 mbar.

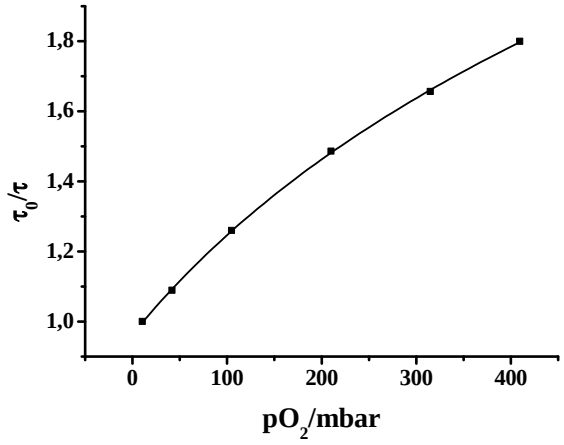

Fig. 9. *Stern-Volmer plot of the quenching of the luminescence intensity of PtTFPL/PSAN particles in a hydrogel matrix in presence of oxygen at different pressures at 24 °C.*

Table 2. *Stern-Volmer constants from the calibration of the oxygen sensitive dye PtTFPL incorporated in PSAN and embedded in a hydrogel matrix.*

Temperature/°C	**f_1**	**f_2**	**$K_{SV1}\cdot10^{-3}$/mbar**	**$K_{SV2}\cdot10^{-3}$/mbar**
24	0.660	0.377	5.27 ± 0.001	0.21 ± 0.0004

5.4.5. Temperature Sensing Properties of the $Eu(tta)_3(dpbt)$/PVC Particles

The response of the $Eu(tta)_3(dpbt)$/PVC particles subjected to the temperature is shown in *Fig. 10.* The temperature dependency of the luminescence lifetime can be described by the Arrhenius equation according to *equation 3*.

$$\tau = \left(k_0 + k_1 \exp\left(-\frac{\Delta E}{RT} \right) \right)^{-1} \qquad \textbf{Eq. 3}$$

k_0 is the temperature-independent decay rate of the excited-state deactivation, k_1 a pre-exponential factor, R the gas constant and ΔE the energy gap between emitting level and higher excited-state level.[5,33] The temperature dependency can be fitted by *equation 3* using the following parameters at 1000 mbar air pressure ($k_0 = 1.7$ ms^{-1}, $k_1 = 1.8\cdot10^8$ ms^{-1}, and $\Delta E =$ 47.6 kJ/mol). The correlation coefficient (r^2) was 0.9985.

The sensitivity is excellent because the lifetime drops by more than 1.8-fold when the temperature is increased from 1 °C to 36 °C. Monitoring of the temperature during an

enzymatic oxidation process is important because the activity of enzymes is mostly temperature dependent. Due to the exceeding temperature sensitivity of $Eu(tta)_3(dpbt)$, even slight temperature changes can be detected.

Glucose oxidase, applied in this work, displays its activity maximum at 35 °C in solutions but the determination of glucose occurs at ambient temperature.[34] Sensing of glucose requires a constant temperature for avoiding activity changes of GOx during the oxidation process. Hence, controlling of the temperature warrants that the activity of GOx is identical during the experiment.

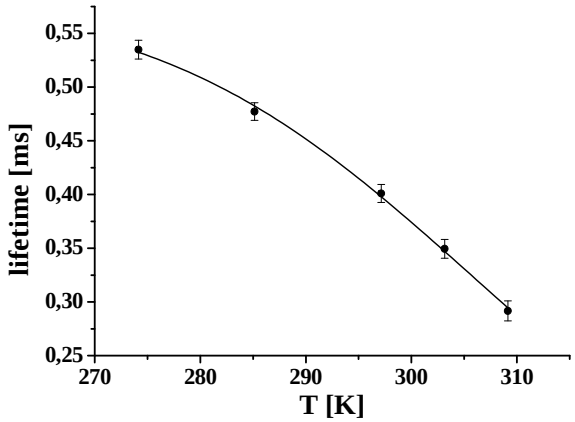

Fig. 10. *Response of $Eu(tta)_3(dpbt)$/PVC particles embedded in a hydrogel matrix to temperatures from 270 to 310 K.*

5.4.6. pH Sensing Properties of the HPTS/p-HEMA Particles

8-Hydroxypyrene-1,3,6-trisulfonate has been evaluated to be the ideal fluorescent indicator for measurement of physiological pH.[35] In this work HPTS was covalently linked to amino-modified poly(hydroxyethyl methacrylate) and embedded in a hydrogel on polyurethane basis. A decrease in the luminescence occurs in the pH range from 7.5 to 9. The pK_a value of the material is 8.4. The pH response curve of HPTS, covalently linked to p-HEMA and embedded in a hydrogel matrix, is shown in *Fig. 11*. A linear relation between pH and luminescence change exists in the pH range from 7.8 to 9. The starting pH for determination of glucose via pH transduction was 8.5 because the production of gluconic acid during the oxidation shifts the pH to lower values.

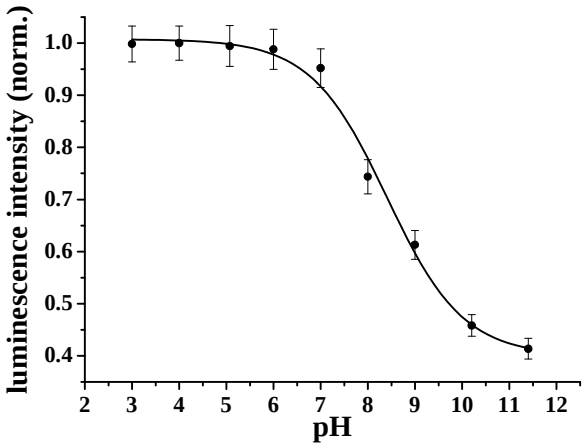

Fig. 11. *pH response of HPTS covalently linked to p-HEMA and embedded in a hydrogel matrix. All measurements are performed at room temperature and air pressure.*

5.4.7. Effect of Experimental Parameters

The pH optimum of GOx is between pH 5.5 to 8 as shown in *chapter 4.3.5* For this measurement a pH of 8.5 was chosen since the pH shift caused by the product gluconic acid can be best detected in the pH range from 7.5 to 9. To compare the results obtained by measurements of the oxygen consumption or the production of gluconic acid, identical buffer systems were applied. All measurements were performed in 0.01 mM Robinson Britton buffer with pH 8.5.

5.4.8. RLD Imaging of Glucose via the Oxygen Transducer PtTFPL

The microtiter plate (MTP) wells were filled with glucose solutions in concentrations from 0 to 3.0 mM and the lifetime of the oxygen transducer was determined by rapid lifetime imaging. The imaging process explained in *chapter 5.3.2 and 5.4.2*. The sensor spots of biosensor membrane BSM5 were located in a MTP according to *Fig 12 (A).* The sensor spots were illuminated by a 405 nm LED and the luminescence of the oxygen sensitive dye is recorded by a CCD camera. In *Fig.12 (B)* the resulting pictures are shown which reflect the luminescence intensity of the biosensor membrane spots BSM5. In the first row the luminescence intensity of PtTFPL is shown in the presence of oxygen, in the following rows the luminescence intensity gets brighter, since luminescence of PtTFPL is less quenched by oxygen due to the consumption of oxygen during the oxidation process of glucose catalyzed by GOx.

It is necessary to cover the biosensor spots placed in the MTP wells to avoid oxygen penetration from the outside. Paraffin oil was applied as cover which is a common sealing of MTP wells for avoiding evaporation of the sample. The assignment of paraffin oil as sealing is most suitable because it is water repulsive, waxen, nontoxic and inert to many chemicals and the oxygen permeability/diffusion is very low.[36]

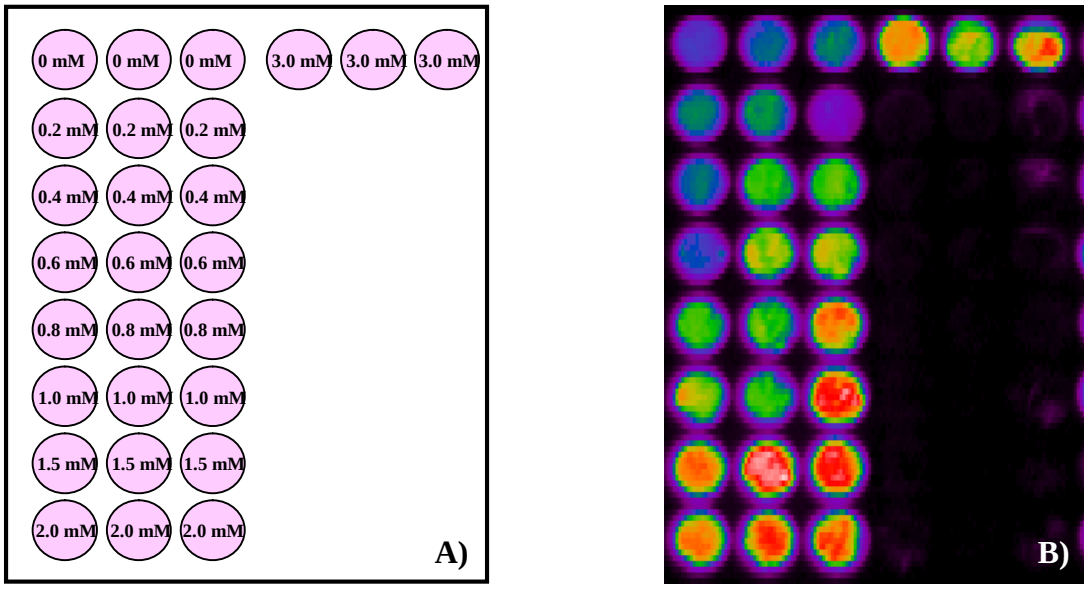

Fig. 12. *(A) Pattern of the biosensor BSM5 spots arranged in the microtiter plate. (B) Luminescence intensity of PtTFPL in presence and absence of oxygen. The blue colour means low luminescence intensity due to quenching by oxygen, red-orange colour means strong luminescence intensity of PtTFPL as result of oxygen consumption during the oxidation process of glucose catalyzed by GOx.*

Fig. 13 shows the calibration plot for the determination of glucose via the oxygen transducer PtTFPL, incorporated in PSAN and embedded in biosensor membrane BSM5. The analytical range and the signal changes depends on the activity of GOx immobilized in the biosensor membrane BSM5. High enzyme activities are responsible for a large oxygen gradient along the biosensor membrane. Therefore, large signal changes are obtained and the analytical range is smaller due to fast consuming of oxygen in the sensor membrane. Good results are achieved by immobilizing GOx with an activity of 770 units. The calibration plot shows a sigmoidal progression, which was fitted by a Boltzmann fit according to *chapter 3.4.8*, with a dynamic range from 0.2 to 1.5 mM. The limit of detection at a signal-to-noise ratio of 3 is 0.2 mM.

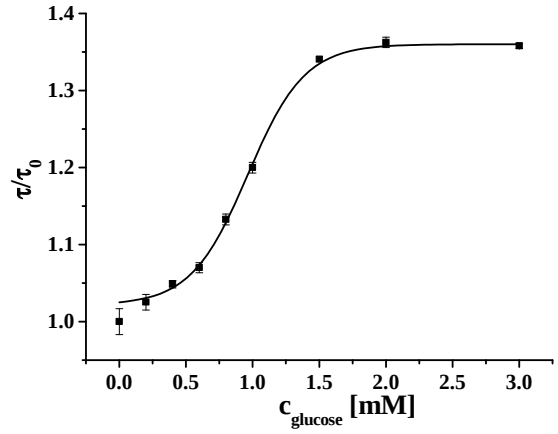

Fig. 13. *Calibration plot for glucose via the oxygen transducer PtTFPL.*

5.4.9. Imaging of the Temperature via the Temperature Transducer $Eu(tta)_3(dpbt)$

Temperature sensing is of highest importance in a broad variety of fields and applications.[23] In this work sensing of temperature is essential for monitoring the temperature during the oxidation process of glucose catalyzed by GOx which has a distinct effect on GOx activity.[37] Changes in temperature can led to changes in the activity. Low temperatures reduce the GOx activity which results in weak response and large deviations in the measurement, and higher temperatures can cause changes in the GOx conformation which reduce the GOx activity as well.[37] All measurements were performed at room temperature because the response resulted in large signal changes. Hence, a constant temperature is necessary for getting constant GOx activity during the measurement. Further on, a constant temperature is

required because the luminescence intensity of the oxygen probe PtTFPL is temperature dependent. Its luminescence is influenced by thermal quenching.

In *Fig. 14* two images of the biosensor are shown at a temperature of 16 °C and 36 °C. In the first image (*Fig. 14A*) the biosensor spot BSM5 was covered with doubly distilled water and the luminescence lifetime was detected. The temperature was determined by referencing the lifetime with the calibration curve for the temperature in *chapter 5.4.5*. In the second image (*Fig. 14B*) the biosensor spot BSM5 was covered with doubly distilled water of 36 °C. The comparison of the investigated lifetime with the calibration plot for the temperature in *chapter 5.4.5* gives the same result. In *chapter 5.4.5* is shown the lifetime decrease with an increase of the temperature. This confirms the images in *Fig. 14* because the luminescence intensity is brighter at 16 °C than at 36 °C. Hence, the application of this temperature sensitive dye is convenient for monitoring during the enzymatic oxidation of glucose.

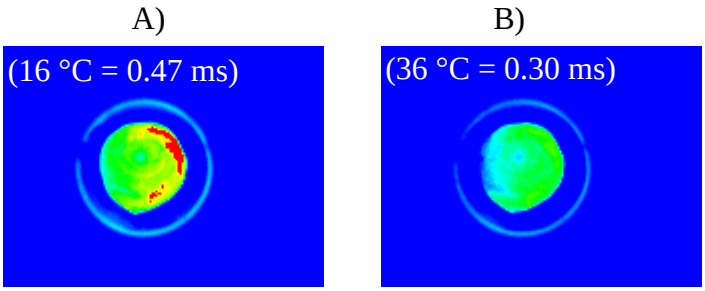

Fig 14. *Two images of the lifetime of the temperature probe embedded in the biosensor membrane BSM5. (A) The spot was covered with doubly distilled water of 16 °C, and (B) 36 °C.*

5.4.10. Luminescence Imaging of Glucose via the pH Transducer HPTS

The typical calibration curve for glucose in 0.01 mM buffer (pH 8.5) is shown in *Fig. 15*. The relative changes of luminescence intensity are dependent on the buffer capacity. Relatively high signal changes are obtained by using a 0.01 mM buffer system. Applying buffer systems in the concentration range from 1 to 10 mM no signal change can be observed. Hence, the buffer capacity is too strong and all produced protons are depleted by the system. For determination of glucose via pH transduction *stand by measurements* were done. A sensor spot was fixed on the bottom of a glass vessel via a titan dioxide (TiO_2) layer which enhances the reflection of the luminescence intensity. Glucose solutions in the concentration range from

0 to 3.0 mM were added and the luminescence intensity was measured after 45 minutes. Compared to flow through cell measurements the products are not washed out of the membrane, but after 45 minutes no steady state signal was achieved. As a result, glucose can be detected in practice only kinetically. The luminescence change can be increased by using air-saturated glucose solutions. The activity of GOx is enhanced and more gluconic acid is produced. Glucose is diffused into the biosensor membrane BSM5 where the enzyme GOx is located, and gluconic acid and hydrogen peroxide are produced. These products will diffuse out of the membrane which leads to a pH gradient inside the membrane. The pH gradient is dependent on the layer thickness, the GOx activity, the pH dependence of the GOx activity and the buffer capacity.[35] The change of the pH was detected by luminescence changes of HPTS whose luminescence is addicted from the pK_a. Further on, the pK_a value of HPTS is highly ionic strength dependent. Constant ionic strength was achieved adding NaCl (0.1 M) to the buffer system.

Fig. 15 shows the calibration plot for determination of glucose via a pH transducer. The error bars for each glucose concentration are very high and the luminescence change is very low despite application of a buffer system with low capacity. For this kind of glucose determination no steady state was obtained after 45 minutes, so the luminescence intensity was always increasing. Hence, glucose was sensed by a kinetic method. Luminescence intensity was measured for each concentration after 45 minutes. The time for returning back to the baseline takes more than 4 hours, which makes the system almost irreversible.

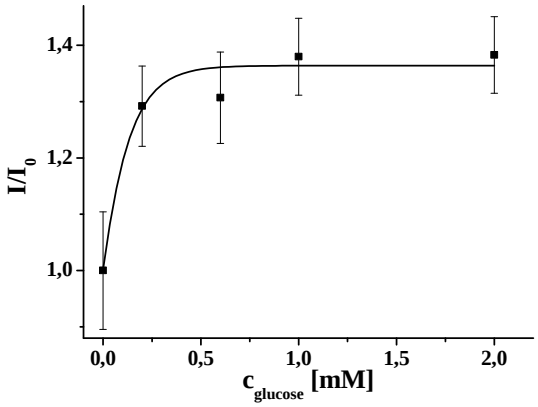

Fig. 15. *Calibration plot of glucose via a pH transducer. The starting pH of glucose solution was 8.5 in 0.01 mM Robinson-Britton buffer containing 0.1 M NaCl. I_0 is the luminescence intensity of the blank (buffer); I is the luminescence intensity of glucose in the concentration range from 0 to 2.0 mM.*

These results are different from the results in *chapter 4.4* because the analytical range for glucose determination is in the molar range. The reason could be that the buffer capacity was too high and therefore the buffer concentration has to be changed from 0.1 mM to 0.01 mM.

5.5. Conclusion

A triple sensor for determination of glucose was developed. The sensor consists of an oxygen, pH and temperature transducer. All indicators are incorporated in particles which are embedded in a hydrogel matrix besides the enzyme glucose oxidase. The aim of this biosensor was the simultaneously determination of glucose via oxygen and pH transduction. The temperature transducer ($Eu(tta)_3(dpbt)$) was used for controlling the temperature during the measurements. Glucose is converted into gluconic acid and hydrogen peroxide catalyzed by glucose oxidase. The oxidation was performed under oxygen consumption which can be detected by dynamic quenching of the luminescence lifetime of the oxygen transducer PtTFPL. The changes in lifetime are equivalent to different glucose concentrations. Determination of glucose via pH transduction is carried out by detection of changes in luminescence intensity of HPTS. The signal changes are equivalent to the glucose concentrations. Glucose determination via oxygen transduction can be easily performed in contrast to the detection via the pH transducer. Here the measurements are not reproducible, steady state conditions cannot be obtained within 45 min. Hence, this biosensor can be simply applied for simultaneously sensing of glucose via oxygen transduction and the temperature.

5.6. References

[1] von Bueltzingsloewen C., McEvoy A. K., McDonagh C., MacCraith B. D., Klimant I., Krause C., Wolfbeis O. S., **Sol-gel based optical carbon dioxide sensor employing dual luminophore referencing for application in food packaging technology** 2002. Analyst 127, 1478-1483

[2] Hyakutake T., Okura I., Asai K., Nishide H., **Dual-mode oxygen-sensing based on oxygen-adduct formation at cobaltporphyrin-polymer and luminescence quenching of pyrene: an optical oxygen sensor for a practical atmospheric pressure** 2008. J. Mater. Chem. 18, 917-922

[3] Schröder C. R., **Luminescent Planar Single and Dual Optodes for Time-Resolved Imaging of pH, pCO_2 and pO_2 in Marine Systems** 2006. Dissertation

[4] Chojnacki P., Mistelberger G., Klimant I., **Separable magnetic sensors for the optical determination of oxygen** 2007. Angew. Chem. Int. Ed. 46, 8850-8853

[5] Kocincová A. S., Borisov S. M., Krause C., Wolfbeis O. S., **Fiber-optic microsensors for simultaneous sensing of oxygen and pH, and of oxygen and temperature** 2007, Anal. Chem. 79, 8486-8493

[6] Khalil G. E., Lau K., Phelan G. D., Carlson B., Gouterman M., Callis J. B., Dalton L. R., **Europium beta-diketonate temperature sensors: effects of ligands, matrix, and concentration** 2004. Rev. Sci. Instrum. 75, 192-206

[7] Kocincová A. S., **New pH sensitive sensor materials. Luminescent fiber-optic dual sensors for non-invasive and simultaneous measurements of pH and pO_2 (dissolved oxygen) in biological systems** 2007. Dissertation, 73

[8] Koese M. E., Carroll B. F., Schanze K. S., **Preparation and spectroscopic properties of multiluminophore luminescent oxygen and temperature sensor films** 2005. Langmuir 21, 9121-9129

[9] Jorge P. A. S., Maule C., Silva A. J., Benrashid R., Santos J. L., Farahi F., **Dual sensing of oxygen and temperature using quantum dots and a ruthenium complex** 2008. Anal. Chim. Acta 606, 223-229

[10] Vasylevska G. S., Borisov S. M., Krause C., Wolfbeis O. S., **Indicator-loaded permeation-selective microbeads for use in fiber optic simultaneous sensing of pH and dissolved oxygen** 2006. Chem. Mater 18, 4609-4616

[11] Cho E. J., Bright F. V., **Pin-printed chemical sensor arrays for simultaneous multianalyte quantification** 2002. Anal. Chem. 74, 1462-1466

[12] Wolfbeis O. S., Weis L. J., Leiner M. J. P., Ziegler W. E., **Fiber-optic fluorosensor for oxygen and carbon dioxide** 1988. Anal. Chem. 60, 2028-2030

[13] Borisov S. M., Krause C., Arain S., Wolfbeis O. S., **Composite material for simultaneous and contactless luminescent sensing and imaging of oxygen and carbon dioxide** 2006. Adv. Mat. 18, 1511-1516

[14] Wencel D., Higgins C., Klukowska A., MacCraith B. D., McDonagh C., **Novel sol-gel derived films for luminescence-based oxygen and pH sensing** 2007. Mat. Sci. 25, 767-779

[15] Yang C., Fu L. M., Wang Y., Zhang J. P., Wong W. T., Ai X. C., Qiao Y. F., Zou B. S., Gui L. L., **A highly luminescent europium complex showing visible-light-sensitized red emission: direct observation of the singlet pathway** 2004. Angew. Chem. Int. Ed. 43, 5010-5013

[16] Stich M. I. J., Nagl S., Wolfbeis O. S., Henne U., Schaeferling M., **Dual luminescent sensor material for simultaneous imaging of pressure and temperature on surfaces** Adv. Funct. Mater., *in press*

[17] Cao Y., Koo Y. E. L., Kopelman R., **Poly(decyl methacrylate)-based fluorescent PEBBLE swarm nanosensors for measuring dissolved oxygen in biosamples** 2004. Analyst 129, 745-750

[18] Koo Y. E. L., Cao Y., Kopelman R., Koo S. M., Brasuel M., Philbert M. A., **Real-time measurements of dissolved oxygen inside live cells by organically modified silicate fluorescent nanosensors** 2004. Anal. Chem. 74, 2498-2505

[19] Zelelow B., Khalil G. E., Phelan G., Carlson B., Gouterman M., Callis J. B., Dalton L. R., **Dual luminophor pressure sensitive paint II. Lifetime based measurement of pressure and temperature** 2003. Sens. Actuators B 96, 304-314

[20] Brandrup J., Immergut E. A., Grulke (Eds) **Polymer Handbook** 1999. Wiley-VCH, New York

[21] Mitsuishi M., Kikuchi S., Miyashita T., Amao Y., **Characterization of an ultrathin polymer optode and its application to temperature sensors based on luminescent europium complexes** 2003. J. Mater. Chem 13, 2875-2879

[22] Guo H., Tao S., **An active core fiber-optic temperature sensor using an Eu(III)-doped sol-gel silica fiber as a temperature indicator** 2007. IEEE Sensors Journal 7, 953-954

[23] Borisov S. M., Klimant I., **Blue LED excitable temperature sensors based on a new europium(III) chelate** 2008. J. Fluoresc. 18, 581-589

[24] Borisov S. M., Wolfbeis O. S., **Temperature-sensitive europium(III) probes and their use for simultaneous luminescent sensing of temperature and oxygen** 2006. Anal. Chem. 78, 5094-5101

[25] Arnaud N., Georges J., **Comprehensive study of the luminescent properties and lifetimes of Eu^{3+} and Tb^{3+} chelated with various ligands in aqueous solutions: influence of the synergic agent, the surfactant and the energy level of the ligand triplet** 2003. Spectrochim. Acta Part A 59, 1829-1840

[26] Leonard J. P., Gunnlaugsson T., **Luminescent Eu(III) and Tb(III) complexes: developing lanthanide luminescent-based devices** 2005. J. Fluoresc. 15, 585-595

[27] Haugland R. P., **Handbook of fluorescent probes and research products 2002**. 9th Edition, 836-837

[28] Schroeder C. R., Weidgans B. M., Klimant I., **pH fluorosensors for use in marine systems** 2005. Analyst 130, 907-916

[29] Liebsch G., **Time-resolved luminescence lifetime imaging with optical chemical sensors set-up, controlling, concepts and applications** 2000. Dissertation, 15-16.

[30] Schröder C., **Luminescent planar single and dual optodes for time-resolved imaging of pH, pCO_2 and pO_2 in marine systems** 2006. Dissertation, 18-19

[31] García E. A., Fernández R. G., Díaz-García M. E., **Tris(bipyridine)ruthenium(II) doped sol-gel materials for oxygen recognition in organic solvents** 2005. Micropo. Mesopo. Mat. 77, 235-239

[32] Roche P., Al-Jowder R., Narayanaswamy R., Young J., Scully P., **A novel luminescent lifetime-based optrode for the detection of gaseous and dissolved oxygen utilising a mixed ormosil matrix containing ruthenium (4,7-diphenyl-1, 10-phenanthroline)$_3$$Cl_2$ (Ru.dpp)** 2006. Anal. Bioanal. Chem 386, 1245-1257

[33] Liebsch G., Klimant I., Wolfbeis O. S., **Luminescence lifetime temperature sensing based on sol-gels and poly(acrylonitrile)s dyed with ruthenium metal-ligand complexes** 1999. Adv. Mater 11, 1296-1299

[34] www.sigmaaldrich.com/catalog/search/ProductDetail/FLUKA/49180

[35] Trettnak W., Leiner M. J. P., Wolfbeis O. S., **Fiber-optic glucose sensor with a pH optrode as the transducer** 1989. Biosensors 4, 15-26

[36] Arain S., **Microrespirometry with Sensor-Equipped Microtiterplates** 2006. Dissertation, 80

[37] Wang X. D., Zhou T. Y., Chen X., Wong K. Y., Wang X. R., **An optical biosensor for the rapid determination of glucose in human serum** 2008. Sens. Actuators B 129, 866-873

Chapter 6

Summaries

English

This thesis describes the development of a microtiter plate assay for determination of uric acid. It also depicts the development, characterization and application of luminescence based optical biosensors for determination of uric acid and glucose.

Chapter 1 gives an introduction on the importance of the determination of uric acid and glucose. Furthermore, an overview on the state of the art of optical sensing of oxygen and pH is given, along with a comparison of optical sensor versus electrochemical sensor technology. In this thesis a microtiter plate assay for uric acid determination is described applying an europium complex as fluorescent probe. Hence, the luminescence emission mechanism of lanthanide complexes is explained in detail.

Chapter 2 describes a microtiter plate assay for uric acid. The hydrogen peroxide sensitive probe europium(III)-tetracycline (Eu_3TC) was applied for sensing hydrogen peroxide that is released by the enzyme uricase during the oxidation of uric acid. Hydrogen peroxide coordinates to Eu_3Tc and enhances its luminescence intensity. The assay is carried out in the time-gated mode. Uric acid can be detected in the concentration range up to 60 µM with a limit of detection of 9.9 µM. The assay cannot be applied to the determination of uric acid in urine unfortunately. Urine a complex matrix contains phosphate which quenches the luminescence intensity of the complex Eu_3TC-HP strongly.

In chapter 3, a biosensor membrane is presented for detection of uric acid. The biosensor membrane consists of a single layer which contains an oxygen probe and the enzyme uricase. The detection of uric acid is based on the measurement of oxygen that is consumed during the oxidation catalyzed by uricase. A ruthenium- or an iridium complex incorporated in organically modified sol-gel is applied as oxygen sensitive probe, whose luminescence intensity is dynamically quenched in presence of oxygen. Uric acid can be detected in the concentration range up to 0.8 mM with a limit of detection of 0.05 mM using the ruthenium complex as oxygen sensitive probe. Applying the iridium complex as oxygen sensitive probe uric acid is detected in the concentration range from 0.02 to 0.6 mM. The

optical biosensor using the ruthenium complex as oxygen sensitive probe is successfully applied to the determination of uric acid in blood serum.

In chapter 4, a biosensor membrane is prepared for determination of glucose. The fundamental idea of this chapter is the simultaneous detection of glucose via (a) oxygen and (b) pH transduction. The first part of this chapter describes a strategy to embed an oxygen sensitive probe and the enzyme glucose oxidase in a hydrogel matrix and apply it to glucose sensing. The detection scheme is based on the principle described in chapter 3. The enzyme glucose oxidase catalyzes the oxidation of glucose under oxygen consumption which is detected using a ruthenium complex as the oxygen sensitive probe. Its luminescence intensity is enhanced in absence of oxygen. Glucose can be detected in the concentration range from 0.2 to 1.0 mM. In the second part glucose is determined via a pH transducer. During the oxidation of glucose one of the end products is gluconic acid which dissociates in gluconate and protons. Hence, the pH of the microenvironment decreases which can be detected in luminescence changes of a pH sensitive probe. Two pH indicators, HPTS and CF, are applied but without the desirable success. The application of CF as pH indicator is disadvantageous due to strong photobleaching. However, the determination of glucose using HPTS as pH transducer is feasible only in the molar concentration range and the reproducibility of the results is very low. Hence, the simultaneous determination of glucose via oxygen and pH transduction is not possible.

In chapter 5, a triple sensor is presented for simultaneous monitoring of glucose via an oxygen and pH transducer along with monitoring the temperature. The oxygen-, pH- and temperature transducers are embedded in a hydrogel matrix along with the enzyme glucose oxidase. The triple sensor is illuminated by one single LED and the resulting emissions of the indicators are imaged by a CCD camera and spectrally separated by using suitable filters. This set up allows the simultaneous monitoring of glucose via oxygen and pH transduction and the temperature. This temperature determination is important because the activity of the enzyme GOx and the luminescence of the oxygen transducer PtTFPL are temperature dependent. Simultaneous sensing of glucose via pH and oxygen transduction along with temperature is successful in the case of monitoring glucose via oxygen transduction along with the temperature. The detection of glucose via pH transduction lacks the desirable success because the response times are very long and the reproducibility of the results is very low.

The following *table* summarizes the work on sensors described in this thesis.

Table. *Overview on successful and unsuccessful sensor work*

Analyte	Transducer	Successful	Unsuccessful
Uric acid	O_2	++	
Glucose	O_2	++	
Glucose	pH	+/-	
Glucose	pH/O_2		++
Glucose	O_2/T	++	
Glucose	pH/T	+/-	
Glucose	pH/O_2/T		++

German

Diese Arbeit beschreibt zum einen die Entwicklung eines Mikrotiterplattentests zur Bestimmung von Harnsäure, zum anderen die Entwicklung, Charakterisierung und Anwendung von optischen Biosensoren zur Bestimmung von Harnsäure und Glucose.

Im ersten Kapitel wird auf die Notwendigkeit der Bestimmung von Harnsäure und Glucose eingegangen. Harnsäure und Glucose können über den Sauerstoffverbrauch bestimmt werden, der aus einer durch die Enzyme Uricase oder Glucose Oxidase verursachten Oxidation resultiert. Beide Enzyme produzieren während der Oxidation Wasserstoffperoxid, welches als indirekter Nachweis für Harnsäure oder Glucose genutzt werden kann. Glucose kann zudem auch über eine Änderung des pH-Wertes während der Oxidation nachgewiesen werden, da das Oxidationsprodukt Gluconsäure in Gluconat und Protonen dissoziiert, die den pH-Wert absinken lassen. Aus diesem Grund wird in diesem Kapitel außerdem ein allgemeiner Überblick über Nachweismöglichkeiten für Sauerstoff, Wasserstoffperoxid und pH gegeben. Für die Bestimmung von Harnsäure und Glucose werden in dieser Arbeit optische Sensoren eingesetzt, welche sowohl Vorteile als auch Nachteile gegenüber elektrochemischen Sensoren aufweisen. Diese Vor- und Nachteile werden genau aufgezeigt und erläutert. Für die Bestimmung von Harnsäure mit Hilfe eines Mikrotiterplattentests wird ein Europiumkomplex als fluoreszierende Sonde verwendet. Der Mechanismus der Fluoreszenzanregung und Emission von diesem Europiumkomplex wird im Detail beschrieben.

Kapitel zwei beschreibt ausführlich einen Mikrotiterplattentest zur Bestimmung von Harnsäure. In Gegenwart des Enzyms Uricase wird Harnsäure zu Allantoin unter Freisetzung von Wasserstoffperoxid oxidiert, das mit einem Europium-Tetracyclin Komplex (Eu_3TC) im molaren Verhältnis 3:1 nachgewiesen werden kann. In Gegenwart von Wasserstoffperoxid nimmt die Fluoreszenzintensität von Eu_3TC zu. Aufgrund seiner langen Fluoreszenzabklingzeit ist die Anwendung von zeitverzögerter Fluoreszenzspektroskopie möglich. Dieser Test ist einfach durchzuführen und Harnsäure kann in einem Konzentrationsbereich von 9,9 bis 60 µM nachgewiesen werden. Die Anwendung dieses Tests zur Bestimmung von Harnsäure in Urin führte zu keinem Erfolg. Urin beinhaltet neben vielen anderen Komponenten auch Phosphat, welches die Fluoreszenzintensität von Eu_3Tc mit koordiniertem Wasserstoffperoxid stark quencht, was die Detektion von Harnsäure in Urin unmöglich macht.

Kapitel drei beschreibt die Entwicklung eines optischen Biosensors zum Nachweis von Harnsäure. Hier wird Harnsäure über den Sauerstoffverbrauch während der Oxidation detektiert. Für den Nachweis von Sauerstoff werden Sauerstoff-sensitive Farbstoffe wie ein Ruthenium- oder ein Iridiumfarbstoff verwendet, deren Fluoreszenz dynamisch durch Sauerstoff gequencht wird. In dieser Arbeit werden die Sauerstoff-sensitiven Farbstoffe in organisch modifizierten Sol-Gel-Partikeln immobilisiert und zusammen mit dem quervernetzten Enzym Uricase in eine Hydrogelschicht eingebettet. Harnsäure kann in einem Konzentrationsbereich von 0,05 bis 0,8 mM für den Sauerstoff sensitiven Rutheniumkomplex und von 0,02 bis 0,6 mM für den Sauerstoff sensitiven Iridiumkomplex nachgewiesen werden. Die Bestimmung von Harnsäure in Blutserum unter Verwendung des Rutheniumkomplexes ist gut durchführbar.

Kapitel vier beschreibt die Entwicklung von optischen Biosensoren zur Bestimmung von Glucose. Die Grundidee dieses Kapitels ist die Entwicklung eines Dualsensors zur gleichzeitigen Bestimmung von Glucose mittels eines Sauerstoff- und eines pH- Transducers. Im ersten Teil dieses Kapitels erfolgt die Bestimmung von Glucose über die Detektion des Sauerstoffverbrauchs. Hier wird ebenfalls ein Rutheniumkomplex als Sauerstoffindikator verwendet, welcher in Sol-Gel-Partikeln immobilisiert ist und dessen Fluoreszenz in Gegenwart von Sauerstoff gequencht wird. Die Indikatorpartikel und das Enzym Glucose Oxidase werden in einer Hydrogelschicht eingebettet. Glucose kann mit diesem System in einem Bereich von 0,2 bis 1,0 mM nachgewiesen werden. Im zweiten Teil dieses Kapitels wird Glucose nachgewiesen indem man die pH-Wert Änderung mit einem pH sensitiven Farbstoff wie HPTS oder CF detektiert. Die erhaltenen Ergebnisse mit zwei verschiedenen

pH-Indikatoren zeigen nicht den gewünschten Erfolg. Die Anwendung von CF als pH-Indikator ist aufgrund der sehr schlechten Photostabilität nicht möglich. HPTS hingegen zeigt zufriedenstellendere Ergebnisse, wobei der Glucosenachweis aber nur im molaren Konzentrationsbereich möglich und die Reproduzierbarkeit dieser Methode sehr niedrig ist.

Im fünften Kapitel wird Glucose mit Hilfe eines Tripelsensors, welcher Sauerstoff-, pH- und Temperatur- sensitive Partikel, sowie Glucose Oxidase in einer Hydrogelschicht enthält, bestimmt. Die Grundidee in diesem Kapitel ist Glucose gleichzeitig über die Messung des Sauerstoffverbrauchs und die pH-Wert Änderung zu detektieren. Während der enzymatischen Oxidation ist es auch wichtig die Temperatur zu verfolgen, da die Aktivität von Glucose Oxidase und die Fluoreszenz des Sauerstoffindikators stark temperaturabhängig sind. Alle verwendeten Indikatoren werden mit einer LED angeregt und die daraus resultierenden Emissionen mit Hilfe einer CCD-Kamera spektral mit geeigneten Filtern voneinander getrennt. Wie schon erwähnt kann Glucose auf drei verschiedene Arten bestimmt werden. Die Temperaturmessung während der Oxidation und die gleichzeitige Glucosedetektion über den Sauerstoffverbrauch und die pH-Änderung liefern keine zufriedenstellenden Ergebnisse. Mit diesem optischen Biosensor ist die Bestimmung der Temperatur und der Glucosenachweis über den Sauerstoffverbrauch möglich. Die Glucosebestimmung über die pH-Wert Änderung ist nicht sehr vielversprechend aufgrund der langen Ansprechzeiten und der geringen Reproduzierbarkeit der Ergebnisse.

Folgende *Tabelle* zeigt eine Zusammenfassung aller Sensoren, die in dieser Arbeit beschrieben werden.

Tabelle. *Überblick über alle in dieser Arbeit entwickelten Sensoren für Harnsäure- und Glucosebestimmung*

Analyt	**Transducer**	**Erfolgreich**	**Nicht erfolgreich**
Harnsäure	O_2	++	
Glucose	O_2	++	
Glucose	pH	+/-	
Glucose	pH/O_2		++
Glucose	O_2/T	++	
Glucose	pH/T	+/-	
Glucose	pH/O_2/T		++

Chapter 7

Abbreviations & Acronyms

PS	polystyrene
PVC	poly(vinyl chloride)
PMMA	poly(methyl methacrylate)
PAH	polycyclic aromatic hydrocarbon
UA	uric acid
Eu_3TC	europium(III)-tetracycline complex
HP	hydrogen peroxide
Eu_3TC-HP	europium(III)-tetracycline hydrogen peroxide complex
TC	tetracycline
MOPS	3-(N-morpholino) propanesulfonate sodium salt
SOP	standard operational protocol
HSA	human serum albumin
BSA	bovine serum albumin
NADP	nicotinamide adenine dinucleotide phosphate
POx	horseradish peroxidase
DMAB	3-dimethylaminobenzoic acid
MTBH	3-methyl-benzothiazoline-2-one
TRIAP	1,1,3-tricyano-2-amino-1-propene
FI	flow injection
LOD	limit of detection
AA	ascorbic acid
GOx	glucose oxidase
HVA	homovanillic acid
CNT	carbon nanotubes
HPTS	8-hydroxypyrene-1, 3, 6-trisulfonate
CF	carboxyfluorescein
p-HEMA	poly(hydroxyethyl methacrylate)
PtTFPL	Pt(II)-5,10,15,20-tetrakis-(2,3,4,5,6-pentafluorophenyl) porpholactone

PSAN	poly(styrene-co-acrylonitrile)
DMF	dimethylformamide
THF	tetrahydrofurane
$Eu(tta)_3(dpbt)$	Eu(III)-tris(thenoyltrifluoroacetonato)-(2-(4-(diethylaminophenyl)-4,6-bis(3,5-dimethylpyrazol-1-yl)-1,3,5-triazine)
RLD	rapid lifetime determination
TiO_2	titan dioxide

Chapter 8

Curriculum Vitae

Personal Data

Surname	Schrenkhammer, nee Suchomel
First Name	Petra
Date of birth	11.01.1977
Place of birth	Aidenbach (Bavaria)
Nationality	German

Education

09/1983 – 07/1987	Primary School, Aldersbach
09/1987 – 06/1997	Gymnasium Vilshofen
06/1997	Abitur

Studies

11/1997 – 09/1999	Study of Technology and Biotechnology of Foods at the Technical University of Munich (Weihenstephan)
11/1999 – 03/2004	Study of Chemistry (Diploma) at the University of Regensburg
05/2004	Exam: Diploma
07/2004 – 03/2005	Diploma Work at the Institute of Analytical Chemistry, Chemo- and Biosensors (Prof. Wolfbeis) at the University of Regensburg (Title: Bestimmung der Aktivität von alkalischer Phosphatase mit Hilfe eines Lanthanoid-Komplexes)
03/2005	Degree: Diplom - Chemikerin (univ.)

since 04/2005	PhD Work at the Institute of Analytical Chemistry, Chemo- and Biosensors (Prof. Wolfbeis) at the University of Regensburg (Title: New optical biosensors for determination of uric acid and glucose)

Extracurricular Activities

04/2005 – 03/2008	Participation at the DFG Graduate College "*Sensory Photoreceptors in Natural and Artificial Systems"*
09/2006	Participation at the 5th Advanced Study Course on Optical Chemical Sensors, Tihany, Hungary

Poster Presentations

02/2005	Deutsches Biosensor Symposium, Regensburg
04/2005	Conference on Ion Analysis (CIA), Berlin
07/2005	Summer School of the Graduate College "*Sensory Photoreceptors in Natural and Artificial Systems"* in Pappenheim
07/2006	Summer School of the Graduate College "*Sensory Photoreceptors in Natural and Artificial Systems"* in Kostenz
07/2007	Summer School of the Graduate College "*Sensory Photoreceptors in Natural and Artificial Systems"* in Regen

Publications

1. Schrenkhammer P., Rosnizeck I. C., Duerkop A., Wolfbeis O. S., Schaeferling M., **Time resolved fluorescence-based assay for the determination of alkaline phosphatase activity and application to the screening of its inhibitors** 2008. J. Biomol. Screening 13, 9-16

2. Schrenkhammer P., Wolfbeis O. S., **Fully reversible optical uric acid biosensors using oxygen transduction** 2008. Biosens. Bioelectron.; *submitted*